Alcoa

JUL 17 1961

TP-10410

ALCOA RESEARCH LABORATORIES

MASTER

Technical Paper No. 10

SECOND REVISION

ALUMINA PROPERTIES

J. W. Newsome

H. W. Heiser, A. S. Russell, H. C. Stumpf

ALUMINUM COMPANY OF AMERICA

PITTSBURGH, PENNSYLVANIA

1960

Technical Paper No. 10

SECOND REVISION

ALUMINA PROPERTIES

BY J. W. NEWSOME
H. W. HEISER, A. S. RUSSELL, H. C. STUMPF

ALCOA RESEARCH LABORATORIES

ALUMINUM COMPANY OF AMERICA
PITTSBURGH, PENNSYLVANIA
1960

2

PREFACE

Second Revision

Much information on alumina has been developed since the first revision of Alumina Properties *appeared in 1956. This, together with the widespread interest in the publication, has justified the preparation of a second revision. As was the case with the previous editions, the authors have had the capable assistance of many associates, as well as the benefit of review by many authorities in the field. We wish to thank all who helped us and particularly to acknowledge the careful study and useful suggestions of E. A. Bloch, J. H. de Boer, H. Ginsberg, W. K. Gummer, J. G. Lindsay, C. Panseri, D. Papée, H. P. Rooksby, C. J. M. Rooymans, W. J. Smothers, S. Teichner, R. Tertian and J. B. Wachtman.*

J. W. NEWSOME
Alumina and Chemicals Division
Alcoa Research Laboratories
East St. Louis, Illinois

ACKNOWLEDGMENT

First Revision

In addition to the generous assistance of many associates, the authors acknowledge the critical reading of the manuscript by Guy Ervin, R. F. Geller, R. Goton, R. W. Kebler, W. O. Milligan, M. Constance Parché, D. Papée, M. Prettre, H. P. Rooksby, E. Ryshkewitch, W. J. Smothers, Persio de Souza Santos, S. Teichner, R. Tertian and H. Thibon.

ALLEN S. RUSSELL
W. H. GITZEN, J. W. NEWSOME, R. W. RICKER, V. M. STOWE,
H. C. STUMPF, J. R. WALL, PAUL WALLACE

Literature values for the properties of the aluminas are compiled critically in this publication. The historical development of the names for the many varieties is traced, and the systems of nomenclature are compared. Three major classifications are distinguished: the high temperature forms that are produced in general by calcination over 1200°C; the transition forms and the hydrates. For each phase the following information is assembled if it is available: occurrence in nature; preparation; crystal structure; optical, thermal, electrical, magnetic, mechanical and surface properties. The interesting phase transformations are given particular attention. Alcoa Activated Alumina is discussed separately with emphasis on its structure and its applications in drying, chromatography, catalysis and oil maintenance. Commercial forms and uses of Alcoa Calcined, Tabular and Hydrated Aluminas are also described. In many cases the data are summarized in figures and tables. An extensive bibliography and subject index are included.

CONTENTS

INDEX OF TABLES

INDEX OF FIGURES

ALUMINA PROPERTIES

ALUMINA is one of the largest-volume pure chemicals on the market today; over four million tons are produced annually in this country at 99% purity. Much of this output is used for the production of aluminum, but an increasing amount is employed in ceramics, refractories, abrasives, paper coatings, rubber goods, desiccants, catalysts, medicinals and many other products. This diversity of application arises from the remarkable range in properties characteristic of the pure oxide, the various hydrated aluminas and the numerous transition phases. Alumina has provided intriguing subjects for research. A compilation of some of the more important results can be of value in connection with present uses and point to future applications.

Alumina, sometimes alone, but usually in combination with silica, is a major constituent of the earth's crust. Bauxite, a product formed by solution of the other materials from aluminous rocks, is the predominant ore for reduction grade alumina by a large margin. Estimated reserves of this ore exceed one billion tons, located principally in Hungary, China, the Guianas, the Caribbean Islands, French West Africa, Gold Coast, Nyasaland, France, Brazil and the United States (War Production Board). Bauxite occurs in blankets, beds or lenses, pockets and detrital deposits, most of which have a definite extent rather than tapering off into gradually diminishing qualities of ore. In 1958 the world production of bauxite was 20,700,000 long tons, and United States consumption was 7,034,000 long tons, of which approximately 3% went into abrasives and about 5% into other nonaluminum applications. Domestic sources, predominantly in Arkansas, supplied 19%. Of the total imports of bauxite, Jamaica supplied 62%, Suriname 31% and British Guiana and Haiti the balance (Minerals Yearbook). The Bayer process for low-silica bauxite and the combination Bayer, lime-soda sinter process for high-silica bauxite are employed almost exclusively for the production of pure alumina. Fulda's and Ginsberg's *Tonerde und Aluminium* is the most complete published discussion on the commercial production of alumina for the aluminum industry.

NOMENCLATURE

Materials with a styptic or astringent taste were designated "alumen" by the Romans. These may have included impure forms both of aluminum sulfate and alum, which occur naturally in volcanic districts. Alumen seems to be the source of our word alumina (Beckman).

The recognition of alumina evolved gradually as the composition of alum became better understood. Hoffman in 1722 held that the base of alum was a true distinct earth and Pott called the base "thonichte erde" or "terre argilleuse" (clay earth). Marggraf in 1754 showed that the earth of alum was a distinct substance, that it existed in natural clays and that it could be extracted by sulfuric acid. His memoirs gave rise to the term "argil" or "argil pur" as the name of the earthy base of alum. De Morveau in 1786 argued that since alum was designated "sel alumineux," the proper name for the base should be "alumine." This latter term has been anglicized to alumina.

A mineral from India, having the composition Al_2O_3 was described in 1798 by Greville under the name corundum, which he believed to be the native name of the stone. The mineral diaspore was described by Haüy in 1801 and was analyzed by Vauquelin in 1802 and shown to be $Al_2O_3 \cdot H_2O$. Haüy named it diaspore from the Greek for "scatter," because it flew apart when heated. In 1805 Davy analyzed a mineral and named it hydrargillite from the Greek for water and clay. Later, however, other workers showed this mineral to be aluminum phosphate. Dewey in 1820 found a mineral he called gibbsite in honor of Gibbs, an American mineralogist. Analyses of it by Torrey in 1822 corresponded with the formula

$Al(OH)_3$ or $Al_2O_3 \cdot 3H_2O$. The name hydrargillite was applied later to a similar mineral found in the Urals, and both names are still employed, but the name gibbsite is preferred.

The name bauxite was derived from the French province Les Baux, an early source of the ore. The term has come to be widely used to cover any aluminum ore consisting of reasonably pure hydrated aluminum oxides. $Al_2O_3 \cdot 2H_2O$, the formula which had been assigned to bauxite, is erroneous and represents a variable mixture of monohydrate and trihydrate phases.

Böhm and Niclassen identified another alumina by using X rays. Böhm found it to be isomeric with diaspore and showed a purified bauxite from Les Baux to consist of this phase. De Lapparent suggested that the hydrate be called böhmite. Böhm also discovered an alumina hydrate isomeric with gibbsite. Fricke (1928) suggested the name bayerite for this material because he thought it was the product of the Bayer process. In the next year, Fricke recognized his error, but the unfortunate name has been continued.

Rankin and Merwin in 1916 assigned the prefix beta to a high-temperature alumina that, according to later experience (Ridgway 1936), must contain alkali or alkaline earth atoms. The pure alumina corresponding to corundum was differentiated as alpha alumina. Inasmuch as several forms of beta alumina have been distinguished, the foreign cation is now made part of the name, i.e., sodium beta alumina. Barlett assigned the name zeta to the phase formed with lithium.

Haber in 1925 divided the aluminas and ferric oxides and their hydrates into two series, alpha and gamma, depending upon the products of their calcination. The failure of this system to differentiate the alumina trihydrates prompted the naming of individual hydrates in *The Aluminum Industry* (Edwards 1930). The symbol alpha was applied to the form more abundant in nature. In this nomenclature, bayerite is beta trihydrate, and the pure alumina phases corresponding to gibbsite, böhmite and diaspore are alpha trihydrate, alpha monohydrate and beta monohydrate, respectively. Weiser and Milligan (1934) and Weiser (1935) later adopted the Haber series names for the individual species and classified bayerite as alpha trihydrate.

The designation gamma was given originally by Ulrich to an undescribed alumina, and this term has been used in many cases for all the alumina transition phases encountered in the low-temperature calcination of aluminum compounds and in the oxidation of aluminum. Stumpf restricted the name gamma to the product whose X-ray pattern is like that in the alpha trihydrate and alpha monohydrate dehydration sequences at 500°C. This phase, present in Alcoa Activated Alumina, had come to be known as gamma alumina. Unfortunately, however, the gamma designation had also been associated with a spinel structure, and Stumpf's gamma is probably not a spinel. Other workers have made the reverse choice and have used the name gamma for the spinel structure.

As new phases have been identified or suspected, they have been assigned Greek letters. Many of these have been disproved. Chi (which might be poorly developed kappa) and delta (which may be a mixture of gamma and theta) are still disputed. The list is probably not complete. Papée and Tertian (1955) proposed the name rho for a phase obtained by thermal dehydration of alpha trihydrate in high vacuum. Steinheil proposed an epsilon alumina from oxidation of aluminum. Cowley assigned the names xi and xi^1 to phases revealed by electron diffraction of the oxide films formed by heating aluminum foil in air on metal grid supports. Shishakov reported a hexagonal $AlO \cdot OH$ as a film on aluminum, identical to the lattice attributed by Steinheil to a cubic Al_2O_3. Van Nordstrand has recently found a new trihydrate phase. Foster (1959) reported an anhydrous alumina phase whose X-ray pattern is very similar to that of mullite. This phase has been named iota alumina.

Table 1 shows the nomenclature systems for those aluminas most frequently confused in the literature. Obviously, a universal standard nomenclature would be highly desirable. An attempt in this direction was made in 1957 when, in Western Germany, a symposium on alumina nomenclature was held. The results of this meeting were reported by Ginsberg. The main agree-

TABLE 1

Nomenclature of Aluminas

ALCOA①	Symposium②		Haber	Weiser and Milligan	Other
ALPHA ALUMINA TRIHYDRATE	Aluminum Trihydroxides	HYDRARGILLITE or GIBBSITE	Gamma Series	GAMMA ALUMINA TRIHYDRATE	Aluminum Hydroxide Orthoaluminic Acid
BETA ALUMINA TRIHYDRATE		BAYERITE		ALPHA ALUMINA TRIHYDRATE	Aluminum Hydroxide Bauxite Dihydrate③
		NORDSTRANDITE			Randomite④ Bayerite II④
ALPHA ALUMINA MONOHYDRATE	Aluminum Oxide Hydroxides	BÖHMITE		GAMMA ALUMINA MONOHYDRATE	Bauxite⑤
					Pseudoböhmite⑥
BETA ALUMINA MONOHYDRATE		DIASPORE	Alpha Series	ALPHA ALUMINA MONOHYDRATE	Meta-aluminic Acid
ALPHA ALUMINA	CORUNDUM			ALPHA ALUMINA	

U.S.A.	Germany	England	France	
ALCOA①	Symposium②	Day and Hill; Rooksby	Thibon	PECHINEY⑦
				rho
gamma	gamma	delta	gamma	gamma
delta	delta	delta +theta	delta	delta
eta	eta	gamma	eta	eta
theta		theta	theta	theta
iota				
chi	chi	chi +gamma	chi	chi +gamma
kappa	kappa	kappa +theta	kappa	kappa +delta
			kappa′	

①Edwards, Frary, Stumpf
②Ginsberg, Hüttig, Strunk-Lichtenberg
③Moiseev
④Teter, Gring, and Keith, U.S. Patent 2,838,375
⑤Böhm
⑥Papée, Tertian, Biais
⑦Tertian, Papée

ment was to abolish the so-called incorrect terms, "hydrate" and "phase." The following nomenclature was suggested, and is also shown to some extent in Table 1, for comparison with others:

(a) Use of the term "hydroxide" instead of "hydrate," namely: aluminum trihy-

TABLE 2

Crystal Structure and Density of Aluminas

Phase	Formula	Crystal System	Space Group	Molecules per Unit Cell	Unit Axis Lengths, Å				Measured Density g/ml	Reference
					a	b	c	Angle		
Molten									2.5	Wartenberg (1936)
Alpha Trihydrate	$Al_2O_3 \cdot 3H_2O$	Monoclinic	C_{2h}^5	4	8.62	5.06	9.70	85°26′	2.42③	Megaw (1934)
Beta Trihydrate	$Al_2O_3 \cdot 3H_2O$	Monoclinic	C_{2h}^5	2	4.72	8.68	5.06	90°11′	2.53③	Unmack
Alpha Monohydrate	$Al_2O_3 \cdot H_2O$	Orthorhombic	D_{2h}^{17}	2	2.868	12.227	3.700	.....	3.01④	Swanson and Fuyat
Beta Monohydrate	$Al_2O_3 \cdot H_2O$	Orthorhombic	D_{2h}^{16}	2	4.396	9.426	2.844	.....	3.44⑤	Swanson and Fuyat
Alpha	Al_2O_3	Hexagonal②	D_{3d}^6	2	4.758	......	12.991	.....	3.98⑥	Swanson and Fuyat
Sodium Beta	$Na_2O \cdot 11Al_2O_3$	Hexagonal	D_{6h}^4	1	5.58	......	22.45	.....	3.24	Beevers and Brohult
Potassium Beta	$K_2O \cdot 11Al_2O_3$	Hexagonal	D_{6h}^4	1	5.58	......	22.67	.....	3.30	Beevers and Brohult
Magnesium Beta	$MgO \cdot 11Al_2O_3$	Hexagonal	D_{6h}^4	1	5.56	......	22.55	.....	....	Bragg
Calcium Beta	$CaO \cdot 6Al_2O_3$	Hexagonal	D_{6h}^4	2	5.54	......	21.83	.....	....	Lägerqvist
Strontium Beta	$SrO \cdot 6Al_2O_3$	Hexagonal	D_{6h}^4	2	5.56	......	21.95	.....	....	Lägerqvist
Barium Beta	$BaO \cdot 6Al_2O_3$	Hexagonal	D_{6h}^4	2	5.58	......	22.67	.....	3.69⑦	Adelsköld
Lithium Zeta	$Li_2O \cdot 5Al_2O_3$	Cubic	O_h^7	2	7.90	......	.....	.....	3.61	Kordes, Braun
Gamma	Nearly Anhydrous Al_2O_3	Cubic	....	..	....	......	.....	.....	(3.2)⑧	Ginsberg
Delta		Orthorhombic	....	12	4.25	12.75	10.21	.....	(3.2)⑧	Stumpf
Delta (Rooksby)		Tetragonal	....	..	7.96	......	23.4	.....	....	Rooymans
Eta		Cubic (Spinel)	O_h^7	10	7.90	......	.....	.....	2.5–3.6⑨	Stumpf
Theta①		Monoclinic	C_{2h}^3	4	5.63	2.95	11.86	103°42′	3.56⑨	Kohn
Iota		Orthorhombic	....	4	7.73	7.78	2.92	.....	3.71⑧	Stumpf
Kappa		Orthorhombic	....	32	8.49	12.73	13.39	.....	3.1–3.3⑨	Stumpf
Chi		Cubic (Not spinel)	....	10	7.95	......	.....	.....	(3.0)⑧	Stumpf

①Anhydrous ②Rhombohedral ③Roth ④Fricke and Severin
⑤Dana ⑥Seemann ⑦Toropov ⑧Estimated ⑨Thibon

droxide, instead of alumina trihydrate; aluminum oxide hydroxide, instead of alumina monohydrate.

(b) Same nomenclature as ALCOA for the transition aluminas, although not using the term "phase," but rather, for example: "chi form," "kappa form," "gamma form," "delta group."

(c) In honor of Van Nordstrand the name Nordstrandite was adopted for the phase of beta trihydrate discovered by him. This name is currently well in use in Europe.

HIGH-TEMPERATURE PHASES

A. *Alpha Alumina*

The occurrence of alpha alumina in rocks, as the mineral corundum, is widespread; the larger crystals are found in igneous rocks. The dark variety of corundum contains magnetite and is known as emery. The alpha form results from solidification of an alumina melt, from calcination of other aluminas and in some circumstances (Wartenberg 1952) from burning aluminum in oxygen.

Recrystallization sintering of alpha alumina occurring at about 1750°C was facilitated by Fe_2O_3, Mn_2O_3, CuO and TiO_2 over certain limits. Fe_2O_3 and Mn_2O_3 also promoted large grains, while MgO and SiO_2 inhibited grain growth. Fine grinding promoted sintering and the growth of large elongated grains (Cahoon and Christensen). Cutler reported that by combinations of added oxides of Mn and Ti or Cu and Ti and small particle size the sintering temperature of 96% alumina bodies was reduced to 1300°C. Kukolev and Leve also investigated the effect of the source and the degree of dispersion of alumina on its sinterability in the presence of additives. PO_4, Cl, NO_3, SO_4, OH, F, Ca, Sr, Ba, Li, K, Na, Ni^2, Mg, Cr^3, Mo^3, Sb^5, Sn^4, La^3, V^5, Si as well as small amounts of hard carbides, silicides and metallic tungsten are claimed to impede grain growth (Bron, Eliasson, Reinhard, Ryshkewitch (1953), Smothers and Reynolds). Pavlushkin studied the effect of nearly all elements in the periodic table as additions to alumina, and classified them according to their effect on sintering and rate of recrystallization. The sintering cycle is claimed of the utmost importance in controlling crystal structure and strength of the corundum, and long soak at low temperatures is not as effective as short holding times at higher temperatures.

Pampuch studied the role of surface energy in the first stages of the sintering process of pure oxides, the possibility of predicting the effect of additives on the sintering of these oxides, and the effect of their structural characteristics. Factors which decrease the surface energy accelerate the sintering process. Experiments with alumina and other metal oxides showed that additives having a lower electronegativity of the metal-O bond than the basis oxide, in general of 1.6-2, improve the sintering process.

The role of structural defects in the sintering of alumina was studied by Jones. Aluminas containing additions of TiO_2, Cr_2O_3, FeO or MnO were sintered at comparatively low temperatures (1200-1500°C) in atmospheres of O, N or H. Diffusion promoted by lattice defects was observed by measurement of bulk density. The densification process was dependent on the sintering atmosphere, indicating that reducing and oxidizing atmospheres can significantly alter the number of lattice vacancies. Kuczynski, Abernethy and Allan studied the chemical aspects of the sintering of aluminum oxide. Their experiments on sintering of alumina single crystal spheres in hydrogen, helium and oxygen atmospheres between 1500 and 2000°C indicate that the predominant mechanism of material transfer in this process is volume diffusion. The sintering rates in purified dry hydrogen were found to be much higher than in oxygen, helium or moist hydrogen. This is probably due to the additional lattice imperfections created in the crystal by reduction of alumina with hydrogen. The heating in dry hydrogen transformed the spheres into polyhedra of hexagonal symmetry. An appreciable loss of oxide due to evaporation of Al_2O and/or AlO was noted. In the presence of impurities in the sintering atmosphere, such as tungsten or molybdenum oxides, the alumina spheres were observed to sinter by viscous flow, presumably because impurity oxides formed a glass or liquid layer on the surfaces.

In actual practice other materials are often added to the alumina to accelerate vitrification at lower temperatures. Fricke and Weitbrecht claimed that silica aided crystallization to alpha alumina, although the opposite effect is more often stated, at least when the alumina is used as a support for active catalysts (for example, Layng, Bailey and Bittner, and Huffman). Voltz and Weller patented the use of thoria and hafnia to stabilize gamma alumina to resist alpha

TABLE 3
X-ray Powder Diffraction Patterns of Aluminas

Interplanar Spacings and Relative Line Intensities
Filtered CuK Radiation, Å

Alpha ① Tri-hydrate		Beta ① Tri-hydrate		Nord-strandite ②		Alpha ③ Mono-hydrate		Beta ③ Mono-hydrate		Chi ④		Gamma ④		Eta ④		Delta ④		Delta ~~④~~ 5		Theta ④		Iota ④		Kappa ④		Alpha ③	
4.82	100	4.72	100	4.790	10	6.11	100	4.71	13							5.02	3	7.97	8	5.2	3	5.45	100	6.2	3	3.479	74
4.34	40	4.36	70	4.373	2	3.164	65	3.99	100					4.6	4	4.55	3	6.58	10	4.5	6	3.47	90	4.5	2	2.552	92
4.30	20	3.19	25	4.310	4	2.346	53	3.214	10							4.07	2	5.07	20	3.53	2	2.92	40	4.2	1	2.379	42
3.35	10	3.08	1	4.205	4	1.980	6	2.558	30					2.8	2	2.87	4	4.05	20	2.85	8	2.72	80	3.04	4	2.165	1
3.31	6	2.69	3	4.153	4	1.860	32	2.434	3			2.7	2			2.73	8	3.56	7	2.72	8	2.59	70	2.79	6	2.085	100
3.17	8	2.45	3	3.880	3	1.850	27	2.386	5							2.58	3	3.40	10	2.56	3	2.46	10	2.70	2	1.740	43
3.08	4	2.34	6	3.600	3	1.770	6	2.356	8	2.40	4	2.41	6	2.40	6	2.43	6	3.28	15	2.43	8	2.34	40	2.57	8	1.601	81
2.44	15	2.28	3	3.462	2	1.662	13	2.317	56	2.27	2	2.28	6	2.27	3	2.28	4	3.21	10	2.31	6	2.24	80	2.41	3	1.546	3
2.42	4	2.21	67	3.022	2	1.527	6	2.131	52			2.18	2					3.03	10	2.24	6	2.15	60	2.32	4	1.510	7
2.37	20	2.14	3	2.845	2	1.453	16	2.077	49	2.11	3	2.09	1					2.783	30	2.11	1	1.99	10	2.26	1	1.404	32
2.28	4	2.06	2	2.706	1	1.434	9	1.901	3	1.98	2	1.98	10	1.97	8	1.99	8	2.737	30	2.01	8	1.94	10	2.16	1	1.374	48
2.23	6	1.97	3	2.490	1	1.412	1	1.815	8			1.95	6			1.95	3	2.593	70	1.91	4	1.88	40	2.11	8	1.276	2
2.15	8	1.91	1	2.478	3	1.396	2	1.733	3							1.91	2	2.457	70	1.80	3	1.73	50	2.06	3	1.239	16
2.03	12	1.83	1	2.451	2	1.383	6	1.712	15							1.80	2	2.311	40	1.73	1	1.61	40	1.99	4	1.190	6
1.98	10	1.76	1	2.390	7	1.369	2	1.678	3	1.53	1	1.54	2			1.54	4	2.277	30	1.61	2	1.55	70	1.95	2	1.160	1
1.95	2	1.71	26	2.261	7	1.312	15	1.633	43					1.52	2	1.51	3	2.156	25	1.54	6	1.492	30	1.87	6	1.147	4
1.90	7	1.68	2	2.217	1	1.303	3	1.608	12							1.49	4	1.989	70}	1.49	4	1.461	40	1.82	3	1.138	1
1.79	10	1.64	1	2.029	1	1.224	1	1.570	4							1.45	3	1.950	65}*	1.45	4	1.435	10	1.74	2	1.125	5
1.74	9	1.59	4	2.013	5	1.209	2	1.522	6					1.40	10	1.40	6	1.793	7	1.43	1	1.410	10	1.64	6	1.099	6
1.67	9	1.56	2	1.898	5	1.178	3	1.480	20	1.39	10	1.39	10			1.39	10	1.701	4	1.40	6	1.370	10	1.54	1	1.083	3
1.65	3	1.55	4	1.777	4	1.171	1	1.431	7							1.29	2	1.616	10	1.39	10	1.346	40	1.49	3	1.078	7
1.63	1	1.52	1	1.717	1	1.161	3	1.423	12							1.26	1	1.602	15	1.34	1	1.325	5	1.45	3	1.043	13
1.58	3	1.48	1	1.698	1	1.134	5	1.400	6					1.21	1			1.543	10	1.29	3	1.288	60	1.43	8	1.018	1
1.57	1	1.47	1	1.680	1	1.092	1	1.376	16			1.14	3	1.14	2	1.14	2	1.507	20	1.26	2			1.39	10	.998	11
1.55	2	1.45	7	1.667	1	1.046	2	1.340	5			1.04	1	1.03	1			1.462	8	1.23	2			1.34	3	.982	2
				1.647	2													1.407	60}								
				1.591	2													1.392	100}*								
				1.569	2													1.250	4								
				1.545	2													1.238	9								
				1.510	3													1.180	4								
				1.475	3													1.134	10								
				1.438	6																						
				1.400	2																						

①Typical diffractometer patterns, scanning speed 1 degree per minute (Stumpf, unpublished)
②Papée, Tertian and Biais
③Swanson and Fuyat, prepared for ASTM X-ray Powder Data File
④Film patterns, intensities estimated visually (Stumpf)
⑤Rooksby (1958)
*These pairs of lines occur in positions corresponding with the 400 and 440 lines for the cubic γ-structure.

Note: See Figure 7, page 36, for X-ray powder diffraction patterns.

alumina formation. Pointud and Caillat found the density of alumina tablets to be near the theoretical maximum after heating at 1600°C under pressures of 150 kg/cm^2.

From measurements of the rate of shrinkage of pressed alumina compacts, Coble found that the growth between single crystals was consistent with bulk diffusion sintering having an activation energy of 165 kcal/mole.

The crystal structure is roughly a hexagonally close-packed agglomerate of molecules in which aluminum ions occur above and below the midpoint of oxygen ion triangles (Pauling and Hendricks). Considerable variation exists in the crystals of corundum, the prismatic, flat and tabular forms being common (Dana). Hoch and Johnston found the crystal structure at 2000°C to be the same as that at room temperature. Belova and Ikornikova reported that sapphires frequently show a mosaic structure. Korenstein investigated the sintering of alumina and, on the basis of examination by electron microscope and X-ray structure analysis, showed sintered alumina to contain a lamellar structure.

TABLE 4

Thermal Properties of Aluminas

Phase	Heat of Formation at 298.16°K kcal/mole	Entropy at 298.16°K cal/deg mole	Reference④
Alpha Trihydrate	−612.7③	33.51	I-59-2①
Beta Trihydrate	−609.4	.....	Russell (1955) and ΔH_f of AlO_2^-
Amorphous Trihydrate $Al(OH)_3$	−304.2	.....	I-59-2①
Alpha Monohydrate	−471.8	23.15	Russell (1955) and ΔH_f of AlO_2^- I-59-2①
Beta Monohydrate	....	8.43③	
Transition Alumina	−384.84	.....	I-59-2①
Product of Alpha Trihydrate Dehydrated at 500°C	−391	.....	Michel (1957) ΔH_f of H_2O I-59-2① and ΔH_f of Alumina Hydrate
Product of Beta Trihydrate Dehydrated at 210-230°C	−390	.....	
Product of Alpha Monohydrate Dehydrated at 210-230°C	−394	.....	
Alpha Alumina	−400.48②	12.186	I-59-2①
Aluminate Ion AlO_2^-	−217.8	.....	Russell (1955) and ΔH_f Alpha Trihydrate I-59-2①

①Selected Values of Chemical Thermodynamic Properties

②Mah noted that the product of the combustion was shown by X ray to be alpha alumina. Schneider and Gattow showed previous values to be 2-3 kcal low because alpha alumina was not formed in the calorimeter.

③Kelley

④Fricke pointed out that different values may be found because of differences in the pre-history of the materials. Torkar and Worel also called attention to this.

TABLE 4—(Continued)

Thermal Properties of Aluminas

<table>
<tr><th>Property</th><th colspan="6">Values</th><th>Reference</th></tr>
<tr><td>Boiling Point</td><td colspan="6">3500°C</td><td>Brewer and Searcy; Wartenberg</td></tr>
<tr><td>Melting Point</td><td colspan="6">2040°C</td><td>II-59-1①</td></tr>
<tr><td>Heat of Fusion</td><td colspan="6">26 kcal/mole</td><td>II-59-1①</td></tr>
<tr><td>Specific Heat (cal/g)</td><td colspan="6"></td><td></td></tr>
<tr><td>Alpha Alumina</td><td colspan="6">$0.34833-8.02\times10^{-6}T-47.852/T$④⑤⑥
0.183, 20°C
0.217, 100°C</td><td>Furukawa⑧</td></tr>
<tr><td>Alpha Trihydrate</td><td colspan="6">$0.2694+6.43\cdot10^{-4}t$④
0.282, 20°C</td><td>Roth</td></tr>
<tr><td>Thermal Conductivity (Metric②)</td><td colspan="6"></td><td></td></tr>
<tr><td>Sapphire</td><td colspan="6">0.08, 2.5°K; 15, 50°K; 1, 100°K (36° from c-axis)</td><td>Berman</td></tr>
<tr><td></td><td colspan="6">0.065, 90-100°C, 60° from axis</td><td>Weeks & Seifert; Ruh</td></tr>
<tr><td rowspan="4">Sintered Alumina③</td><td>100°C</td><td>200°C</td><td>400°C</td><td>600°C</td><td>800°C</td><td>1000°C</td><td rowspan="4">Kingery</td></tr>
<tr><td>0.072</td><td>0.054</td><td>0.031</td><td>0.022</td><td>0.017</td><td>0.015</td></tr>
<tr><td>1200°C</td><td>1400°C</td><td>1600°C</td><td>1800°C</td><td></td><td></td></tr>
<tr><td>0.013</td><td>0.013</td><td>0.015</td><td>0.018</td><td></td><td></td></tr>
<tr><td>Activated Alumina</td><td colspan="6">$4.3\cdot10^{-4}$, 100°C</td><td>Activated Alumina: Its Properties and Uses</td></tr>
<tr><td>Compressed Powder, 1.84 g/ml.</td><td colspan="6">0.00161, 468°C</td><td>Tomashov and Inzhenerov</td></tr>
<tr><td>Linear Expansion Coefficient (All values have been multiplied by 10^6)</td><td colspan="6"></td><td></td></tr>
<tr><td>Alpha Alumina⑦</td><td colspan="6">5.5, 25°C; 7.3, 800°C; 10.0, 1300°C</td><td>Schwartz</td></tr>
<tr><td></td><td colspan="6">7.12⊥c-axis, 7.2 ∥ c-axis, 500°C</td><td>Shalnikova and Yakovlev</td></tr>
<tr><td></td><td colspan="6">$6.58+0.0_2500t+0.0_5258t^2$, ∥ c-axis, 50-700°C
$5.43+0.0_2553t+0.0_5288t^2$, ⊥c-axis, 50-700°C</td><td>Megaw 1933; Sharma</td></tr>
<tr><td></td><td colspan="6">8.32 ∥ c-axis, 0-1442°C
7.75⊥c-axis, 0-1442°C</td><td>Mauer and Bolz</td></tr>
<tr><td>Synthetic Sapphire Rod</td><td colspan="2">∥ c-axis</td><td colspan="2">⊥c-axis</td><td colspan="2">∥ rhombohedral axis</td><td>Geller and Yavorsky</td></tr>
<tr><td>25-200°C</td><td colspan="2">6.8</td><td colspan="2">5.7</td><td colspan="2">6.2</td><td></td></tr>
<tr><td>25-400°C</td><td colspan="2">7.7</td><td colspan="2">6.9</td><td colspan="2">6.9</td><td></td></tr>
<tr><td>25-600°C</td><td colspan="2">8.2</td><td colspan="2">7.5</td><td colspan="2">7.5</td><td></td></tr>
<tr><td>25-800°C</td><td colspan="2"></td><td colspan="2">7.5</td><td colspan="2">7.9</td><td></td></tr>
<tr><td>25-1000°C</td><td colspan="2"></td><td colspan="2">7.7</td><td colspan="2">8.3</td><td></td></tr>
<tr><td>Alpha Trihydrate ⊥to given plane, 25-100°C</td><td colspan="6">(010), 10.9; (001), 15.4; (100), 13.1; $(10\bar{1})$, 39; (101), -5.6</td><td>Megaw 1933</td></tr>
<tr><td>Beta Alumina</td><td colspan="6">5.1-5.7, 25-200°C; 6.0-7.6, 600-700°C</td><td>Nat. Bur. Stds. News Bull. p. 39, April 1934</td></tr>
<tr><td>Zeta Alumina</td><td colspan="6">6.0, 25-200°C; 7.7, 600-700°C</td><td>Nat. Bur. Stds. News Bull. p. 39, April 1934</td></tr>
</table>

For effect of pores and for detailed data see J. Am. Ceram. Soc. **37**, 67-110 (1954).

①Selected Values of Chemical Thermodynamic Properties

②Metric Conductivity Units=cal/cm, °C, sec. Multiply metric value by 0.806 to convert to Btu/sq ft, in., °F, sec.

③Calculated to zero porosity by dividing measured conductivity by (1-volume pore fraction)

④T in °K, °K=273.1+°C, t in °C

⑤Equation applies 400-1200°K. Results tabulated in reference from 13-1170°K

⑥Also measured from 100-900°C by Gomel'skii, and from 1100-1400°C by Rodigina and Gomel'skii

⑦Klein showed that within small limits of error the ratio c/a was constant between 20 and 1750°C.

⑧Tscherbow and Tschernjak obtained values in fairly close agreement with these.

Levin has compiled phase-diagrams for systems consisting of Al_2O_3 with the following compounds:

- Al_4C_3
- AlF_3-CaF_2-NaF
- AlF_3-LiF
- AlF_3-LiF-NaF
- AlF_3-NaF
- BaO
- BaO-H_2O
- BaO-SiO_2
- BeO
- BeO-MgO
- BeO-ThO_2
- BeO-TiO_2
- BeO-ZrO_2
- B_2O_3-SiO_2
- CaF_2
- CaF_2-CaO
- CaO
- CaO-Cr_2O_3
- CaO-Cr_2O_3-MgO-SiO_2
- CaO-FeO-SiO_2
- CaO-Fe_2O_3
- CaO-Fe_2O_3-K_2O
- CaO-Fe_2O_3-MgO
- CaO-Fe_2O_3-MgO-SiO_2
- CaO-Fe_2O_3-Na_2O
- CaO-Fe_2O_3-SiO_2
- CaO-H_2O
- CaO-H_2O-SO_3
- CaO-K_2O
- CaO-K_2O-MgO-SiO_2
- CaO-K_2O-Na_2O-SiO_2
- CaO-K_2O-SiO_2
- CaO-MgO
- CaO-MgO-Na_2O-SiO_2
- CaO-MgO-SiO_2
- CaO-Na_2O
- CaO-Na_2O-P_2O_5-SiO_2
- CaO-Na_2O-SiO_2
- CaO-Na_2O-SiO_2-TiO_2
- CaO-P_2O_5
- CaO-P_2O_5-SiO_2
- CaO-SiO_2
- CaO-SiO_2-TiO_2
- CeO_2
- CO_2-H_2O-MgO
- CoO
- Cr_2O_3
- Cr_2O_3-FeO-Fe_2O_3
- Cr_2O_3-MgO
- Cu_2O
- FeO
- FeO-Fe_2O_3
- FeO-Fe_2O_3-SiO_2
- FeO-K_2O-SiO_2
- FeO-MnO
- FeO-Na_2O-SiO_2
- FeO-SiO_2
- Fe_2O_3
- Fe_2O_3-MgO-SiO_2
- Fe_2O_3-SiO_2
- Fe_3O_4
- Ga_2O_3
- Ga_2O_3-H_2O
- H_2O
- H_2O-K_2O-Na_2O-SiO_2
- H_2O-K_2O-SiO_2
- H_2O-MgO
- H_2O-MgO-N_2O_5
- H_2O-MgO-SiO_2
- H_2O-Na_2O-SiO_2
- H_2O-SiO_2
- H_2O-SO_3
- K_2O-MgO-SiO_2
- K_2O-Na_2O-SiO_2
- K_2O-SiO_2
- La_2O_3
- Li_2O-MgO-SiO_2
- Li_2O-SiO_2
- MgO
- MgO-SiO_2
- MgO-SiO_2-ZrO_2
- MgO-TiO_2
- MgO-ZrO_2
- MnO
- MnO-SiO_2
- MnO-SiO_2-Y_2O_3
- Mn_3O_4
- Na_2O-SiO_2
- NiO
- PbO
- PbO-SiO_2
- P_2O_5
- SiO_2
- SiO_2-SrO
- SiO_2-TiO_2
- SiO_2-ZnO
- SiO_2-ZrO_2
- SrO
- ThO_2
- TiO_2
- TiO_2-ZrO_2
- UO_2
- ZnO
- ZrO_2

Optical evidence for the existence of $(11\bar{2}0)$ slip planes with $[1\bar{1}00]$ slip direction was reported by Klassen-Neklyudova (1953). The structure of alpha alumina, the dislocations which it allows, and the atomic movements during motion of a dislocation were discussed at length by Kronberg. The intersection of dislocations with the surface can be revealed by etching with boiling phosphoric acid, according to Gibbs.

Sapphire is uniaxial negative. Refractive indices for the ordinary and extraordinary rays are given in Table 8. A strong peak in the absorption at 0.55 microns caused by Cr in ruby was reported by Mandarino who also determined the change of indices of refraction with compressive stress applied parallel to the c-axis. The absorption coefficient of sapphire doped with various impurities was measured by Bates and Gibbs during optical studies of corundum.

Pure alumina is neither phosphorescent nor fluorescent, although .001% of chromic oxide produced a distinct fluorescence (Kröger). Thermoluminescence was induced in alpha alumina by high gamma ray exposure, the intensity increasing with calcination and being greatest for synthetic sapphire. The luminescence structure was relatively simple with a principal peak at 160°C and a smaller peak at 300°C (Rieke).

Levy showed that irradiating sapphires in a reactor produced color centers at 2,040 Å that could not be formed by purely ionizing radiation. Coloring was removed by annealing the alumina to 450°C but was restored by Co^{60} gamma ray irradiation, while annealing above this temperature removed coloring that was not restored by subsequent Co^{60} irradiation. Presumably the fast reactor neutrons formed centers by radiation damage processes that were then colored by ionization processes.

Bhagavantam and Venkatarayudu predicted 18 frequencies for alpha alumina, of which two symmetric and five doubly degenerate ones should be Raman active. Krishnan found the Raman frequencies and their relative intensities to be 375 (8), 417 (10), 432 (4), 450 (2), 578 (3), 642 (6), 751 (7) cm^{-1}. The Raman spectrum of alpha alumina was confirmed by Raman in 1951. The infrared spectra are summarized in Table 10.

Synthetic sapphire of 0.5-cm thickness had 83% transmission at 10,000 Å, the loss being largely Fresnel reflection. Its 20% transmission limits extended from 1,500 to 57,000 Å (Klevens and Platt, Bauple, Seeman, Gilles). Gilles showed that absorption at the shorter wave lengths increased as temperature increased, and that there was a smooth decrease in the transmission of synthetic sapphire from 2,800 to about 1,450 Å.

The emissivity of alumina decreased from 0.98 at room temperature to 0.9 at 100°C, 0.8 at 400°C, 0.5 at 750°C, 0.3 at 1000°C, 0.18 at 1600°C and 0.12 at 2760°C (Heilman, Michaud, Kilham, Taylor and Edwards, Leedy). The monochromatic emissivity at 0.655 micron was 0.15 from 1000 to 1600°C (Michaud).

Many of the thermal properties of aluminas are given in Table 4. Alpha alumina has been recommended as a calorimetric standard, and the specific heat was determined by Furukawa and co-workers over the range 13-1170°K. They also prepared tables of enthalpy and entropy, and Gibbs' free energy values over the range 0-1200°K.

The thermal conductivity of sapphire and alumina at high temperatures has been studied extensively. References were given by Charvat and Kingery, who included values up to 1200°C for single crystals. Values of thermal diffusivity measured directly by a heat-wave propagation method were reported by the Alfred University group, who also investigated the heat transfer properties of polycrystalline alumina at very low temperatures (Berman and Soxman).

Electrical properties of alpha alumina are shown in Table 5. In a survey, Cohen found that the electrical conductivity of sapphire varied by a factor of 100 or more, depending on the impurities, microstructure and surface state of the specimen. Gibbs suggested that impurities penetrate into the body of sapphire along dislocation lines. This is assumed to affect the structure in such a way as to provide high-conductivity "tubes" surrounding the dislocation lines. It was stated that these high-conductivity regions also give rise to dielectric-loss peaks, and that these can be eliminated by heating the material sufficiently to drive out the impurity atoms.

Bárta, Bartuška and co-workers investigated the effects of impurities on the specific resistance of sintered alumina in the range of 400-700°C with low-voltage direct current. Alkaline impurities were found to decrease the resistance considerably, whereas SiO_2, CaO and Fe_2O_3 in small amounts had little influence. TiO_2 and Cr_2O_3, even in large amounts, did not affect the resistance. V_2O_5 decreased it noticeably, and MnO increased it. The fine-grained material had a higher resistance than the coarse-grained.

O'Connor deduced from streaming potential that freshly ground corundum in water had a positive surface, but on ignition to 1000°C this was changed to negative. Modi and Fuerstenau found the point of zero charge at pH 9.45. These findings were supported by Pike and Hubbard.

Selwood studied the magnetic properties of solid solutions of Cr_2O_3 and of Fe_2O_3 in Al_2O_3. Magnetic resonance of 0.1% Cr_2O_3 in Al_2O_3 was detected, and ruby single crystals have been used as the working substance in maser amplifiers (Makhov, Kikuchi and co-workers).

Many of the mechanical properties of alpha alumina are listed in Table 7; and, as a result of current intense investigations, more and more related data are being rapidly obtained and published.

McCandless and Yenni reported that single crystal alumina bodies could be stretched into rod and bent when they were heated, the stretched portions becoming opaque while the body remained a single crystal after the bending operation. Saucier reported that sapphires split on a plane containing the optic axis.

Ryshkewitch (1944) reported that both the shrinkage and elasticity increased sharply with firing temperature from 1500 to 1750°C. He also (1953) found that an increase of 10% in porosity decreased the compression strength of sintered pure alumina by one-half. Pores perpendicular to the pressure direction decreased strength more than those parallel to the pressure direction. Attinger concluded from measurements with a Knoop diamond indenter that sapphires with pores normal to the optic axis were the softest. Fissures were obtained mostly at 45° to the optic axis.

Roberts and Watt confirmed observations first made by Ryshkewitch (1941) that fracture of well-sintered alumina bodies (RAE, specific gravity 3.8) was both trans- and inter-crystalline. They thus regarded it as improbable that the bend strength of this alumina could be increased appreciably. Because of delayed fracture effects, they doubted that sintered alumina would find application where it must withstand tension.

Pearson found the fracture time of sintered alumina to increase from one second to 10^6 seconds when the stress was reduced in the ratio 1.3:1. The delayed-fracture effect was eliminated by heat treatment and testing in vacuo, which suggests an association with water vapor.

In support of this view, Charles found that at 240°C the modulus of rupture in a constant loading rate experiment changed from 116,500 psi in dry nitrogen to 68,000 psi in saturated water vapor.

The elastic constants of sapphire were recently redetermined by Wachtman and co-workers. Elastic moduli for polycrystalline alumina at room temperature were given by Lang. Young's modulus of sapphire was found to decrease linearly with increasing temperature up to at least 1500°C. For polycrystalline alumina, Young's modulus measured at 1 kilocycle/sec decreased linearly to about 950°C and then fell rapidly accompanied by an increase in the internal friction (Wachtman and Lam). A value of the activation energy for grain boundary slip of 200 kilocalories/mole was determined from internal friction measurements by Chang. The variation of elastic moduli of polycrystalline alumina with porosity was studied by Coble and Kingery, who found good agreement with equations derived by MacKenzie. His formula assumes spherical pores, but data by Lang on alumina with nonspherical pores indicate that in this case MacKenzie's equation seriously underestimates the effect of porosity. Bienvenue and Dixon showed that irradiation with gamma rays caused Young's modulus to decrease to a minimum 0.7% below the initial value at 2×10^{15} photons/cm^2. Further irradiation caused a subsequent recovery to a value 0.6% below the starting value. These effects were paralleled by an initial increase in the internal friction followed by a return to its original value. The internal friction of sapphire at room temperature depends on its microstructure; values ranging from 2×10^{-6} to 1×10^{-3} were reported (Wachtman, Lam and co-workers). Chang studied the secondary internal friction peaks caused by small amounts of La and Cr acting in conjunction with grain boundaries. Wachtman and Maxwell found the stress required to cause breakage decreased as the tests were extended over longer times. They found plastic deformation beyond a definite yield point in sapphire above 900°C; (0001) was the slip plane and $[11\bar{2}0]$ the slip direction. The creep curves showed three stages: an increasing creep rate, a large but decreasing creep rate, and a small and nearly constant creep rate. In one experiment at constant load, 70 hours elapsed without measurable creep, after which more than 2% elongation took place. Chang studied the "second" or steady stage of creep and obtained an activation energy of 7.8 ev. He concluded that dislocation climb by self-diffusion is the most likely rate-determining process. Small amounts of partially recoverable creep in polycrystalline aluminum oxide in the range 1000-1200°C were observed by Wachtman and Maxwell, who interpreted them as relaxation of shear stress on grain boundaries accompanied by elastic deformation of grains. At higher temperatures, Chang reported much larger creep strain which he attributed to the Nabarro-Herring vacancy diffusion mechanism. Negative creep due to residual internal strains from firing sintered corundum was observed by Cahoon and Christensen. The residual strains could be eliminated by annealing.

As variables in their creep-rate studies, Cahoon and Christensen also investigated various sources of alumina, method of preparation, control, amount of impurities and temperature.

Kronberg showed that plastic bending of sapphire, followed by heat treatment, results in polygonization. That is, dislocations of the same sign segregate and form plane walls perpendicular to the slip plane. May studied the kinetics of this process over the range 1750-1850°C and found an activation energy of 140 kcal/mole. The modulus of rupture of both sapphire and alumina were studied as a function of temperature by Jackson and Roberts. They found that for single-crystal sapphire the modulus of rupture passed through a minimum at 600°C and returned to the room temperature value at 1000°C. The same minimum and subsequent rise was found by Wachtman and Maxwell for single crystals favorably oriented for plastic deformation. Crystals with unfavorable orientations showed a much smaller rise. The results were interpreted to mean that the increase in strength at 1000°C over that at 600°C found by Jackson and Roberts is associated with relief of stress concentrations by small amounts of plastic deformation.

Kiyoura and Sayta reported that CoO, NiO, MgO and Cr_2O_3 (2-5%) were especially effective in increasing the transverse strength of sintered alumina at 1000°C.

Webb and Forgeng produced small euhedral crystals of alpha alumina by oxidizing aluminum in wet hydrogen between 1300 and 1450°C. These crystals were up to 10 mm long in the form of tapered hexagonal needles from 1 to 50 microns thick and blade-shaped platelets from 0.5 to 10 microns thick. The growth process appeared to involve aluminum suboxide. The needles could be elastically bent to strains greater than 2% before failing by brittle fracture. Dragsdorf and Webb measured the lattice twist from screw dislocations which accounts for the growth mechanism. The position of the dislocations was clearly shown by a capillary hole along the core.

Carnahan found that the contact angle of liquid aluminum on alumina at 1243°C and 10^{-6} mm Hg pressure decreased to a steady value of 60° in 20 minutes. On sapphire at 1201°C, the drops spread and then suddenly contracted to a contact angle of 80°. The spreading and contraction were repeated cyclicly. This behavior was explained by the reaction of the alumina and aluminum to form aluminum suboxide gas.

Alpha alumina usually has surface area less than 1 m^2/g and is, therefore, nonsorptive. However, a higher surface area form can be prepared; Missouri diaspore after heating at 600°C had a surface area of 85 m^2/g although the X ray showed only alpha alumina (Russell and Cochran). Schwiersch reported that such a product had a lower refractive index than either beta monohydrate or alpha alumina, and took this to indicate a fine-grained porosity. Herold and Dodd found that similarly heated diaspore had an increased solubility in hydrochloric acid. Knapp measured the internal surface of alpha alumina by low-angle X-ray scattering to be much larger than that found by gas diffusion or vapor adsorption.

Additional information on the mechanical properties of sintered alumina is in the work of Desmarquest.

B. Beta and Zeta Aluminas

The beta aluminas are isomorphous compounds containing small quantities of Na_2O, K_2O or one of the alkaline earth oxides. They have been identified with varying contents of Na_2O (4.9 to 5.3%) and K_2O (6.8 to 7.5%). However, the forms containing alkaline earth oxides apparently are stoichiometric compounds. These include $MgO \cdot 11Al_2O_3$, $CaO \cdot 6Al_2O_3$, $BaO \cdot 6Al_2O_3$ and $SrO \cdot 6Al_2O_3$. These phases have never been identified in nature.

Sodium oxide reacted with alumina at 900°C to form beta alumina, and this product with excess sodium oxide formed sodium aluminate at 1200°C (Yamauchi and Kato 1944). Gallup reported that sodium beta alumina converted to alpha alumina at 1300°C in vacuum or hydrogen, but that 1650°C was necessary in air or argon. According to Funaki, beta alumina was stable at 1700°C if it contained more than 5% sodium, magnesium or calcium oxide. Brownmiller crystallized potassium beta alumina from alumina plus 3.5% K_2O heated to 1550°C.

Saalfeld investigated the effect of various double fluorides on alpha alumina at elevated temperatures. Molten cryolite and cryolite vapor, potassium cryolite and the alkali iron hexafluorides caused alpha alumina to be transformed into beta alumina at about 1000°C.

Akiyama produced zeta alumina by adding 2% lithium oxide at 1700°C. Zeta alumina is apparently formed when lithium ions occupy vacant lattice sites of a spinel lattice (Smith and Beeck). Little change in the basic lattice results. Zeta alumina crystallizes in octahedra (Barlett).

Bor found that the beta alumina present in corroded glass tank firebrick usually crystallized in extremely thin, sharp-edged, perfect hexagons embedded in glass. He pointed out that these hexagons were often mistaken for alpha alumina.

The spectral distribution of the luminescence from these aluminas with manganese activation was reported in detail by Kröger. Bragg found no piezoelectric effect in sodium and magnesium beta aluminas.

Sodium beta alumina is much softer than alpha alumina, and penetrated plate glass only one-fiftieth as much as fused alpha alumina in an air-jet abrasion test (Ridgway 1933). Care is usually taken to remove sodium from aluminous abrasives.

TABLE 5

Electrical Properties of Alpha Alumina

Temp. °C	Resistivity (ohm-cm)	Alumina	Reference
14	10^{16}	Sintox	Singer and Thurnauer
300	$1.2 \cdot 10^{13}$	Sintered	Gerdien
500	10^{11}	Sapphire	Linde Air Products Co.
800	$3.5 \cdot 10^{8}$	Sintered	Gerdien
600–900	10^{6}	Sintered	Railton
1000	10^{6}	Sapphire	Linde Air Products Co.
1000	$2.5 \cdot 10^{6}$	Sapphire	Wachtman and Maxwell (1954)
1000	$1.0 \cdot 10^{8}$ ①	Sapphire①	Wachtman and Maxwell (1954)
1075	10^{5}–10^{6}	Sintered	Rögener
1214	10^{6} ②	Sapphire	Seemann
1227	$7.7 \cdot 10^{6}$	Sintered	Wartenberg and Prophet
1231	10^{6} ③	Sapphire	Seemann
1327	$2.0 \cdot 10^{6}$	Sintered	Wartenberg and Prophet
1400	$1.3 \cdot 10^{5}$	Sapphire	Wachtman and Maxwell (1954)
1400	$5.0 \cdot 10^{5}$ ①	Sapphire①	Wachtman and Maxwell (1954)
1500	$0.5 \cdot 10^{6}$	Sapphire	Linde Air Products Co.
1600	$5.2 \cdot 10^{3}$	Sintered	Werner
1800	$4.30 \cdot 10^{3}$ ④	Sintered	Podszus
2000	10^{3}	Sapphire	Linde Air Products Co.

①Previously plastically deformed ②$\perp$ c-axis ③$\parallel$ c-axis

④Lowest in hydrogen, intermediate in nitrogen, highest in vacuum

For additional resistance measurements see Arizumi and Tana, Miyazawa and Okada. Hensler and Henry found Cr_2O_3, NiO and MgO to increase and SiO_2 to decrease resistivity of alumina.

TABLE 5—(Continued)

Electrical Properties of Alpha Alumina

Phase	Preparation	Per Cent Loss on Ignition	Dielectric Constant	Reference
Amorphous	Stock	49.6	20.6	Glemser
Alpha Trihydrate	Fricke and Wullhorst	34.6	8.7	Glemser
Beta Trihydrate	Fricke and Wullhorst	34.6	9.4	Glemser
Alpha Monohydrate	Fricke and Severin	17.4	20.5	Glemser
Amorphous	Heated 13 hr 600°C	21.4	9.3	Glemser
Amorphous	Heated 13 hr 800°C	....	9.6	Glemser
Amorphous	Heated 13 hr 1200°C	....	11.3	Glemser
Beta Trihydrate	Heated 13 hr 600°C	0.88	13.1	Glemser
Beta Trihydrate	Heated 13 hr 1000°C	....	11.8	Glemser
Alpha Monohydrate	Heated 13 hr 600°C	0.13	10.6	Glemser
Alpha Monohydrate	Heated 13 hr 800°C	....	10.0	Glemser
Alpha Monohydrate	Heated 13 hr 1000°C	....	10.0	Glemser
Alpha①	Synthetic or Corundum	....	12.3	Glemser
Alpha①	Sintox 10^6 cycles/sec	....	9.6	Singer and Thurnauer
Alpha①	Sintox 10^3 cycles/sec	....	10.0	Singer and Thurnauer

Property	Conditions	Values	Alumina	Reference
Dielectric Strength	50 cycles/sec	$0.48 \cdot 10^6$ v/cm	Sintox	Singer and Thurnauer
	50 cycles/sec	$0.82 \cdot 10^6$ v/cm	Sintox	Singer and Thurnauer
	50 cycles/sec	$2 \cdot 10^6$ v/cm	....	Ueda and Okada
	<100 Å Thick, 15°C, Vacuum	$11 \cdot 10^6$ v/cm	Anodized Film	Lomer
	>100 Å Thick, 15°C, Vacuum	$6 \cdot 10^6$ v/cm	Anodized Film	Lomer
Thermionic Emission, T in °K, amp/cm^2	....	$47.0\ T^2$ exp. $11{,}600 \cdot 2.70/T$	C.P.	Rueger
Secondary Electron Emission	30-500 microsecond Pulses 50/sec 1400-1900°C	Max. of 3 at 500 volts	10 micron thick spectroscopically pure	Shul'man and Rozentsveig
Activation Energy for Conductivity	....	2.38-2.50 ev	....	Heldt and Haase
Activation Energy for Electrical Breakdown	....	5 ev	....	Miyazawa and Okada

①See page 21.

TABLE 5—(Continued)

Temperature	Frequency	Dielectric Constant		Dielectric Loss Tangent (Dissipation Factor)		Dielectric③ Constant	Dielectric Loss Tangent (Dissipation Factor)
		Sapphire①		Sapphire①		Sintered Alumina① (99.9% Al_2O_3)	
°C	Cycles/sec	⊥ Optic Axis	∥ Optic Axis	⊥ Optic Axis	∥ Optic Axis		
25	10^2	9.34	11.55		0.000012	10.5	0.00066
	10^3	9.34	11.55			10.5	0.00031
	10^4	9.34	11.55			10.5	0.00011
	10^5	9.34	11.55			10.5	
	8.5 x 10^9	9.34	11.55	0.00003	0.000086	9.6	0.00049 (0.00026)②
50	10^2	9.36	11.58	0.00001	0.000018	10.6	0.0015
	10^3	9.36	11.58			10.6	0.00056
	10^4	9.36	11.58			10.6	0.00019
	10^5	9.36	11.58			10.6	0.0001
	8.5 x 10^9	9.36	11.58	0.000032	0.00009	9.7	0.0005 (0.00027)
100	10^2	9.41	11.68	0.00002	0.000038	10.7	0.008
	10^3	9.41	11.68		0.00001	10.7	0.002
	10^4	9.41	11.68			10.7	0.00059
	10^5	9.41	11.68			10.7	0.00029
	8.5 x 10^9	9.41	11.68	0.000036	0.000096	9.7	0.00053 (0.00028)
200	10^2	9.53	11.87	0.00012	0.00017	12.0	0.20
	10^3	9.53	11.87	0.000036	0.000034	10.8	0.033
	10^4	9.53	11.87	0.000012	0.00001	10.8	0.0067
	10^5	9.53	11.87			10.8	0.0018
	8.5 x 10^9	9.53	11.87	0.000047	0.00011	9.8	0.00062 (0.0003)
300	10^2	9.65	12.09	0.00062	0.00066	21.6	1.4
	10^3	9.65	12.09	0.00023	0.00015	12.8	0.33
	10^4	9.65	12.09	0.000078	0.00005	11.2	0.06
	10^5	9.65	12.09	0.000037		11.1	0.012
	8.5 x 10^9	9.65	12.09	0.000062	0.00013	9.9	0.00076 (0.00034)
400	10^2	9.82	12.35	0.0033	0.003	100	1.03
	10^3	9.78	12.3	0.001	0.0009	21.5	1.17
	10^4	9.78	12.3	0.00036	0.0003	13.1	0.30
	10^5	9.78	12.3	0.00018		11.5	0.062
	8.5 x 10^9	9.78	12.3	0.00008	0.00014	10.0	0.001 (0.00039)
500	10^2	10.02	12.7	0.026	0.015	257	0.83
	10^3	9.95	12.55	0.005	0.0035	69	1.10
	10^4	9.92	12.55	0.0012	0.0017	19.0	0.90
	10^5	9.92	12.55	0.00056	0.0011	13	0.24
	8.5 x 10^9	9.92	12.55	0.000093	0.00015	10.1	0.0016 (0.00048)
600	10^2	10.55	13.15	0.23	0.16		
	10^3	10.17	12.83	0.032	0.021		
	10^4	10.07	12.83	0.0054	0.0036		
	10^5	10.07	12.83	0.0011	0.0017		
	8.5 x 10^9	10.07	12.83	0.00013	0.00017	10.2	0.003 (0.00062)
700	10^3		13.15				
	10^4	10.26	13.15				
	10^5	10.26	13.15				
	8.5 x 10^9	10.26	13.15	0.00021	0.00019	10.3	0.0059 (0.00093)
800	8.5 x 10^9	10.40	13.50	0.00043	0.00021		

①Data from MIT Technical Report 126; von Hippel (1958).

②Values in parentheses were obtained from a different sample of sintered alumina.

③All measurements of sintered alumina at 8.5 x 10^9 were made with electric field perpendicular to the direction of processing. At other frequencies the field was parallel.

De Pablo-Galan and Foster investigated the alumina-rich portion of the system Na_2O-Al_2O_3-SiO_2. The results of their studies also confirmed the status of beta alumina as a discrete compound, and were believed to justify the insertion of an additional tie line, linking beta alumina to carnegieite, in the soda-alumina-silica diagram.

Smith and Beeck suggested the use of calcium beta alumina as a thermostable catalyst support, but it is doubtful that this material has had extensive commercial application. Yamanouchi and Kato suggested the use of sodium beta alumina in glass-melting crucibles.

CALCINED AND TABULAR ALUMINAS

Many branches of technology owe much to the development of aluminas to meet and anticipate exacting requirements. Rigid demands are placed upon aluminas for high-temperature refractories, mechanical ceramics, abrasives and metal-working tools, electronic ceramics, and ceramics for missiles.

The use of alumina for these various purposes is growing at a phenomenal rate. High-alumina ceramics have excellent mechanical strength, high thermal conductivity, extremely good dielectric properties, and a particularly low dielectric loss factor at high temperatures. Alumina ceramics are dense, hard, abrasion resistant, highly resistant to chemical attack, and can be readily metallized for ceramic-to-metal seals. Without doubt, one of the most significant contributions to this growth is the continuing availability of high-purity, low-cost aluminas.

In addition to its widely expanded use in high-alumina porcelain for spark plugs, one of the more glamorous applications of alumina is the production of bodies for radio, television, military communication and radar tubes. In fact, these are used wherever high voltages and high frequencies must be handled because of outstanding dielectric characteristics and high-temperature stability of ceramic aluminas.

The abrasive industry is one of the largest consumers of calcined alumina. Bayer aluminas are processed to obtain a wide variety of grits and powders for grinding and polishing, and for the production of grinding wheels and cutting tools. Some of the requirements of a good cutting tool are extreme hardness, good strength and wear resistance. It must be resistant to high temperatures and must be made available at a reasonable cost. In the last few years alumina compositions, that meet all these requirements and can be formed into dense bodies, have been developed from an experimental product into a commercial reality.

Aluminas are finding other applications in fabricating practices, particularly in ceramic parts of mechanical equipment in which metal cannot stand the high temperatures, abrasion and corrosive conditions involved.

More and more alumina is being required in the production of high-temperature refractories. Substantial amounts of alumina are used, not only in making large fused blocks and refractory brick, but also in the production of castable refractories for service at high temperatures.

As a refractory, ceramic alumina is also finding further application, as radomes, rocket nose-cones, jet-engine linings and orifices subjected to high temperatures, corrosion and erosion.

Alcoa Aluminas satisfy the requirements for the manufacture of the numerous ceramic, refractory and abrasive products now in demand. Alcoa Calcined Aluminas, Alcoa Tabular Aluminas, and Alcoa Low-Soda Aluminas are commercial products, readily available in several grades. The various properties and uses of each of these specific aluminas are covered in more detail in the following descriptions and tables.

A. Commercial Forms and Uses

Alcoa Series A Calcined Aluminas are prepared by sufficiently high-temperature calcination of Bayer process hydrate that the surface area created at low temperatures is largely destroyed. The particles are more or less firmly bonded aggregates of small ultimate crystallites (Figure 1) whose size, shape and rate of growth on subsequent heating must be controlled for many applications. They are made in a variety of grades. The principal use of Alumina A-1 is in the manufacture of fused alumina abrasives.

Smaller tonnages are used in enamel, porcelain and glass mixes, high-temperature refractories and as a constituent of the slag in alloy steel production. Alumina A-2 is more highly calcined. It has uniform fine particle size and low shrinkage on firing. It grinds readily. Alumina A-3 is a high-porosity alumina, whose shrinkage on heating is reasonably uniform and greater than A-2.

Their principal uses are in low-cost electrical insulators, electrical supports, kiln furniture for china and pottery, for improving the strength of refractories and refractory clays, and for the manufacture of abrasive products. Alumina A-5 is a specially calcined alumina having more sharply defined plate-shaped crystals. Aluminas A-10 and A-14 are low-soda aluminas prepared especially for high-grade ceramic shapes and for electrical insulators such as spark plugs (Figure 2) where alkalinity impairs dielectric properties. A-10 has more soda than A-14 but has less shrinkage on firing.

Smothers and Reynolds measured shrinkage, grain size and specific gravity of A-10 containing 1% additives after heating at 1300, 1400 and 1700°C. Bogoroditskii and Polyakova studied the dielectric properties of various crystal modifications of alumina. The low dielectric losses for corundum are explained by the ionic and electronic polarization in the crystals, whereas in the beta modifications structural polarization seems to predominate, owing to the loose lattice of the crystals. Variation in the dielectric properties of alumina ceramic materials is attributed to the formation of beta alumina during an oxidizing calcination. When calcined under reducing conditions, the beta modification is converted to the alpha, and the impurities are either volatilized or changed to a vitreous phase.

Austin found that the use of alumina in ceramic whiteware bodies improved their properties. Geller (1946) studied binary and ternary mixtures of alumina with other oxides and the use of these mixtures as porcelains.

Alcoa Tabular Alumina is massive sintered alumina that has been thoroughly shrunk and has coarse, well-developed alpha alumina crystals. The crystals bear no relation to the original trihydrate particles. The principal applications of Tabular Alumina T-60 include high-temperature refractories, bricks, glass tank blocks and burner tips, where the presence of some soda is not objectionable and where high density and low porosity are important. Tabular Alumina T-61, a grade with lower soda content, is used in large tonnage for the production of electrical insulators and low-porosity catalyst supports. Tabular Alumina T-71 has porosity in the range of 30-50%, and even higher porosities can be made.

Tabular Alumina Balls T-160 are rough and they may have spherical laminations, chips, cracks and other imperfections. They are not suitable for such dynamic uses as pebble heaters and grinding balls. Tabular Alumina Balls T-162 have a smooth surface and are suitable as catalyst reactor and desiccant bed supports or for ballast where exposed to high temperature or severe corrosive conditions. Possibility of catalyst contamination from these balls is very small because of their high chemical purity and inertness. They have reasonably good heat shock, mechanical shock and abrasion resistance. Tabular Alumina Balls T-164 (Figure 3) have a smooth surface and have excellent thermal and mechanical shock resistance as well as very good resistance to abrasion. They make excellent grinding balls. Commercial use of T-164 balls in pebble heaters where temperature cycles go from a high of approximately 2600°F to a low of about 400°F has demonstrated that there is an insignificant loss from spalling and a very low loss from abrasion.

B. Refractories

Refractories containing up to about 70% Al_2O_3 can be made from diaspore clay blended with flint or plastic clay (Harbison-Walker). There is, however, increasing interest in higher alumina refractories. Large tonnages of calcined bauxite or Alcoa Tabular Alumina are used to improve the properties of fireclay refractories. One important reason for the preference for high-alumina refractories is evident from the alumina-silica phase diagram (Figure 4). With less than 72% Al_2O_3, a eutectic liquid melting at 1595°C is en-

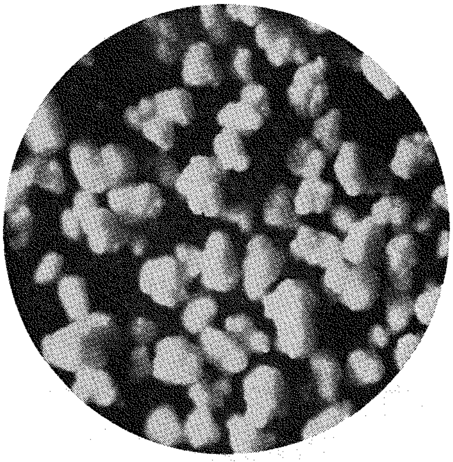

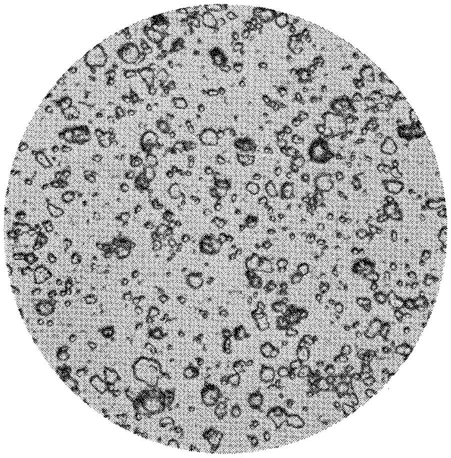

Left—Alumina A-2
Unground Grain
Magnification 75X

Right—Alumina A-2
Ultimate Crystals
Magnification 500X

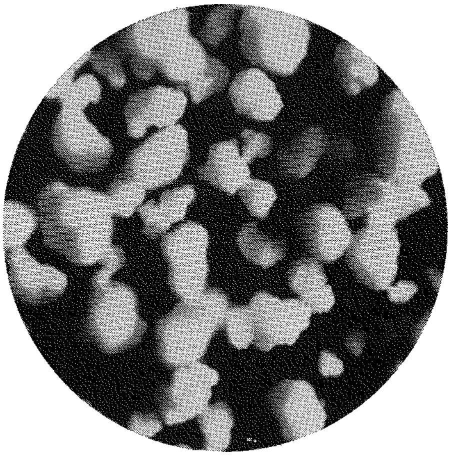

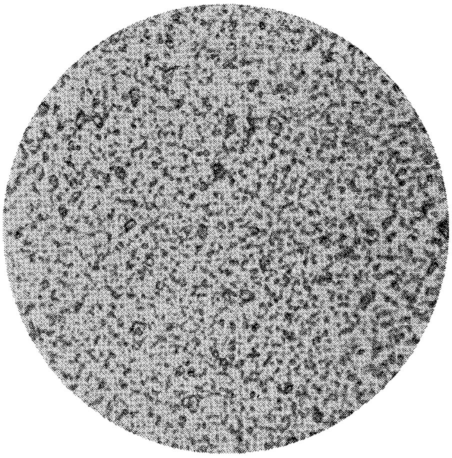

Left—Alumina A-3
Unground Grain
Magnification 75X

Right—Alumina A-3
Ultimate Crystals
Magnification 500X

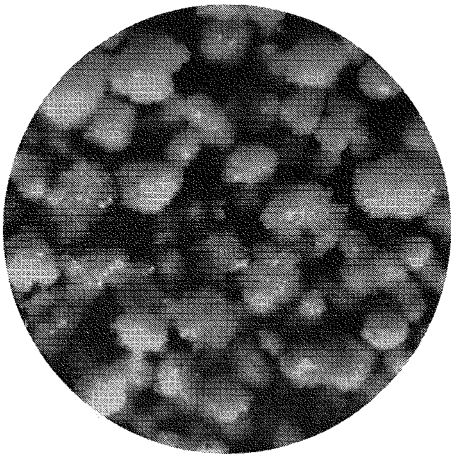

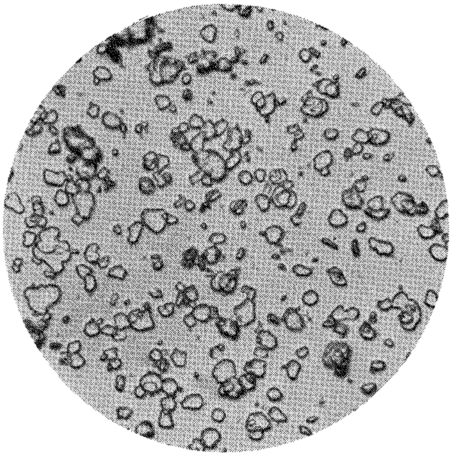

Left—Alumina A-5
Unground Grain
Magnification 75X

Right—Alumina A-5
Ultimate Crystals
Magnification 500X

Fig. 1—Micrographs of Particles and Ultimate Crystallites of Alcoa Calcined Aluminas

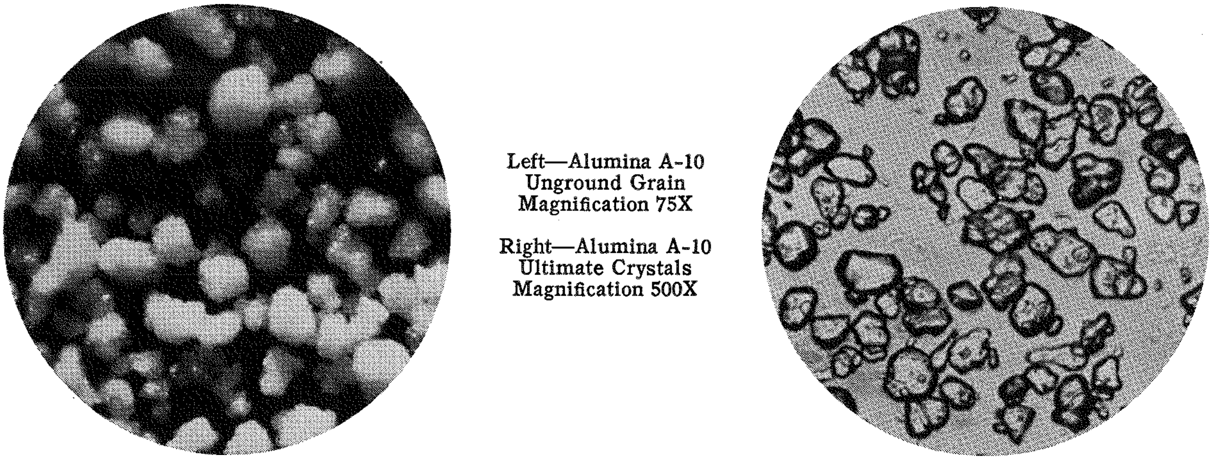

Left—Alumina A-10
Unground Grain
Magnification 75X

Right—Alumina A-10
Ultimate Crystals
Magnification 500X

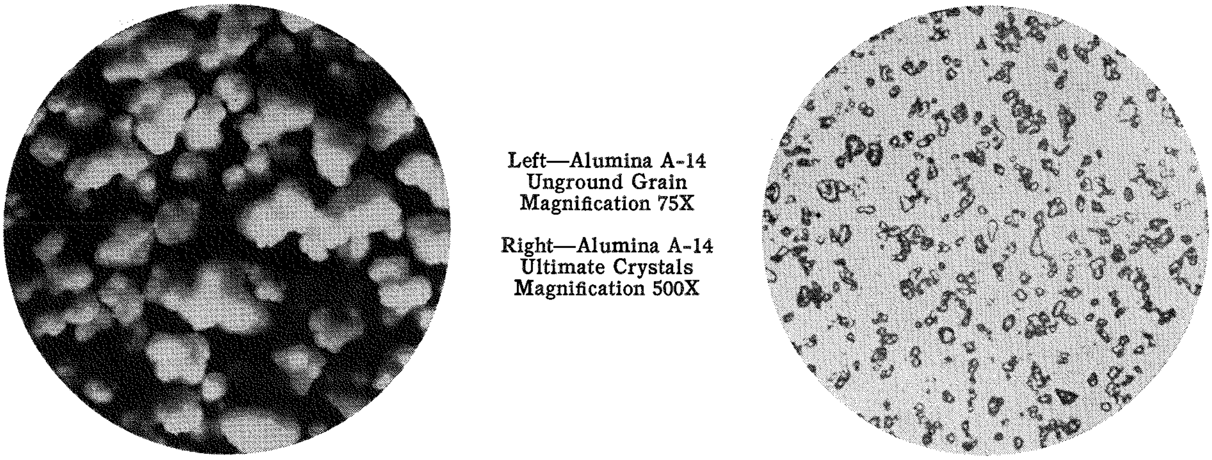

Left—Alumina A-14
Unground Grain
Magnification 75X

Right—Alumina A-14
Ultimate Crystals
Magnification 500X

W. H. Gitzen

Fig. 1 (Continued)—Micrographs of Particles and Ultimate Crystallites of Alcoa Calcined Aluminas

countered. Bayer alumina is used to produce synthetic mullite and also to increase the mullite content produced from natural mineral sources. In the higher alumina range, the lowest melting phase is at 1825°C, and the useful range of the refractory increases steadily as the alumina content is increased (Figure 5). Refractories of 90 to 99% Al_2O_3 are used where especially high temperatures are encountered, as in the burners of rapid-combustion furnaces (Chesters). Fused aluminas, as well as sintered and calcined, are used in refractories of this type. Solid blocks of alumina formed by casting the fused material with added soda (beta alumina) or chromic oxide find wide application in glass tank construction.

Castable refractories comprised of Alcoa Tabular Alumina bonded with a hydraulic-setting calcium aluminate cement or with phosphoric acid are receiving increased attention. Pure calcium aluminate cement produced from alumina extends the range of refractories beyond 1650°C. Calcined bauxite, Alcoa Tabular Alumina or other suitable refractory material may be used as the grog. Cal-Tab® is a high-quality castable refractory, made from Alcoa pure calcium aluminate cement with Alcoa Tabular Alumina as the grog. Refractory castables composed of sintered alumina bonded with phosphoric acid, Phos-Tab,®

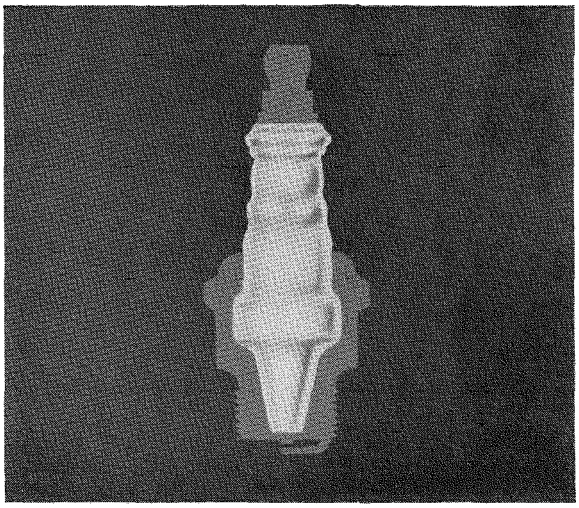

Fig. 2—Spark Plug Body

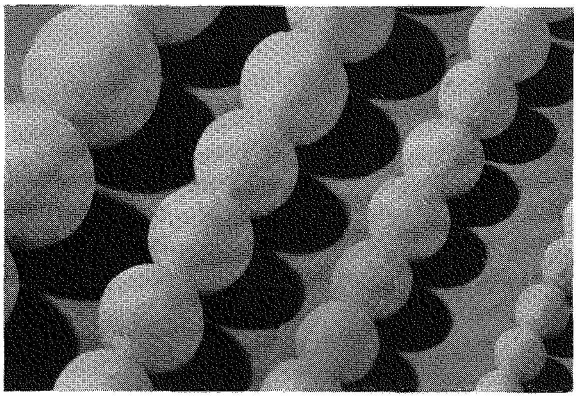

Fig. 3—Alcoa Tabular Alumina Balls

also have been developed (Gitzen). These castables are matured at 343°C and are characterized by high bond strength and remarkable erosion resistance over a wide temperature range.

Another type of refractory is made from alumina bubbles. Fused alumina is poured from the electric furnace so that the molten stream flows

TABLE 6

Magnetic Susceptibility of Aluminas

Units of 10^{-6}; Data of Selwood

Alpha	−0.23
Gamma-Type	−0.34
Alpha Monohydrate	−0.37
Alpha Trihydrate	−0.43
Beta Trihydrate	−0.46

See also Rao and Leela for more values on alpha alumina.

Pascal found partially dehydrated alpha trihydrate nearly identical with alpha alumina.

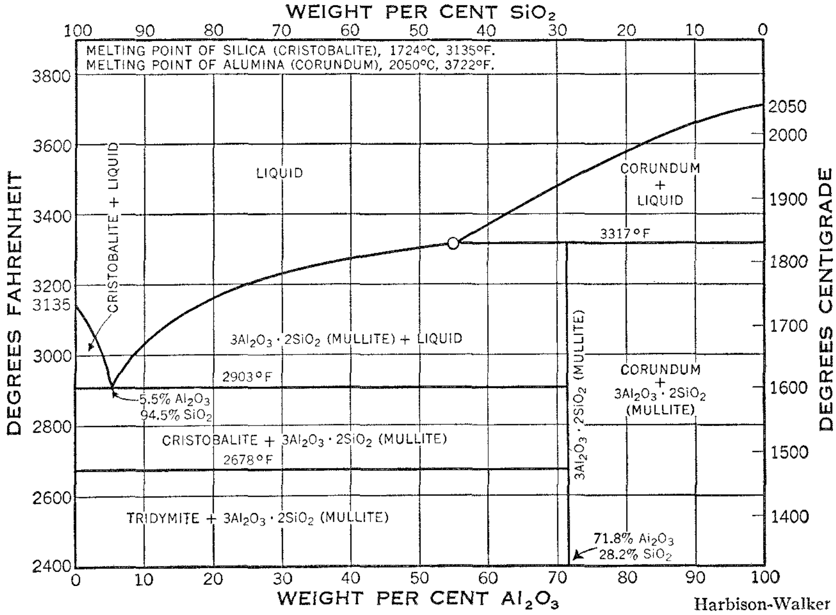

Harbison-Walker

Fig. 4—Alumina-Silica Phase Diagram by Bowen and Greig with Correction by Schairer. Partridge and Rooksby, Toropov and Galakhov, and Budnikov determined the congruent melting of mullite and showed a minimum in the liquidus line at 77.3% Al_2O_3.

past an air jet. The bubbles thus produced are bonded and pressed into lightweight bricks. The bubbles may be used to make an insulating castable refractory (Parché).

C. Abrasives

Advantage is taken of the extreme hardness of alpha alumina in many grinding, buffing and polishing operations. In general, fused alumina abrasive wheels are used for grinding materials of high tensile strength, and silicon carbide wheels are used on materials of low tensile strength. The fused alumina may be one of the following types: regular grain (2% TiO_2), high-titania grain (3% TiO_2), finely crystalline grain and pure white grain. Most grinding operations use the regular grain. The tougher, high-titania grain is used in wheels for heavy stock removal and in coated abrasive products. The finely crystalline type is used for lighter grinding. The more porous-

TABLE 7

Mechanical Properties of Alpha Alumina

25°C Unless Otherwise Noted

Property	Conditions	Values, psi	Alumina	Reference
Elastic Constants.....	C_{11}	$68.6\cdot10^6$	Corundum	Rao; Bhimasenachar
	C_{12}	$18.3\cdot10^6$	Corundum	Rao; Bhimasenachar
	C_{13}	$17.0\cdot10^6$	Corundum	Rao; Bhimasenachar
	C_{14}	$14.1\cdot10^6$	Corundum	Rao; Bhimasenachar
	C_{33}	$81.6\cdot10^6$	Corundum	Rao; Bhimasenachar
	C_{44}	$34.3\cdot10^6$	Corundum	Rao; Bhimasenachar
Young's Modulus......	....	$66\cdot10^6$	Corundum	Rao
	....	$49\cdot10^6$	Sintered	Ryshkewitch (1942)
	....	$74\cdot10^6$	Sapphire	Ryshkewitch (1942)
	....	$51\cdot10^6$	Sintered	Schwartz
	800°C	$48\cdot10^6$	Sintered	Schwartz
	1000°C	$37\cdot10^6$	Sintered	Ryshkewitch (1942)
	1300°C	$28\cdot10^6$	Sintered	Schwartz
	1500°C	$20\cdot10^6$	Sintered	Ryshkewitch (1942)
	30° to c-axis	$55\cdot10^6$	Sapphire	Seemann
	45° to c-axis	$51\cdot10^6$	Sapphire	Seemann
	60° to c-axis	$50\cdot10^6$	Sapphire	Seemann
	75° to c-axis	$56\cdot10^6$	Sapphire	Seemann
Compressive Strength.	....	240,000	Sintox	Singer and Thurnauer
	....	300,000	Sapphire	Seemann
	....	420,000	Sintered	Ryshkewitch (1941)
	1000°C	130,000	Sintered	Ryshkewitch (1941)
	1500°C	14,000	Sintered	Ryshkewitch (1941)
Tensile Strength......	....	21,000	Sintered	Schwartz
	20°C	37,400	Sintered	Ryshkewitch (1941)
	800°C	19,500	Sintered	Schwartz
	800°C	33,900	Sintered	Ryshkewitch (1941)
	1300°C	11,600	Sintered	Schwartz
	1300°C	6,400	Sintered	Ryshkewitch (1941)
	1400°C	7,300	Sintered	Schwartz
	1400°C	4,200	Sintered	Ryshkewitch (1941)
	1460°C	1,500	Sintered	Ryshkewitch (1941)
	1500°C	0	Sintered	Ryshkewitch (1941)
	30° to c-axis	100,000	Sapphire	Seemann
	45° to c-axis	78,000	Sapphire	Seemann
	60° to c-axis	65,000	Sapphire	Seemann
	75° to c-axis	94,000	Sapphire	Seemann

TABLE 7—(Continued)

Mechanical Properties of Alpha Alumina

25°C Unless Otherwise Noted

Property	Conditions			Values, psi	Alumina	Reference
Bending Strength	Plates			44,300-115,600⑤	Corundum	Klassen-Neklyudova
				24,000-36,000	RAE sintered⑦	Roberts and Watt
	1000°C			16,000-22,000	Sapphire	Roberts and Watt
	25°C			37,000① 28,000②	Sapphire	Roberts and Watt
	1000°C			43,000① 32,000②	Sapphire	Roberts and Watt
	Plane③	**Direction③**				
	24°	25°		43,000-131,000	Sapphire	Wachtman and Maxwell
	45°	46°		94,000-155,000	Sapphire	Wachtman and Maxwell
	51°	55°		17,000-50,000 (540°C)	Sapphire	Wachtman and Maxwell
Modulus of Rigidity				$27 \cdot 10^6$	Sapphire	
Poisson Constant	25-1000°C			0.32⑥	Sintered	Ryshkewitch
	1400°C			0.45⑥	Sintered	Ryshkewitch
Volume Change④				0.00355⑥	Sapphire	Bridgman
Impact Strength				43,000	Sintered	Moore
Torsion Strength	800°C			27,000	Sintered	Stavrolakis and Norton
	1000°C			24,000	Sintered	Stavrolakis and Norton
	1150°C			16,000	Sintered	Stavrolakis and Norton
	1300°C			11,000	Sintered	Stavrolakis and Norton
	1500°C			3,400	Sintered	Stavrolakis and Norton
	Temp.	**Tension, psi**	**Duration hr**			
Creep Strain	1300°C	....	...	Observable	Sintered	Stavrolakis and Norton
	1000°C	7,200	402	$< 10 \cdot 10^{-2}$%	RAE sintered⑧	Roberts and Watt
	1000°C	20,000	769	$1 \cdot 10^{-2}$%	RAE sintered⑨	Roberts and Watt
	1000°C	15,100	77	0.49%	Sapphire	Wachtman and Maxwell
	1000°C	12,000	431	1.52%	Sapphire	Wachtman and Maxwell
	1100°C	17,100	95	.08%	Sapphire	Wachtman and Maxwell
	1100°C	13,100	431	2.06%	Sapphire	Wachtman and Maxwell
	1200°C	12,100	53	0.7%	Sapphire	Wachtman and Maxwell
	1300°C	7,250	3	2.34%	Sapphire	Wachtman and Maxwell
	1300°C	8,620	44	32%	Sapphire	Wachtman and Maxwell

①Optic axis ⊥ length of test piece. Bent in plane of optic axis

②Optic axis ⊥ length of test piece. Bent ⊥ to plane of optic axis

③Four-point loading. Angle between rod axis and slip

④10,000 kg/cm^2 (142,200 psi)

⑤Heating 1500-1900°C followed by slow cooling increased strength

⑥No units

⑦Specific gravity 3.48—3.82

⑧Specific gravity 3.61

⑨Specific gravity 3.78

grained (from soda in the Bayer alumina) friable white type is desirable for a freer and cooler cutting action as in grinding hard, heat-sensitive, high-alloy tool steels (Parché). By petrographic techniques, Baumann showed high-titania alumina made from bauxite to be characterized by large crystalline areas of alpha alumina with slag-like inclusions of siliceous groundmass and numerous included microcrystals of titanium and aluminum compounds. The toughness of the abrasive grain was ascribed to this residual matrix. Yamaguchi and Tanabe said that Bayer process alumina calcined at 1100 to 1250°C mixed with fatty acid was a good metal-finishing abrasive. Cannon suggested the use, in a universal metallographic polishing method, of 0.3-micron alpha alumina and 0.03-micron gamma-type alumina.

Russell and Lewis emphasized the tremendous range of abrasive properties available with aluminas derived from the Bayer process and gave values for their abrasive action. Typical properties of Alcoa Calcined Aluminas and Alcoa Tabular Aluminas are shown in Table 11. Alcoa

TABLE 8

Mineralogical Properties of Aluminas

Phase	Index of Refraction n_d				Cleavage	Brittleness	Mohs Hardness	Luster	Reference
	α	β	γ	Average					
Alpha Trihydrate...	1.568	1.568	1.587	......	(001) Perfect	Tough	2½ to 3½	Pearly Vitreous	Dana
Beta Trihydrate...	......	......	......	1.583	......	....	....	....	Montoro
Alpha Monohydrate.	1.649	1.659④	1.665	......	(010)	....	3½ to 4	....	Ervin and Osborn Bonshtedt-Kupletskaya
Beta Monohydrate.	1.702	1.722	1.750	......	(010)③ Perfect	Brittle	6½ to 7	Brilliant Pearly	Dana
	ϵ	ω		Average					
Alpha①......	1.7604	1.7686		....	None③	Tough when compact	9②	Pearly Adamantine	Dana
Sodium Beta.	1.635–1.650	1.676		....	......	....	....	....	Rankin and Merwin
Magnesium Beta.........	1.629	1.665–1.680		....	......	....	....	....	Rankin and Merwin
Barium Beta.	1.694	1.702		....	......	....	....	....	Toropov
Lithium Zeta.	....	....		1.735	......	....	....	....	Kordes
Transition...	....	....		1.696	......	....	....	....	Hansen and Brownmiller
Eta.........	....	....		1.59–1.65	......	....	....	....	Thibon
Theta........	....	....		1.66–1.67	......	....	....	....	Thibon
Kappa........	....	....		1.67–1.69	......	....	....	....	Thibon
Iota.........	....	....		1.604	......	....	....	....	Foster, P.A.

①Chromatic Dispersion $\epsilon_{4861\text{Å}} - \epsilon_{6563\text{Å}} = \omega_{4861\text{Å}} - \omega_{6563\text{Å}} = 0.011$ (Seemann). N_o along optic axis $= 1.74453 + \dfrac{101.0\ \text{Å}}{\lambda - 1598\ \text{Å}}$ (Kebler) (3600–6600 Å)

②Knoop hardness 1525-2000 sapphire (Seemann)

③Conchoidal fracture

④Value in Ervin and Osborn is misprint

Tabular Aluminas were as abrasive as fused alumina in air-jet abrasion tests, but certain of the hydrates and partially calcined aluminas were essentially nonabrasive.

D. Sintered Ware

Fully sintered alumina is characterized by considerable chemical inertness (Table 9). Concentrated H_2SO_4, HCl, HNO_3, H_3PO_4 and 20% NaOH at their boiling points did not dissolve more than 0.02% of a 30 x 35 mm crucible in a six-hour treatment. Forty per cent hydrofluoric acid caused a weight loss of 0.08% (Winzer).

A comprehensive investigation by Jaeger and Krasemann of the resistance of sintered alumina crucibles (Degussa) to corrosion greatly extended the earlier work. Weight loss values from multiple tests were given in many instances. Alumina crucibles may be cleaned safely with sea sand, hydrochloric acid or chromic-sulfuric acid; pyrosulfate or 33% caustic must be used with care since some weight loss will occur. The crucibles lost little weight on successive heating. However, in many cases after treatment with acid (especially with 1:1 hydrochloric acid) the crucibles shattered or broke off lens-shaped pieces on subsequent heating. This was not prevented by long drying at 120°C, but it was avoided by "stabilized crucibles." Borax gave a special polishing action on the surface. The most aggressive melt was Na_2O followed by $Na_2S_2O_7$, Na_2O_2 and KOH, $Na_2CO_3 + KNO_3$, $Na_2CO_3 + S$, NaOH, Na_2CO_3, K_2CO_3 and $NaKCO_3$. The results on ashing precipitates were as follows:

No Adherence	Small Adherence	Strong Adherence
SiO_2	Fe_2O_3	MnS
Al_2O_3	Cr_2O_3	CuS
$BaSO_4$	$CaSO_4$	$Mg_2P_2O_7$
CaO		
BeO		
SnO_2		
ZnO		
Graphite		

Alumina laboratory ware with excellent resistance to chemical reagents is now being marketed. Alumina can be freed of gas only by heating in a vacuum system at temperatures over 1000°C. Highly sintered laboratory ware is vacuum tight (Stott 1938).

Alumina filters can be made by partial sintering of alumina (Deadmore) and extraction thimbles are commercially available. Ryschkewitch (1939) pointed out that a capillary hole in alumina retains its original dimensions after firing. Porous media for filters and diffusers are made from ceramic-bonded, fused alumina granules (Parché).

Uses of high-alumina (80 to 95% Al_2O_3) bodies, employed for their electrical properties, include insulators, printed circuit bases, condenser shafts, capacitor and resistor cores, vacuum tube spacers and radomes. Use is made of their mechanical and chemical properties in many wear-resistant parts, such as pump liners, ball mill liners, bearings, high-density grinding balls, agitators exposed to chemical action and cutting tools. Their high-temperature mechanical properties are utilized in jet engines, rocket nozzles, recoilless rifles, brake liners for aircraft, thermocouple and pyrometer tubes and in many furnace and burner applications.

All ceramic forming processes can be applied to alumina. These include plastic extruding, dry

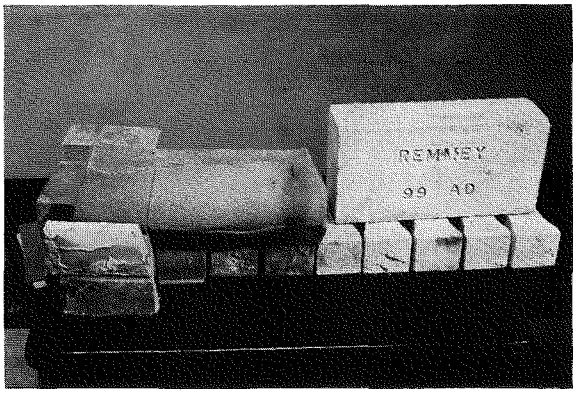

G. B. Remmey American Ceramic Society

Fig. 5—Photograph Showing 91% Alumina Resting on 99% Alumina Brick and 99% Alumina Sample on the Right After Heating Five Minutes at 1927°C (3500°F)

TABLE 9

Resistance of Sintered Alumina to Attack by Oxides and Elements

Oxide	Results	Reference
Alkaline oxides	No effect	Singer and Thurnauer
Beryllium oxide	Reacts with alumina at 1900°C	Jaeger and Krasemann
Carbon dioxide	No attack	Singer and Thurnauer
Iron oxide	Attack	Singer and Thurnauer
Lead oxide	Attack	Singer and Thurnauer
Magnesium oxide	Forms spinel with alumina over 1700°C	Jaeger and Krasemann
Manganese oxide	Attack	Singer and Thurnauer
Potassium hydroxide	Less aggressive than sodium oxide	Jaeger and Krasemann
Silicates	Some are harmful, many glasses can be melted in alumina	Singer and Thurnauer
Sodium oxide	Aggressive attack when heated by Bunsen burner but can be handled in alumina at 1350°C	Jaeger and Krasemann
Steam	No attack after 24 hours at 150 atmospheres	Singer and Thurnauer
Thorium oxide	Reacts with alumina at 1900°C	Jaeger and Krasemann
Tungsten anhydride	Attack	Singer and Thurnauer
Uranium oxide	Reacts with alumina at 450°C	Gmelin, Al [B] 97
Zirconium oxide	Can employ alumina underplate at 1900°C	Jaeger and Krasemann

Element	Results	Reference
Alkalis	Resistant to melts	Singer and Thurnauer
Aluminum	Forms Al_2O at 1100°C; AlO at 1600°C	Hoch and Johnston
Antimony	No attack	Jaeger and Krasemann
Beryllium	Inert to 1600°C	Economos
Bismuth	Resistant to 1400°C	Reed
Calcium, Strontium, Barium	Inert to boiling points	Jaeger and Krasemann
Carbon	Reduction above 1700°C	Jaeger and Krasemann
Chlorine	No attack at high temperatures except with carbon present	Singer and Thurnauer
Chromium	Wetting at 1650°C in reducing atmosphere	Blackburn
Fluorine	Attack at 1700°C	Winzer
Gallium	Inert to 1000°C	Kelman
Hydrogen	Darkens on heating. Not reduced at melting point	Jaeger and Krasemann
Iron, Cobalt, Nickel	Can be melted in alumina in hydrogen atmosphere Wet alumina at 1600°C in air	Jaeger and Krasemann Blackburn
Lead	No reaction at melting point	Kelman
Lithium	Reacts with molten melt. Poor resistance at 600°C	Winzer; Kelman
Magnesium	No attack on alumina at melting point	Jaeger and Krasemann
Manganese	Prepared at high purity by vacuum distillation from alumina	Jaeger and Krasemann
Mercury	No reaction at 300°C	Kelman
Molybdenum, Tungsten	No reaction with molten alumina. Alumina used to support molybdenum heating wires becomes gray	Jaeger and Krasemann
Nitrogen	No attack	Jaeger and Krasemann
Palladium	Can be melted in alumina in air. Attack at 1200°C in hydrogen	Jaeger and Krasemann
Phosphorus, Arsenic	No attack even at moderately high temperature	Jaeger and Krasemann
Platinum	Can be melted in alumina	Jaeger and Krasemann

TABLE 9—(Continued)

Element	Results	Reference
Silicon	Melts react	Jaeger and Krasemann
Sodium	Resistant at 900°C	Reed
Sodium-Potassium	Resistant at 500°C. Attack at 600°C	Kelman
Sulfur, Selenium	No attack	Jaeger and Krasemann
Thorium	No reaction	Jaeger and Krasemann
Tin	No reaction at 1000°C	Reed
Titanium, Zirconium	React at 1400°C. No reaction with titanium in vacuum or reducing atmospheres to 1500°C	Economos
Uranium	No reaction to 1200°C	Jaeger and Krasemann

and semi-dry pressing, plastic molding and slip casting. Conventional organic binders and plasticizers as well as thermoplastic and thermosetting resins are employed in extruding, pressing and molding processes. Blackburn dry pressed alumina tile at 5000 psi from -325 mesh Alcoa Tabular Alumina T-61 using 5% of a water solution containing 1% polyvinyl alcohol as a temporary binder. The tile was sintered at 1316°C and fired one hour at 1982°C. Directions for slip casting and firing alumina laboratory ware were published by Hauth, Watt, Roberts, Carruthers, Scott, Stott, Thompson and Mallett, and Yamauchi and Kondo. Lecuir suggested that sintering was improved by coating the pure oxide grains with an organic material such as urea. Casting slips are made by suspending enough very finely ground alumina to give a specific gravity of 3.0 in hydrochloric acid solution (pH 3) or a basic solution (pH 12), but casting slips near neutral pH are also feasible. Alumina can be ball milled dry or in aqueous media. The slip is poured into a plaster of paris mold where it gradually solidifies as the water is absorbed. The bodies are then dried and fired. They can be given a final shaping if necessary after drying or after heating at about 1000°C. Ernst and Wartenberg reported that crystallites in sintered alumina articles have their c-axes perpendicular to the surface.

Normally, the first stage in making sintered ware is to grind the alumina substantially to complete disintegration of the grain into ultimate crystals. Carruthers and Gill showed that alumina derived from alpha trihydrate calcined at 1200°C broke down by attrition of loosely bound crystallites from the surface. For higher calcination temperatures, the crystallites appeared to be larger and more firmly held together and crushing became the important mechanism. The packing density of the calcined hydrates increased over the first few hours grinding, but in some cases diminished again as grinding was prolonged. Aluminas derived by calcining commercial alpha monohydrate increased in packed density more rapidly than did those from alpha trihydrate and did not cake so readily during milling.

General Electric Research Laboratories developed a polycrystalline alumina ceramic called Lucalox. This ceramic withstands heat better than quartz and, unlike ordinary ceramic, is very translucent. This material is stable up to 3600°F. Production of Lucalox calls for extremely fine-grain, high-purity Al_2O_3; and during processing all of the pores must be eliminated.

E. Sapphires

Transparent, water-white alpha alumina single crystals are called sapphires. Additions of up to 8 mol per cent Cr_2O_3 produce a pink to deep red color, changing to green with more Cr_2O_3. At 8 mol per cent Cr_2O_3, isolated Cr^3 ions contact neighboring Cr^3 ions in the alumina lattice and cause abrupt changes of properties (Thilo). Shubnikov discussed the influence of impurities on properties of synthetic corundum crystals. Crystals containing small amounts of iron oxides and

TABLE 10

Infrared Spectra of Aluminas

microns

Phase	OH-Stretch	OH-Bend	Unassigned	Al-O Stretch	Reference
Alpha Trihydrate....	2.765(m), 2.842(s), 2.917(vs), 2.960(m), 2.975(s)	9.85(vs), 10.37(m)	11.0(w), 12.1* 12.58(s)	13.48(s)	Frederickson Hannah
Beta Trihydrate.....	2.830(m), 2.842(m), 2.895(m), 2.940(m)	9.84(s), 10.25(s)	11.6(m), 12.3(m)* 13.9(m)*	12.88(s)	Frederickson Hannah
Alpha Monohydrate..	3.065(s), 3.247(s)	8.75(m), 9.35(s)		13.5(s)	Frederickson Hannah
Beta Monohydrate...	3.42(vs), 4.27(m), 4.73(m), 5.04(m)	9.35(s), 10.42(s)		13.89(vs)	Cabannes-Ott
Alpha Alumina......			15.58(m), 16.61(s) 17.89(m), 20.41(w) 22.21(s)	13.16(vs)	Hannah Kolesova
Alumina "Gel"......		8.5, 8.3, 9.8	6.9, 7.7 10.7, 12.3	13.5	Imelik (1954)
Anodic Oxide........	4.15	8.4-8.7	10.2-10.6		Fichter

m=Medium intensity s=Strong vs=Very strong *=Shoulder w=Weak

titania are generally known as blue sapphires. By adding less than 1% titania, a star effect emerges (Figure 6) by precipitation of fine needles along prominent crystallographic planes of the crystal during heat treatment of the boule at 1100 to 1500°C. Cutting and polishing *en cabachon* (dome shaped) with the c-axis of the crystal normal to the flat base of the stone is required. Disks up to 5-in. diameter and rods up to 0.29-in. diameter are produced commercially by Linde Company employing a modified Verneuil flame process with high-purity ammonium alum powder as the starting material. Splitting along a principal plane or annealing the boules at 1950°C relieves strain and permits them to be sawed and drilled without fracturing. The rod can be bent into a helix and flame polished. Industrial uses include bearings, precision gages, guides, styli, ball points for pens, orifices, optical parts and electrical insulators. The synthetic materials sell for about 1¢ per carat (Seemann).

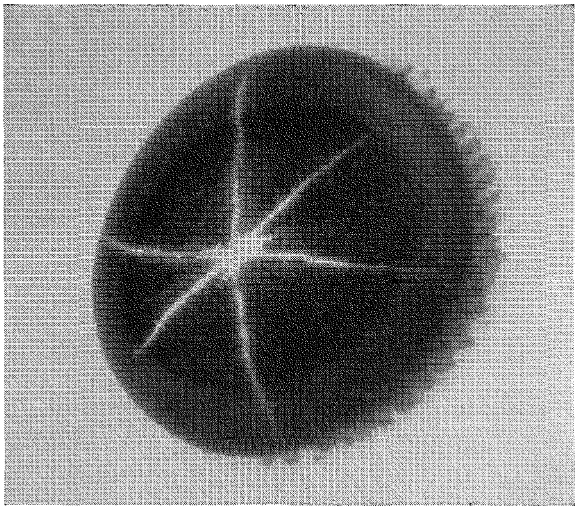

Fig. 6—Linde Synthetic Star Sapphire

TRANSITION ALUMINAS

Transition aluminas are encountered in the moderate calcination of some aluminum compounds, alumina hydrates (with the exception

TABLE 11

Typical Properties of Calcined and Tabular Aluminas

Chemical Analysis, %	Calcined Aluminas①					
	A-1②	A-2	A-3	A-5	A-10	A-14
Al_2O_3	99	99	99	99	99.5	99.6
Na_2O	0.50	0.50	0.50	0.50	0.10	0.04
Fe_2O_3	0.04	0.04	0.04	0.04	0.04	0.04
SiO_2	0.025	0.025	0.025	0.025	0.05	0.06
Loss on Ignition 1100°C	0.75	0.30	0.50	0.30	0.15	0.15
Water Adsorbed at 50% Humidity	1.25	0.10	1.00	0.10	0.10	0.10
Alpha Alumina Content, %	....	+90	80	+90	+95	+95
Physical Properties						
Bulk Density, Packed, lb/ft³	68	68	68	63	80	83
Bulk Density, Loose, lb/ft³	55	52	55	48	60	63
Specific Gravity	~3.7	3.7-3.9	3.6-3.8	3.7-3.9	3.8-3.9	3.8-3.9
Ultimate Particle Diameter, microns	....	<5	0.8	5-15	4-15	2-5
Ultimate Particle Thickness, microns	....	<0.5	0.2	1	2	1
Surface Area, m²/g	20-70	0.4	5	0.4	0.1	0.2
Pore Volume, ml/g	~0.25	0.25	....	0.26	0.12	....
Pore Diameter, Å	~1,000	15,000	....	20,000	15,000	....
Shrinkage in 1 hr at 1800°C, %	~22	16-18	20-22	16-18	14-16	16-18

①Screen Analysis, %: +100 mesh=2-6; +200 mesh=50-70; +325 mesh=88-96; −325 mesh=4-12
②Specifications permit wide tolerance in physical properties

of beta alumina monohydrate), in the hydrolysis of amalgamated aluminum and aluminum alcoholates, and in the oxidation of aluminum. None of these has been identified in nature or in hydrothermal equilibrium experiments. The X-ray patterns are in some cases diffuse and similar. The morphology of the crystals is strongly influenced by the starting materials. For these reasons, many workers (e.g., Ginsberg, Hüttig, Strunk-Lichtenberg) have considered these phases to represent increasing degrees of crystallinity or various orientations of the crystallites.

There is increasing warrant from other investigations for designating distinct phases in the dehydration sequences of the alumina hydrates. Foster and Stumpf noted that the end product of the gallia transition sequence was isomorphous with theta alumina. Roy (1953) identified a gallia phase which was isomorphous with kappa alumina and formed a complete series of solid solutions with it. These workers established a similar series of solid solutions between theta alumina and a gallia isomorph. Kohn established theta alumina as a distinct polymorph of alumina. Caglioti and D'Agostino produced a transition alumina by blowing a stream of air rapidly through molten aluminum. Eta alumina is formed from the oxidation of aluminum at temperatures near the aluminum melting point (Hunter and Fowle), as well as in electrolytic oxidation of aluminum under some conditions. Kimberlin and Gladrow prepared eta alumina by hydrolyzing aluminum alcoholates followed by 20 to 65 hours aging. The beta trihydrate thus obtained was heated at 650-1200°F to produce eta alumina. Following the indications of Burgers, and Gorbunova and Vaganova, Stumpf and Russell (unpublished) identified transition aluminas on

TABLE 11—(Continued)

Typical Properties of Calcined and Tabular Aluminas

Chemical Analysis, %	Tabular Aluminas①②		
	T-60	T-61	T-71
Al_2O_3	99.5+	99.5+	99.5+
Na_2O	0.13	0.02	0.03
Fe_2O_3	0.03	0.03	0.03
SiO_2	0.02	0.02	0.02
Loss on Ignition 1100°C	0.0	0.0	0.0
Water Adsorbed at 50% Humidity	0.0	0.0	0.0
Alpha Alumina Content, %	100	100	100
Physical Properties			
Bulk Density, Packed, lb/ft^3	120-140③	120-140③	85
Bulk Density, Loose, lb/ft^3	....	....	76
Specific Gravity	4.0	4.0	4.0
Surface Area, m^2/g	....	0.04	0.5
Pore Volume, ml/g	0.015	0.015	0.10-0.20
Shrinkage in 1 hr at 1800°C, %	< 10	< 10	....

①T-160 is selected imperfect cylinders, usually between ½ in. and ⅞ in. T-162 is a ball form available in nominal sizes of ¼ in., ⅜ in., ¼ in. and ¾ in. diameter. T-164 balls have a smooth surface and excellent resistance to thermal and mechanical shock as well as very good resistance to abrasion. They are available in nominal sizes of ¼ in. and ⅜ in. diameter.

②Standard Sizes: ½ in. to ¼ in.; ¼ in. to 8 mesh; 8 to 14 mesh; 14 to 28 mesh; imperfect cylinders 1 in. dia x ⅝ in.

③Minus ½ in. = 120 lb/ft^3; minus 14 mesh = 135 lb/ft^3; minus 325 mesh = 140 lb/ft^3

heating ammonium alum. Rooksby (correspondence, 1950) noted kappa alumina in the thermal decomposition of hydrated aluminum chloride. Fricke and Jockers found gamma type alumina upon heating $AlCl_3 \cdot 6H_2O$.

Two X-ray patterns for delta alumina are given in Table 3. Until the situation is clarified, a choice cannot be made as to which is the better pattern. The Alcoa pattern is from products of calcination of pure alpha monohydrate in air or steam for a few hours. Rooksby obtained a better crystallized delta with slightly different X-ray pattern by calcination of hydrates for long times or by addition of a mineralizer. Rooymans showed that Rooksby's delta has a tetragonal cell of axial ratio 2.94:1, analogous with the cell of gamma ferric oxide (van Oosterhout and Rooymans), for which the axial ratio is 3:1. Saalfeld, and Brindley and Nakahira, also referred to the tetragonal distortion exhibited by aluminas from dehydration of alpha trihydrate and alpha monohydrate.

A fused alumina-aluminum nitride mixture, analyzing 0.34% N, yielded a pattern similar to that of the Rooksby delta (Foster, Long and Stumpf, unpublished). Delta alumina has also been obtained by combustion of aluminum in air or oxygen, and of aluminum carbide in oxygen (Foster (1956), Wartenberg (1952), Schneider and Gattow). Plummer found that gamma or alpha alumina passed through an oxyhydrogen flame formed well-developed crystals of delta and theta alumina, providing the final particles were less than 15-μ spheres. Larger particles were alpha alumina. Thus, extremely rapid solidification of molten pure alumina, and possibly contamination by nitrogen or carbon, stabilize delta alumina.

Patterns by H. C. Stumpf

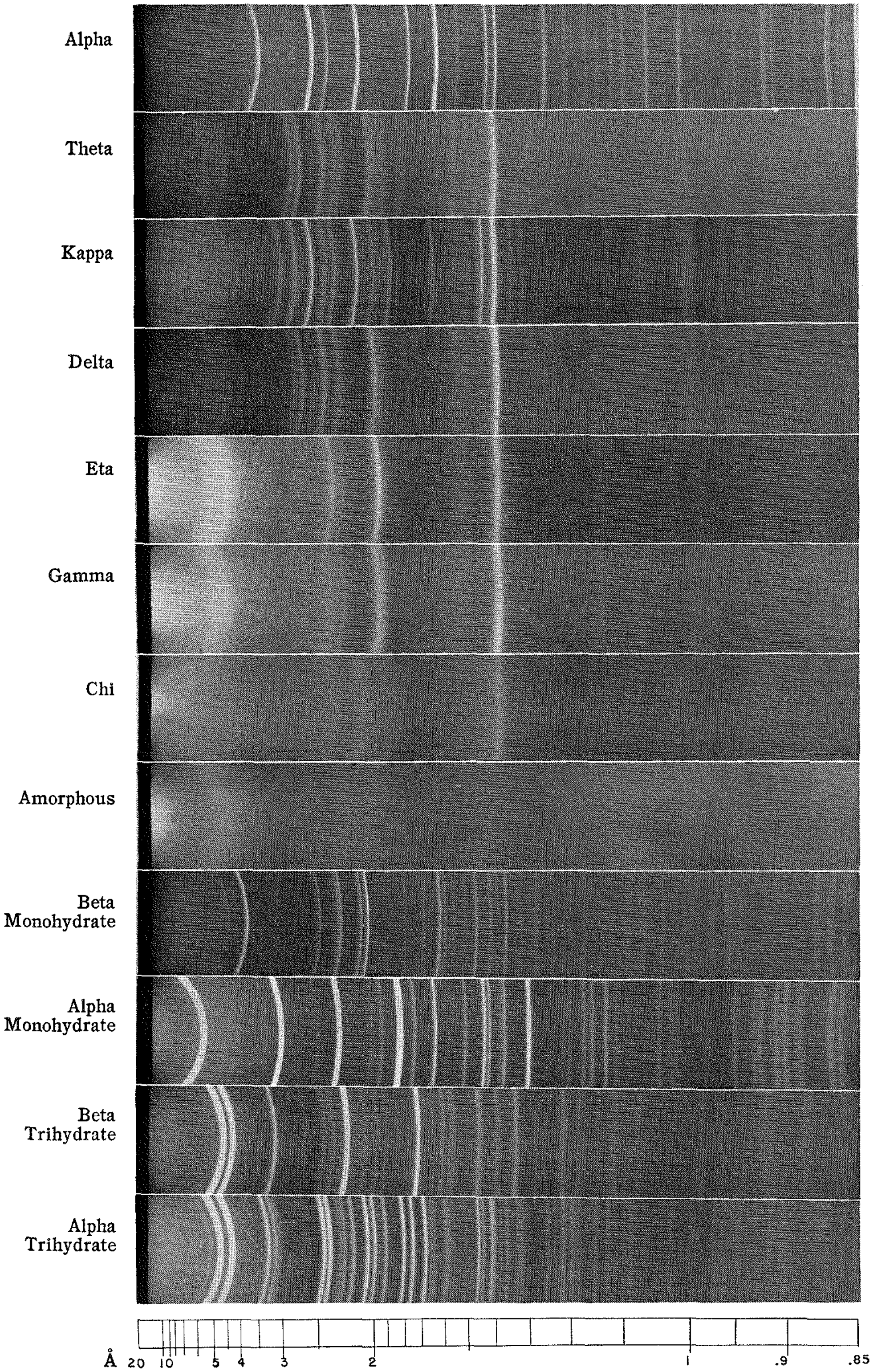

Fig. 7—X-ray Powder Diffraction Patterns of Alumina Phases

Note: See Table 3, page 12, for d-Values and intensities.

Teichner (1959) has prepared nonporous spheres of delta alumina in an oxyhydrogen flame. Their essential characteristic is uniformity of diameter. This is controlled from 100 Å to 1500 Å by the quantity of chloride and flame temperature. The 100 Å particles did not lose oxygen appreciably on evacuation at 500°C, but they became black, oxygen-deficient, nonstoichiometric n-type semiconductors under pressures of 1 to 5 tons per square inch.

Foster (1959) reported a new phase of anhydrous alumina having an X-ray pattern very similar to that of the aluminum silicate, mullite. This material, now designated iota alumina, formed during very rapid quenching of cryolite-alumina, melts and appears to be the only alumina phase formed in this procedure. Slow cooling gave corundum as the only equilibrium phase. This new mullite-like phase is metastable and transformed through eta alumina to alpha alumina on heating.

The principal alumina phases increase in crystallinity as follows: amorphous; rho, chi and eta; gamma; theta, kappa and delta; alpha. Pure rho, chi and kappa can be prepared from fine alpha trihydrate; eta and theta from fine beta trihydrate; gamma and delta from alpha monohydrate. Tertian and Papée (1955) prepared all of the phases by suitable dehydration and rehydration treatments starting with a single sample of fine-particle alpha trihydrate. Papée, Tertian and Biais (1958) have published X-ray data for pseudoböhmite. X-ray powder diffraction values for gamma and eta alumina have been obtained also by Biegler (1957).

Verwey deduced that the unit cell of spinel structure alumina contains only $21\frac{1}{3}$ aluminum ions, distributed over the 24 cation sites, with the $2\frac{2}{3}$ vacancies on the octahedral position, and having the formula $Al_8[Al_{13\frac{1}{3}}\square_{2\frac{2}{3}}]O_{32}$. The crystals of the spinel-structure alumina specimen (with a very small percentage of Li_2O) prepared by Kordes give the same superstructure reflections as the spinel $LiAl_5O_8$ or $Al_8\,[Al_{12}Li_4]\,O_{32}$, with the Li-ions on definite octahedral sites (Braun 1952). These superstructure lines have led also to suggestions about a hydrogen-aluminum-spinel $Al_8\,[Al_{12}H_4]\,O_{32}$ (De Boer and Houben). The great number of extra reflections mentioned by Kordes, and ascribed by him to beta radiation and impurities, were suggested by Rooymans (1959) to be indications of the same superstructure as found in gamma Fe_2O_3 (van Oosterhout and Rooymans, 1958).

Extra spots and line segments observed in single-crystal electron-diffraction patterns of eta alumina were interpreted by Cowley in terms of faults in the cubic close packing of the oxygen atoms. The vacant aluminum sites in eta alumina were suggested as occurring preferentially at unfavorable positions along fault planes, where they would be nearer than usual to other aluminum sites.

Ervin pointed out that the X-ray powder diffraction patterns of transition aluminas have in common one strong line at 1.39 Å, which corresponds to the oxygen ion radius and is indexed as the $\{440\}$ line for the spinel unit cell. Planes giving rise to this reflection have the unique property of passing through the centers of all the anions and the possible cation positions for anions in cubic close packing. By inference, therefore, all of these structures have oxygen ions in nearly cubic close packing and aluminum ions in the interstices. The $\{400\}$ line of the spinel pattern at about 1.99 Å comes from planes through all the anion positions and the octahedral cation positions. Its intensity is affected only by the relative distribution of cations between these two types of positions. On this basis, the varying degree of aluminum ion order within an unchanging oxygen ion network is responsible for the multiplicity of transition aluminas. Fricke and Eberspächer suggested that these aluminas are built up of single crystals (possibly octahedra because in some cases the particle size calculated from wide angle scattering with the $\{440\}$ interference is 1.4 times that from the $\{400\}$ interference) arranged like a fluid, although areas of secondary arrangement may exist.

Ginsberg noted that the transition aluminas at 500-800°C had broad X-ray lines, although electron microscopy showed well-developed 5- to 0.25-μ rhombic plates having the habit of alpha monohydrate. He therefore assumed lattice disturbance as the cause of the broadening. This viewpoint is strengthened by the fact that the line intensities never reached those of the well-ordered alpha alumina. For samples of transition aluminas, consisting by electron microscopy of 2-μ aggregates of 200-Å crystallites, the X ray, which penetrates deeply into the specimens, showed chi or gamma where electron diffraction showed a surface coating of eta alumina.

König reported that the lattice constant of aluminas formed on aluminum varied from 7.73 to 8.06 Å, although all alumina films that were in contact with aluminum at 800°C gave a constant of 7.89 Å ± 0.01, regardless of their previous history. Alumina films heated in oxygen had the highest value, and the lowest came from heating the films in vacuo.

The oxide formed on aluminum at low temperatures is amorphous and, according to Hass, became crystalline at 500°C in contact with aluminum, but separated layers of oxide did not crystallize below 680°C. Mahl reported the oxide formed in air at 500 to 600°C to be scaly crystallites oriented on the $\{111\}$ and $\{110\}$ planes.

According to Taylor (1945) the oxide from electrolytic oxidation of aluminum was structureless if the formation voltage was less than 100, and was eta at higher formation voltages. Burnham and Robinson, on subjecting high-purity aluminum to high voltages in boric, citric and tartaric acids, produced nonporous, platelike microcrystals of gamma-type alumina with hexagonal symmetry. The boundaries of these microcrystals coincided with those of the original aluminum grains. Bergmann studied the electrolytic oxidation of aluminum in dilute aqueous hydrogen peroxide and carbon dioxide solutions in order to obtain high-purity aluminas. Using high-purity aluminum as cathode and platinum as anode, he observed the formation of predominantly amorphous products of the composition $Al_2O_3 \cdot 2.94H_2O$ to $Al_2O_3 \cdot 3.02H_2O$ containing varying amounts of beta alumina trihydrate (hydrogen peroxide series) and alpha alumina monohydrate-beta alumina trihydrate mixtures (carbon dioxide series), respectively. The most distinct X-ray powder diffraction patterns were obtained at bath temperatures of 20-60°C.

LeChatelier may have been the first to report that substantial heat is evolved on slow heating to 850°C of alumina prepared from nitrates and chlorides, but not for alumina from sodium aluminate. Heat evolution in this case can be induced by traces of volatile fluorides This finding has been substantiated by many workers (e.g., Avdalian). Parravano and Montoro noted the exothermic reaction on heating aluminum chloride hexahydrate, and Roth found that alumina, formed electrolytically in oxalic acid solution, evolved heat and became incandescent when heated to 1100°C.

Foster and Stumpf found two exothermic peaks on heating aluminum nitrate nonahydrate with 2% added ammonium fluoride to catalyze the phase transformations. The first, at 700°C, corresponded to an amorphous-gamma transition, while the second was gamma to alpha (no intervening phase). Theta alumina with ammonium fluoride gave a smaller peak at 1000°C as it transformed to alpha alumina.

Tran-Huu-The and Prettre have shown a change from absorption to the evolution of heat when alpha trihydrate from the Bayer process was slowly calcined past the point where the residual alumina had one-half mole of water. This temperature of 350°C is decidedly lower than that where the exothermal transformations have been recorded previously.

By continuous weighing in the furnace and thermographic methods, Komarov and Chernikova found that some hydroxides added to hydrated alumina during dehydration reduced the number of endothermic maxima, representing an evolution of water at the highest rate, and reduced the temperature intervals between the maxima. The specific surface of the impure hydrate and of the alumina obtained from it was always smaller than the specific surface of pure alumina.

Charrier (1953) and Papée (1954) reported that the product from vacuum heating of normal alpha trihydrate gave a well-characterized exothermic effect at a temperature (200 to 700°C) which decreased with increasing water content of the specimen. The exothermic effect connected with transformation of the rho alumina was accompanied by an increase in crystallinity and index of refraction and by a lessened tendency toward rehydration; chi-alumina containing products obtained under atmospheric pressure did not give the exothermic effect. The same difference was found between vacuum and air dehydration products of beta trihydrate. Finely divided alpha trihydrate heated under vacuum did not give the exothermic effect; this was assumed to be due to more progressive transformation and broadening of the thermal effects.

Thermoluminescence may be induced in most transition aluminas by a high gamma-ray exposure (Rieke). The total number of protons produced by gamma-rays increased as the degree of calcination increased. Peaks have been found at 103, 123, 164 and 235°C, the 123°C peak being the most characteristic. The peak at 235°C depends on sodium impurity (Rieke and Daniels). A blue-green luminescence can also be observed in unirradiated samples on heating. The emission occurred generally over a rather broad temperature range, starting at about 300°C and producing a broad peak in the vicinity of 350°C. When the samples were repeatedly heated and cooled in the dark after having been drained, no further emission occurred. However, exposing the samples to light at room temperature caused the glow to reappear on heating. Emission occurred for as long as 10 or 15 minutes. Water vapor quenched this luminescence.

Winter showed an initially rapid, first-order exchange of O^{18} between oxygen and transition alumina, the rate constant being about 0.001 min^{-1} at 500°C and the heat of activation 37 kcal/mole. This was followed by a slow reaction. Whalley and Winter observed a similar exchange for water vapor containing O^{18}. Karpacheva and Rozen determined the exchange of O^{18} between alumina and water vapor to attain 20, 30 and 50% equilibrium at 200°C, 400°C and 600°C, respectively. Winter, and Winter and Houghton found an activation energy between 27 and 30 kcal/mole for the exchange of O^{18} between oxygen gas and transition alumina. The initial first-order exchange was independent of oxygen pressure and was ascribed to surface oxygen ions; rate constants increased from 0.0067 to 0.0146 min^{-1} from 485 to 592°C, respectively. The heat of activation was 37.3 kcal/mole. A subsequent slow exchange was ascribed to less active parts of the surface, or diffusion of oxygen ions from the second layer to the surface. Karpacheva and Rozen found that alumina after exposure to water vapor containing O^{18} exchanged at 200 and 400°C with ethyl alcohol vapor. The rate curves were of the same shape, although dehydration of the ethyl alcohol occurred only at the higher of these temperatures. The exchange with alcohol was about one-third as fast as with water. The similarity of the kinetic curves suggested an identical mechanism.

Dontsova found the rate of exchange of O^{18} in CO_2 with alumina at 1100°C to be less than that with Fe_2O_3 and greater than that for SiO_2.

Fricke (1937) set the lower limit of the surface energy as 560 erg/cm². Fricke and Keefer gave pH = 8.00 as the isoelectric point.

Alumina as calcined for electrolytic reduction to aluminum may contain mixtures of kappa and theta, or theta and alpha phases. Chi and gamma aluminas (along with alpha monohydrate) are principal constituents of Alcoa Activated Aluminas.

STRUCTURE AND PHASE TRANSFORMATIONS

A. Heated Alpha Trihydrate

Granules of alpha trihydrate lose water on heating and recrystallize to higher density aluminas without shrinking appreciably. This process creates the porous structure of Alcoa Activated Alumina F. Sufficiently high temperatures collapse the structure and lead eventually to a dense sintered particle. Information is available from several techniques on the structures and transformations accompanying this heating.

The temperature for decomposition of alpha trihydrate depends on the pressure, particle size, atmosphere, impurities and heating rate. Figure 8 shows 140°C as the temperature for decomposition of alpha trihydrate to alpha monohydrate in room air, or in water under a pressure of 10,000 psi (680.5 atm).

Ginsberg (1957) reported conversion of alpha trihydrate to alpha monohydrate above 60°C in

170 g/l NaOH, and conversion detectable by X ray in a few hours in air at 105°C. Alpha monohydrate was observed by phase contrast microscopy at temperatures below the detection limit by X ray.

Blanchin reported decomposition of the trihydrate at 100°C in vacuum. Fricke and Severin found long heating at 165°C necessary for nearly complete transformation in air of finely ground alpha trihydrate to alpha monohydrate. For heating periods of one hour in air, the dehydration was slight below 200°C and well advanced by 250°C. Prettre, Blanchin and co-workers followed the equilibrium water content vs temperature for heating periods of twenty hours. Water content decreased uniformly in a 70°C interval from $Al_2O_3 \cdot 3H_2O$ at 100°C in vacuum (or 150°C at one atmosphere) to $Al_2O_3 \cdot \frac{1}{2}H_2O$, and there showed an 80°C arrest before the loss of water was again appreciable. Dehydration was essentially complete at 400°C in vacuum or 500°C at one atmosphere. The presence of a discontinuity at the composition $Al_2O_3 \cdot \frac{1}{2}H_2O$ is one manifestation of the interesting behavior in this system.

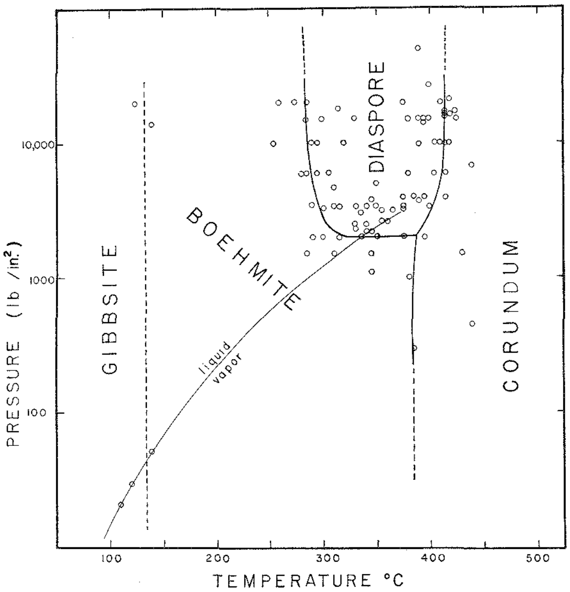

The University of Chicago Press

Fig. 8—Equilibrium diagram of Ervin and Osborn for the system Al_2O_3-H_2O. Circles refer to runs. Heavy lines delineate regions of stability of the crystalline phases. Light line is the vaporization curve for water; and, in view of the low solubility of alumina in water, this curve approximates the vaporization curve for solutions in this system. Parts of this diagram have been confirmed by Friedel. Less complete versions were given by Laubengayer and Weisz and by Cooke and Haresnape.

Thermal-dehydration curves, in relation to time and temperature, are shown for alpha trihydrate in Figures 9 and 10, and for beta trihydrate in Figures 11 and 12 (Alcoa Research Laboratories). De Boer has plotted a thermal-dehydration curve (Figure 13) for alpha trihydrate, showing the water content as a function of the heating temperature, and pointed out the three steps in which the three products, alpha monohydrate, chi alumina, and gamma alumina form. De Boer represents these steps even more clearly in Figure 14, which is a differential curve derived from Figure 13, and which is similar to the type of curve obtained by actual differential thermal analysis.

Eyraud, Goton and co-workers found that after a short induction period the rate of decomposition was constant at a given temperature to about $Al_2O_3 \cdot H_2O$ beyond which the rate diminished. For Bayer hydrate, particle diameter 50 microns, the rate of weight loss for a one-gram sample at 10^{-3} mm pressure increased from 0.13 mg/min at 188°C to 2.8 mg/min at 235°C. In the presence of 4.5 mm of water, the rate at 235°C was reduced to 1.3 mg/min, although it was still linear with time. From the plot of logarithm of the rates vs reciprocal of absolute temperature, an apparent energy of activation of 31 kcal/mole was deduced. This increased rapidly in the presence of water. The constant decomposition rate at a fixed temperature (zero order reaction) resulted from the laminar structure of the trihydrate by which succeeding layers could react uninfluenced by the reaction products of outer layers.

These workers also measured the electrical energy required for the dehydration at a fixed heating rate of 4.5°C/min. The following heat effects occurred: an endothermicity with a maximum at 240°C, a much greater endothermicity with a maximum at 327°C, a slight exothermic effect between 350-400°C and a final small endothermic effect with a maximum at 500°C. Adding all these led to a heat requirement for the dehy-

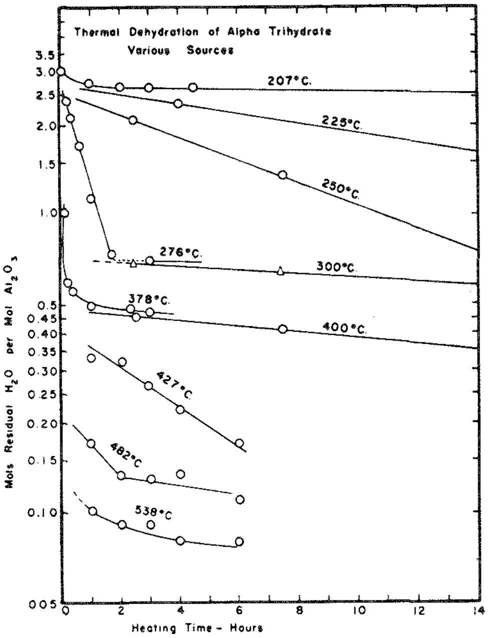

Fig. 9

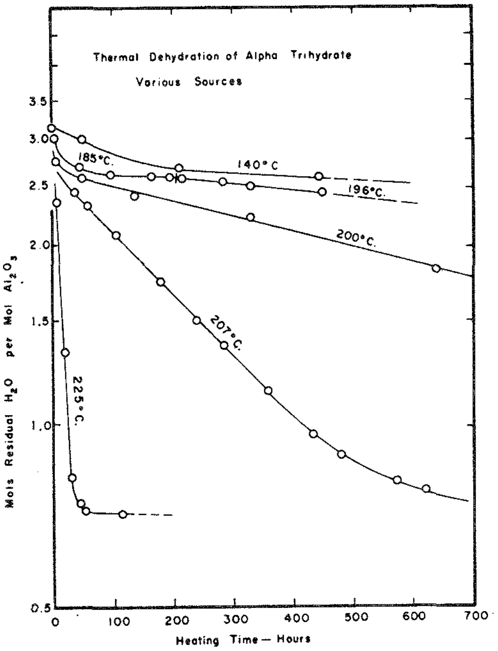

Fig. 10

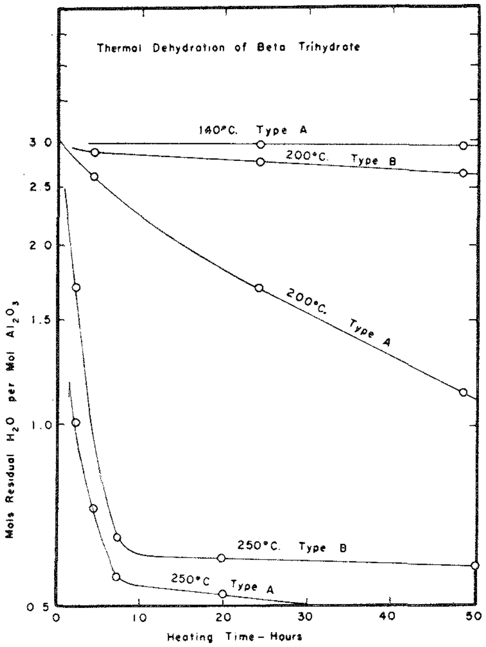

Fig. 11

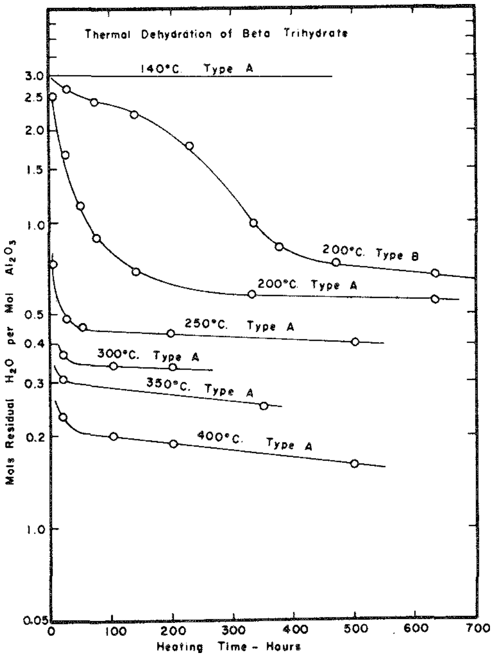

Fig. 12

Thermal Dehydration of Alumina Trihydrate in Relation to Time and Temperature. (Type A beta trihydrate was obtained by treating sodium aluminate solution with carbon dioxide at 25-30°C. Type B was prepared by reaction of an aluminum-mercury couple with water at room temperature.)

dration of 73.7 kcal/mole. By combining the measurements of weight loss and energy absorption in a single apparatus they determined the energy required for each step of the dehydration. The initial dehydration to $Al_2O_3 \cdot 2.8\,H_2O$ required 3.5 kcal/g H_2O removed. This fell abruptly to 0.9 kcal/g H_2O and then recovered to a constant value of 1.1 kcal/g H_2O over the entire range $Al_2O_3 \cdot 2.7H_2O$ to $Al_2O_3 \cdot 0.5H_2O$ beyond which the value increased to about 2.0 kcal/g H_2O. When the energy input was stopped with a sample at 230°C dehydrated to $Al_2O_3 \cdot 2.9H_2O$, the loss of weight continued, to a final composition $Al_2O_3 \cdot 2.5H_2O$. These results were interpreted to mean that the initial dehydration required a great deal of energy which was offset in large measure after the initial step by a compensating simultaneous exothermic reaction to $Al_2O_3 \cdot 0.5H_2O$. Beyond this composition, the energy corresponded simply to alpha monohydrate decomposition. The heat absorbed in the first step was close to that for the transformation to alpha monohydrate.

Courtial, Trambouze and Prettre determined that alpha trihydrate subjected to various heat treatments was, successively or simultaneously, transformed into crystalline alpha monohydrate and into a more or less hydrated amorphous substance. Based on the thermogravimetric, calorimetric and chemical methods, equations were devised to calculate water contents. Later, Courtial and Trambouze offered a tentative interpretation of the dehydration mechanism.

Tertian and Papée measured vacuum dehydration equilibrium water content for both Bayer and finely divided alpha trihydrate at 180-400°C. The finely divided alpha trihydrate had the lower water content in its dehydration product. In both cases, the maximum water content of the transition alumina phase corresponded to about $Al_2O_3 \cdot 0.45H_2O$. Results were similar for air dehydration. In the latter case, the maximum surface area of chi alumina amounted to 350-400 m^2/g, for both varieties of alpha trihydrate. These results clearly showed that the interfacial properties of active aluminas of this type are related to their transition alumina content.

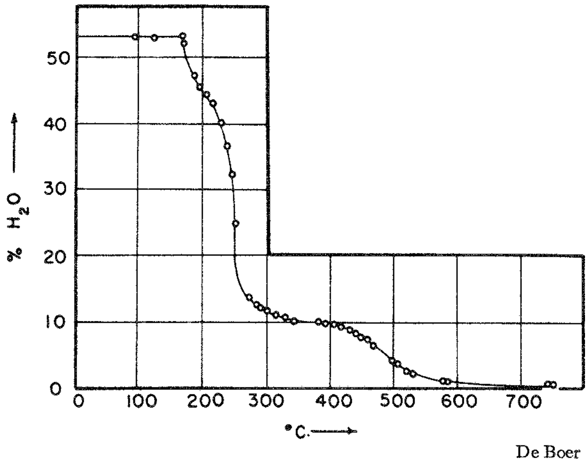

De Boer

Fig. 13—Water Content as a Function of the Heating Temperature of Alpha Trihydrate (Per cent H_2O is on Al_2O_3 basis)

Papée and Tertian pointed out that the increase in surface on heating alpha trihydrate was proportional to the development of transition aluminas and was independent of the amount of alpha monohydrate formed. The circumstance that only alpha monohydrate and not transition alumina was formed in the first step of the dehydration accounted then for the absence of area on first heating alpha trihydrate. The surface area of alpha trihydrate heated in air was much greater than when heated in vacuum. Under conditions

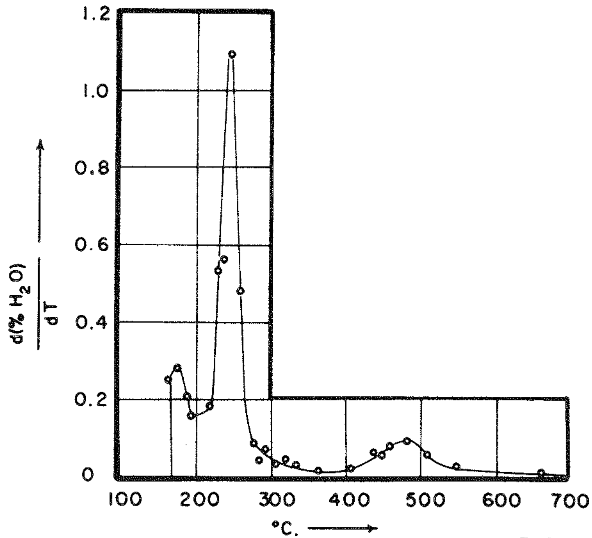

De Boer

Fig. 14—Differential Curve Derived from Fig. 13

where air activation gave 265 m^2/g by cyclohexane and 285 m^2/g by nitrogen, activation in vacuum gave 25 m^2/g and 50 m^2/g, respectively. The vacuum-activated material (rho alumina) had its surface located in extremely narrow pores which were inaccessible to cyclohexane or even to nitrogen.

Surface area as a function of calcination temperature is plotted in Figure 15. Russell and Cochran reported that the surface area (as measured by n-butane) did not reach 2 m^2/g until the weight loss was 8%. Thereafter it rose to a peak of about 350 m^2/g for one-hour calcination at 400°C in dry air. Surface areas were lowered by water vapor at high temperatures. Blanchin pointed out that the maximum surface area occurred at a composition of $Al_2O_3 \cdot \frac{1}{2}H_2O$ for many combinations of activation temperature, time and atmosphere. The relation between surface area and calcination temperature has been reported by many workers including Blanchin, Fricke and Jockers (1951), Gregg and Sing (1951), R. J. Taylor and *Industrial Chemist 22*, 651-5 (1946). Carruthers and Gill reported surface areas of 5, 3, 1 and 0.3 m^2/g for alpha trihydrate heated two hours at 1200, 1400, 1600 and 1720°C. Calvet used a microcalorimeter to determine the surface area of calcined trihydrates.

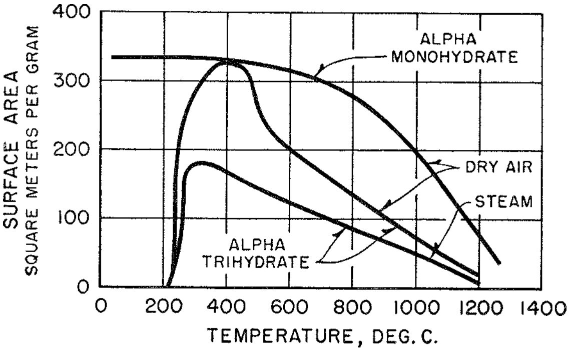

Russell and Cochran

Fig. 15—Surface Area of Heated Alumina Hydrates

For heated alpha trihydrate, A. G. Foster determined a Gaussian distribution of particle size with a maximum at 26 Å by application of the Kelvin equation to water sorption data. Gregg and Sing (1951) presented general features of the pore structure from carbon tetrachloride isotherms. Drake and Ritter measured the macropore size distribution after 16 hours heating at 540°C by observing the change in apparent volume as mercury was compressed into the pores. Two-thirds of the 0.123 ml/g macropore volume was in pores greater than 1000 Å diameter. Total pore volume was 0.388 ml/g. De Boer (1958) distinguished two types of pore structure in the transition to chi alumina. At about 225 to 250°C pores of about 30 Å were formed by the initial release of water, resulting in surface area of about 60 m^2/g. As the dehydration proceeded, a second, rod-shaped structure developed having pore diameter of about 10 Å and additional surface area of about 200 to 250 m^2/g. The rod structure was retained through several transitions to alpha alumina at temperatures to 1200°C, but pore size increased and surface area fell. Sanlaville observed two distinct maxima in pore size distribution of the transition aluminas: the first covering a range of 7 to 18 Å (surface area 235 m^2/g), the second of 18 to 300 Å (surface area 36 m^2/g). Pore generation reached a maximum of 6.5 Å for the composition $Al_2O_3 \cdot \frac{1}{2}H_2O$. Jellinek and Fankuchen, by measurement of X-ray line breadth, found crystallite diameters to increase from 45 to 67 Å on heating alpha trihydrate from 649 to 982°C.

Tertian and Papée (1958) finally proved that the alpha monohydrate resulted from rehydration of the primary decomposition product. Heating small-particle alpha trihydrate slowly in air led to chi alumina and in vacuum to rho alumina, both free of alpha monohydrate. Slow dehydration of Bayer hydrate always formed some alpha monohydrate. Even dehydration at 170°C for 80 hours under high vacuum gave 19% alpha monohydrate in the product. Similar dehydration in a water-rich atmosphere raised this amount to 42%.

Today's knowledge of the air dehydration is represented in Table 12. Dehydration of both alpha and beta alumina trihydrate can proceed in two different ways. The following is a plausible explanation for the different routes. In the inner part of the granules the water molecules can escape only with great difficulty. With rapid heating, this gives rise to high vapor pressures in the coarse crystals. This, particularly with alkali present, is the condition necessary for the formation of alpha monohydrate. When the pore system reaches the surface of the granules, the water vapor pressure falls to one atmosphere, the reaction to alpha monohydrate stops and the rest of the trihydrate decomposes to chi or eta alumina.

Tertian and Papée (1958) have published a more detailed form of the dehydration sequences giving attention to various combinations of origin, heating rate, particle size and pressure. The phase sequences and the temperature scale given in Table 12 should be considered only approximate at best. In addition to the conditions listed in Table 12, mineralizers can alter the sequence and the temperature of the phase changes. This applies particularly to the change to alpha alumina where fluorides may lower this temperature to 900°C, and where water at high pressure can drop it to 400°C and can cause alpha monohydrate to change directly to alpha alumina.

Ginsberg (1957) noted that the stability of chi alumina (400-900°C) was displaced downwardly and narrowed (300-700°C) in case the starting alpha trihydrate was produced under potassium hydroxide. Alpha monohydrate stability was not affected by the amount of alkali. Gamma alumina continued in low-alkali material to 1000°C and in alkali-rich material to 1200°C, although in one case it was observed to transform to delta alumina at 700°C.

According to Achenbach and Damerell, alpha alumina trihydrate crystals after dehydration still showed their original habit (hexagonal prisms or lamella) but had lost their smooth surface and transparency and consisted of fine-grained fibers parallel to the hexagonal surface. If decomposition was carried out slowly, the refractive index rose immediately, but if decomposition was rapid, the refractive index dropped initially because of the formation of evacuated spaces. Thibon and Charrier further investigated the retention of habit on heating alpha trihydrate.

Hüttig and Ginsberg showed micrographs of the crystal form resulting from the heating of alpha alumina trihydrate. They concluded that dehydration takes place as a continuous process preceding lattice change, the transition phases being fragments in the crystal structure. During alpha monohydrate formation, the form of the trihydrate crystal was best retained when the transformation was in alkali; next when it was carried out in water; and last, when the dehydration was in air. Transparency was lost from the interior of the original trihydrate crystal, and small rhombic segments were easily observed. On further heating, the form of the trihydrate crystals was retained even to 1200°C. The segments in the interior of the crystal were altered, going finally into small alpha alumina crystals of different orientations. By heating to 1300°C, a large part of the aggregate broke into small crystals.

Ginsberg related the stabilizing effect of alkali for alpha trihydrate to the numerous vacancies expected in the structure and for chi, kappa, gamma and delta to their fragmented lattice arrangement.

Nahin and Huffman published electron micrographs of heated alumina hydrates. Voids apparently generated by dehydration are shown for theta alumina, and crystal holes are evident in high-temperature gamma-type alumina. An Alcoa Activated Alumina calcined at 1040°C, where it showed a diffuse pattern transition alumina, was sharply microcrystalline and of isometric habit, ranging in size from less than 100 to 250 Å on edge. A few micrographs indicated pores in the 40 to 60 Å range.

Stirland, Thomas and Moore published electron micrographs of alumina phases during thermal transformations. Electron diffraction and electron microscope techniques were used to study the alumina phases encountered in the thermal decomposition of hydrated aluminum chloride. An attempt was made to explain the structures found in these specimens. The importance of the findings in relation to sintering mechanisms was discussed. The material formed at 500°C is amorphous ($Al_2O_3 \cdot 0.7H_2O$) and probably a mixture of fine crystals of alpha monohydrate and amorphous Al_2O_3. Shrinkage occurs at 840-1000°C and the plate-like particles contain hexagonal and angular "inclusions" which may be micro-crystallites of gamma or chi alumina. At 1100°C the final transformation to alpha alumina begins.

Another technique for investigating structure and phase changes in sorptive aluminas is the emanation method of Otto Hahn. The alumina was impregnated with thorium salt and the change in radioactivity measured as the alumina was subjected to various thermal treatments. In this way, Gregory and Moorbath found discontinuities at 300 to 450, 850, 890, 1020, 1070, 1090, 1140 and 1190°C on heating alpha trihydrate prepared from reaction of hot hydrated aluminum sulfate solution with ammonia. Moorbath was unable to correlate these discontinuities with structural changes observed with X-ray photographs. Jockers correlated emanating power with surface area.

Petitjean followed the infrared absorption of alpha trihydrate during its thermal dehydration. Bands at 9.9, 10.5 and 11.0 microns gradually lost intensity and disappeared below $Al_2O_3 \cdot H_2O$. The 9.35 band of alpha monohydrate showed first at $Al_2O_3 \cdot 2.5H_2O$ and the 8.7 band at $Al_2O_3 \cdot H_2O$. After heating at 500°C to give essentially anhydrous alumina, the spectrum was characterized by transparency increasing from 8 microns and absorption beyond 11 microns. From $Al_2O_3 \cdot 0.8H_2O$ to $Al_2O_3 \cdot 0.2H_2O$ the pattern was like alpha monohydrate but less intense. At $Al_2O_3 \cdot 0.1H_2O$ the OH bands had disappeared (Orsini and Petitjean).

Iwase investigated alumina phase changes by observing changes in the cathode luminescence spectra of Sm incorporated into alumina. Tromimov and Tolkachov similarly followed the transformations by noting the change in phosphorescence spectra of added Eu.

Trambouze and Perrin found the acidity, measured by dioxan titration of heated alpha trihydrate in benzene suspension, to change regularly with the surface area.

Newsome obtained excellent, relatively large crystals of alpha alumina at 450°C and 4500 psi by hydrothermal decomposition of alpha trihydrate at 350-500°C, and at steam pressures ranging from 1000 to 4700 psi.

B. Heated Beta Trihydrate

There is a marked similarity between the structures and stabilities of the products formed on heating alpha trihydrate and dense beta trihydrate prepared by carbon dioxide precipitation from sodium aluminate solution. But the finely divided beta trihydrate prepared by the action of water on amalgamated aluminum has a significant surface area before calcination, and it has greater stability toward transformation on heating (Russell and Cochran). Structural properties determined by Fricke and Jockers (1951), and Fricke and Eberspächer are listed in Table 13. Densities for heated beta trihydrate shown in Figure 16 are in reasonable agreement with the work of de Kayser.

Imelik (1954) and Petitjean found the dehydration of dense beta trihydrate to proceed as follows: Per mole of Al_2O_3 the initial content of $3.15H_2O$ went to $3.0H_2O$ between 25 and 80°C; to $1.0H_2O$ (after a slight break at $Al_2O_3 \cdot 2.5H_2O$) between 120 and 160°C; to $0.5H_2O$ between 160 and 220°C; to $0.3H_2O$ between 220 and 340°C; to $0.1H_2O$ between 340 and 370°C; to $0.0H_2O$ between 370 and 400°C. The dehydration was more rapid in vacuum. Accompanying these changes, the surface area increased rapidly at 150°C to a maximum of 320 m^2/g for $0.5H_2O$ as in the dehydration of alpha trihydrate. From X-ray studies, alpha monohydrate began to appear at 120°C and eta alumina at $1.5H_2O$. The trihydrate disappeared at 160°C, the eta alumina was stable up to 900°C. The thermal dehydration of beta trihydrate was also discussed by de Kayser.

Goton found the rate of decomposition of dense beta trihydrate, particle diameter 100 microns, to be much like that for alpha trihydrate. After a short induction period, in which excess water beyond the stoichiometric composition was lost, the rate of decomposition at a given temperature was constant to $Al_2O_3 \cdot 0.5H_2O$; beyond this point it fell rapidly. The rate of weight loss for a one-gram sample at 10^{-3} mm increased from 0.51 mg/min at 174°C to 5.67 mg/min at 225°C. In the presence of 4.5 mm of water, the rate at 225°C fell to 5.25, although it was still linear with time. At higher water pressure, the constancy of

TABLE 12

Decomposition Sequence of Alumina Hydrates

Conditions Favoring Transformations①

Conditions	Path a	Path b
Pressure	>1 atm.	1 atm.
Atmosphere	moist air	dry air
Heating Rate	>1° C/min.	<1° C/min.
Alkali	present	absent
Particle Size	>100 microns	<10 microns

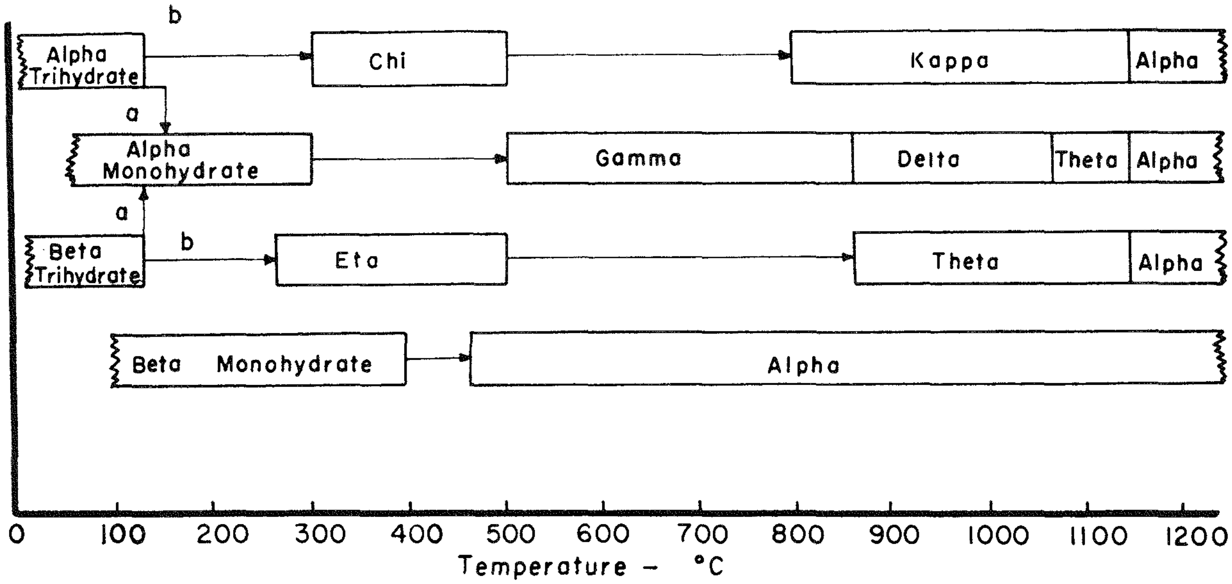

Note: Enclosed area indicates range of stability.
Open area indicates range of transition.
①Pollak.

rate disappeared and the order of the reaction increased. The apparent energy of activation for dehydration at 10^{-3} mm was 23 kcal/mole (less than alpha trihydrate) and this increased sharply when the water pressure increased.

The heat effects on dehydration at a temperature increase of 4.5°C/min were similar to those for alpha trihydrate: small endothermicity at 250°C, large endothermic peak at 330°C, no exothermic peak (in contrast to alpha trihydrate) and a weak endothermicity at 450-500°C. With a sample of fine beta trihydrate, the two peaks at

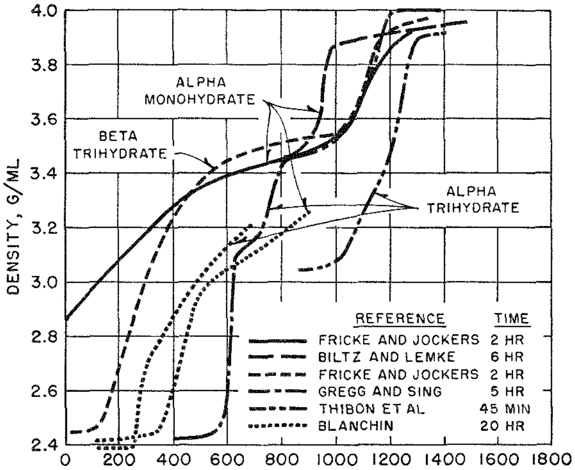

Fig. 16—Density of Heated Alumina Hydrates

250°C and at 450-500°C were both eliminated, thus showing their interdependence. The heat requirements for dehydration were 72.2 kcal/mole.

By differential thermal analysis, Petitjean found rapid dehydration to alpha monohydrate beyond 220°C. Between 240 and 290°C an exothermic effect offset the endothermic dehydration, but the endothermic effect prevailed, and was maximum at 360°C. A transition phase was evident above 300°C. The alpha monohydrate disappeared beyond 520°C and was marked by a weak endothermal effect. The curve obtained with the solid heated in advance to $Al_2O_3 \cdot 3H_2O$ did not differ from that of the original sample; but further heating to $Al_2O_3 \cdot 2.5H_2O$ lost the first endothermal peak at 220°C without affecting the balance of the curve. The sample heated to $Al_2O_3 \cdot 1.5H_2O$ was like $Al_2O_3 \cdot 2.5H_2O$ but had a lesser endothermic peak. $Al_2O_3 \cdot 0.5H_2O$ showed no thermal effects until 530°C where the usual weak endothermal curve resulted.

Petitjean found that the characteristic infrared bands at 9.8 and 10.4 microns gradually lost intensity and disappeared at $Al_2O_3 \cdot H_2O$, and the 9.35 and 8.7 bands of alpha monohydrate appeared when dehydration was carried to $Al_2O_3 \cdot (2\text{-}2.5)H_2O$. Transparency of the nearly anhydrous phase resulting from heating at 500°C was greater beyond 7.2 microns than for the corresponding phase from heating alpha trihydrate. Densities in mercury and helium were used to compute porosities increasing from 0.27 ml/g for the initial product to 0.63 ml/g.

Petitjean found the acidity measured by dioxane titration of a benzene suspension of partially calcined beta trihydrate was zero until $Al_2O_3 \cdot 1.5H_2O$ where the only decomposition phase shown by X ray was alpha monohydrate. This had a surface area of 150 m^2/g. Beyond this point acidity increased rapidly to 1.6 me/g at $Al_2O_3{:}0.5H_2O$, surface area 280 m^2/g, eta alumina. On further heating, surface area fell, the alumina became better crystallized and acidity fell rapidly to zero.

Funaki and Shimizu said that beta trihydrate did not transform into alpha trihydrate at room temperature during a ten-year aging period. The permanent adsorption of water vapor on dehydrated beta trihydrate was a maximum at 250°C (Papée).

The X-ray decomposition sequences, assuming the validity of a dual mechanism, are listed in Table 12. An amorphous, or poorly crystallized phase may be produced analogous to rho alumina. The transformations found by X ray have been verified by infrared and differential thermal analysis investigations.

Russell and Cochran measured the surface area by n-butane sorption of rocklike beta trihydrate. Slightly greater areas were found at the optimum calcination than for alpha trihydrate.

Chrétien and Papée investigated the microporosity of sorptive alumina prepared by calcining alpha monohydrate gel and beta trihydrate at 400°C for 14 hours. They determined the sorption of water, carbon tetrachloride, chloroform and trichloroethylene, and calculated the macroporosity from the difference between the microporosity and the total pore volume determined by immersion. Macroporosity was little influenced and microporosity much influenced by calcination.

Laubengayer and Weisz found a metastable transition of beta trihydrate to alpha monohydrate in superheated steam close to the alpha trihydrate decomposition point of 155°C, whereas Fricke and Severin, from experiments at atmospheric pressure, gave the point as about 120°C.

TABLE 13

Structural Properties of Heated Alumina Hydrates

BETA TRIHYDRATE (Fricke and Jockers 1951; Fricke and Eberspächer)

Property	Room Temperature	2 Hr-Calcination						
		400°C	600°C	800°C	1000°C	1100°C	1200°C	1300°C
Pore Diameter (sorption), Å	20	14	48	79	230	144	......	......
Surface Area, m^2/g	28	431	174	108	33	33	......	......
Particle Size (line width), Å	171	48	69	77	85	......	......	......
Xylol Density, g/ml	2.45	3.23	3.44	3.51	3.54	3.70	3.93	3.96
Mercury Density, g/ml	0.77	0.54	0.55	0.56	0.55	0.58	0.58	0.58

ALPHA MONOHYDRATE (Fricke and Jockers 1951; Fricke and Eberspächer)

Property	Room Temperature	2 Hr-Calcination						
		400°C	600°C	800°C	1000°C	1100°C	1200°C	1300°C
Pore Diameter (sorption), Å	63	69	89	144	140	140	......	......
Surface Area, m^2/g	196	211	181	138	84	37	......	......
Particle Size (line width), Å	87	43	49	59	64	......	......	......
Xylol Density, g/ml	2.86	3.28	3.40	3.45	3.54	3.67	3.86	......
Mercury Density, g/ml	0.80	0.66	0.69	0.69	0.80	1.05	1.48	......
Average Spacing (Xray), Å	161	140	132	126	151	......	......	......

ALPHA MONOHYDRATE (Blanchin)

Property	Room Temperature	20 Hr-Calcination		
		265°C	355°C	450°C
H_2O/Al_2O_3	1.5	1.0	0.5	0.1
Helium Density, g/ml	2.41	2.40	2.40	2.60
Mercury Density, g/ml	0.89	0.80	0.80	0.85
Pore Volume, ml/g	0.71	0.83	0.83	0.79
Surface Area, m^2/g	310	310	310	285
Pore Radius, Å	41	54	54	55

ALPHA TRIHYDRATE (Blanchin)

Property	Room Temperature	20 Hr-Calcination					
		200°C	205°C	208°C	210°C	250°C	400°C
H_2O/Al_2O_3	3.0	2.50	2.00	1.50	1.00	0.50	0.10
Helium Density, g/ml	2.38	2.39	2.40	2.48	2.60	2.76	3.01
Mercury Density, g/ml	2.25	1.88	1.69	1.60	1.58	1.65	1.87
Pore Volume, ml/g	.025	.114	.175	.222	.248	.244	.203
Surface Area, m^2/g	0	5	50	125	250	325	225
Pore Radius, Å	....	400	70	36	20	15	18

C. Heated Alpha Monohydrate

The structure of alpha monohydrate depends strongly on its method of preparation. The structure resulting from heating the trihydrates in air has been discussed in the preceding two sections.

The dense alpha monohydrate formed by subjecting the trihydrates to water or caustic at high pressure undergoes structural changes on heating in air that are in principle like those for the trihydrates. The temperature of decomposition is higher. Ervin and Osborn set the upper stability limit at 375°C at pressures below 2,000 psi; at higher pressure, the alpha monohydrate transformed to beta monohydrate at temperatures above 275°C. Variable results on heating in air were ascribed by Hüttig and Ginsberg to low thermal conductivity.

Haber said that alpha monohydrate lost 1% of its weight at a water pressure of 10 mm of mercury in thirty minutes at 300°C. It lost weight rapidly between 400 and 450°C, creating a surface area of 100 m^2/g on relatively narrow pores. Further heating caused a rapid loss of area. Thin platelets of alpha monohydrate resulting from heating alpha trihydrate in concentrated sodium hydroxide solution became dehydrated at the temperature characteristic of the larger particle monohydrate but developed less additional area on activation (Russell and Cochran).

Petitjean, and Eyraud and co-workers reported that the initial water content of $Al_2O_3 \cdot 1.15H_2O$ was reduced on evacuation to $Al_2O_3 \cdot H_2O$ at 330°C, $Al_2O_3 \cdot 0.1H_2O$ at 380°C and $Al_2O_3 \cdot 0.0H_2O$ at 800°C. Slightly higher temperatures were required on heating in air to effect this loss of water. The characteristic infrared bands at 8.7 and 9.35 microns lost intensity as the sample was heated and disappeared at $Al_2O_3 \cdot 0.1H_2O$ where a maximum transparency at 7.2-9 microns was created. After the initial water was evolved, the decomposition followed a simple rate law of order 2/3. The apparent activation energy of 42 kcal/mole for a sample of 50 microns diameter at 10^{-3} mm was increased in the presence of water vapor which inhibited the reaction. Thermal analysis at a heating rate of 80°C/min showed a strong endothermic-exothermic phenomenon at 280 to 370°C whose magnitude diminished as the initial water content of the sample was decreased by prior heating. Goton for a heating rate of 4.5°C/min found the strong endothermic peak at 510°C. The total heat (first peak being deduced) required for the dehydration was 35 kcal/mole. Surface area, initially reflecting only the geometric surface of the grains, increased to 100 m^2/g at 450°C where the composition corresponded to $Al_2O_3 \cdot 0.1H_2O$. The products lost area on further calcination.

Much more important in present-day technology is the alpha monohydrate produced from alumina gel. The alumina gel precipitated by alkali or ammonia from aluminum salt solutions usually consists of a hydrous mass of minute crystals of alpha monohydrate. During aging or drying, these fibrils coalesce and under some conditions form a hard structure. This structure is, however, extremely porous and may have a surface area of 500 m^2/g without any heating. Generally the pores are uniform in contrast to those resulting from calcination of the dense trihydrate or the dense hydrothermal alpha monohydrate. Heating this structure above about 400°C resulted in the decomposition of the alpha monohydrate. Accompanying this loss of water was an increase in pore volume but usually little change in surface area (Russell and Cochran).

Boerskov (1952 and 1953) measured properties, after stepwise heating to 1200°C, of gels prepared from aluminum nitrate solutions by precipitation with ammonia. The structures as determined by sorption and mercury porosimeter methods were unaffected by heating up to 600°C. At higher heat-treating temperatures, surface area and the number of fine pores diminished, but the number of large pores increased. On heating to 1200°C, the surface area decreased by a factor of 60 and the pore volume decreased by less than a factor of 2. The specific activity for dehydration of ethyl alcohol increased twofold on heating slightly below 1200°C but it fell rapidly at higher calcination temperatures accompanying the conversion to alpha alumina.

Papée, Tertian and Biais studied the differences between dense and gel type alpha monohydrate (or pseudoböhmite). They pointed out that pseudoböhmite cannot be simply considered as a finely divided or poorly crystallized alpha monohydrate. The different structure was evidenced by the strong variation in the first interference, which increased from 6.11 for true alpha monohydrate to 6.6-6.7 Å; on the other hand, the X-ray pattern did not show the usual modifications observed for disturbed crystals. Pseudoböhmite showed the same atomic arrangement at short distances as that of alpha monohydrate. The relationship between the particular properties of pseudoböhmite was illustrated in hydrothermal evolution experiments, with this solid going progressively to true alpha monohydrate. Even under mild conditions (18 hours at 200°C) there was an important shift of the first interference from 6.6-6.7 to 6.19 Å and a substantial decrease of the excess water from 60 to 12%. Under more severe conditions (18 hours at 285°C) the excess water fell to 1%, while the X-ray pattern showed only slight differences from that of the alpha monohydrate. After a treatment of 48 hours at 300°C the solid reached the theoretical composition of alpha monohydrate and showed its exact X-ray pattern in all details. The decrease of the specific surface area was much slower than in the case of excess water; this fact supports the idea that this excess water is not to be considered as merely adsorbed at the surface of a finely divided solid having otherwise the properties of true alpha monohydrate, but rather as situated between the elemental structure layers, thus leading to an enlargement of the basal spacings and conferring particular properties to the solid. Thermogravimetric experiments confirmed these views.

Alumina gels are discussed further in the section titled "Amorphous and Gel Aluminas."

D. Heated Beta Monohydrate

Ervin and Osborn established the stability range for beta monohydrate to be between 275 and 425°C above 2,000 psi. Fricke and Severin found the temperature at which beta monohydrate lost 1% in weight at a water pressure of 10 mm of mercury in 30 minutes to be 420°C.

One of the most interesting properties of beta monohydrate is its direct conversion into alpha alumina at 450 to 600°C without destruction of the external form of the crystal (Deflandre). No intermediate phases were found in the transition sequence on heating, in contrast to the other hydrates (Stumpf). Garrido found that the lattice of beta monohydrate was not disorganized during dehydration. K. Wefers, quoted by Hüttig and Ginsberg, showed that, on heating, loss of water preceded lattice rearrangement.

According to Kengott, beta monohydrate interspersed with alpha alumina occurs similarly oriented in nature. Schwiersch proved by optical experiments that after beta monohydrate was dehydrated the alpha alumina crystals were located parallel to each other, with the a-axis of beta monohydrate the triple main axis of alpha alumina, and the c-axis of beta monohydrate the [010] direction of alpha alumina. Boehm and Jäntsch used a wide angle X-ray diffraction method to verify again that the original single crystals of beta monohydrate became an oriented aggregate of microcrystals of alpha alumina. The abc axes of the rhombohedral beta monohydrate changed to cab in the hexagonal alpha alumina after the thermal decomposition.

Ervin pointed out that the hexagonal close-packed arrangement of the oxygen ions in beta monohydrate is responsible for its transition to alpha alumina without going through the intermediate cubic transition phases. A relatively coarse beta monohydrate, with cleavage parallel to (010) and its (020), (040) and (060) lines greatly intensified, gave on calcining a corundum pattern with the $(10\bar{1})$ reflection greatly intensified at 2.375 Å, which corresponds to the (040) reflection of beta monohydrate at 2.355 Å.

E. Rehydration

Ervin and Osborn were unable to rehydrate low surface area alpha alumina within several hundred hours under the pressure and temperature conditions where the monohydrates are stable. No attempt to rehydrate high surface area alpha alumina has been reported. There is extensive literature on the rehydration of various transition aluminas (van Nieuwenburg and Pieters, Hüttig and Kölbl, Laubengayer and Weisz, Bentley and Feachem, Fricke and Jockers (1947), Ervin and Osborn, Day and Hill). Rehydration of the high area transition phases is usually reported to proceed well at 100°C to alpha monohydrate in a matter of days. Some alpha or beta trihydrate may be formed by prolonged rehydration. Lower or higher temperatures may be employed. The rehydration may proceed through the water chemisorbed on the surface (Thibon). Papée (Thesis A2737) found that the quantity of water permanently adsorbed corresponded to that entering into the rehydration under some conditions although the take-up of water was more rapid than its rearrangement into the new crystal.

Tertian and Papée investigated rehydration of a vacuum-dehydrated Bayer hydrate containing about 25% alpha monohydrate, the remainder being a poorly crystallized transition alumina. Quantitative X-ray analysis of the product rehydrated at 25°C showed the alpha monohydrate to be unchanged, while the transition alumina transformed to beta trihydrate.

Similar results were obtained with rho alumina prepared from beta trihydrate. The ability of rho to rehydrate was strongly affected by the conditions of water vapor escape during previous dehydration. If in the course of this operation water vapor was allowed to accumulate in contact with the solid, this ability was greatly reduced, while the surface became more accessible to cyclohexane; such a solid no longer showed the X-ray pattern of pure rho alumina. A method of manufacturing granulated active alumina, by Pingard, is based on the ability of dehydrated Bayer alumina to rehydrate.

Calvet and Thibon (1954) also investigated this rehydration phenomenon by means of microcalorimetric experiments. Microcrystalline alpha trihydrate activated at 205°C under vacuum formed $Al_2O_3 \cdot 0.47H_2O$ which rehydrated to beta trihydrate with the evolution of 150 cal/g. When activated at 440 to 520°C under vacuum, it formed Al_2O_3 which rehydrated less efficiently and evolved 100 cal/g. When activated at approximately 500°C at atmospheric pressure, the alumina did not rehydrate and the only heat evolved was that due to sorption. Bayer alpha trihydrate activated at 180°C under vacuum formed alpha monohydrate and rho alumina (total composition $Al_2O_3 \cdot 0.6H_2O$) which hydrated in two stages (heat evolution peaks at approximately 5 hours and approximately 15 hours at 35°C) giving a heat of 128 cal/g after correcting for the unhydratable alpha monohydrate content. At higher temperature and under atmospheric pressure, rehydration was less efficient. Even when activated under vacuum, the beta trihydrate samples rehydrated less efficiently.

The gamma alumina created from dense alpha monohydrate had little tendency toward rehydration, although the transition phase (eta?) from calcination of high area alpha monohydrate had a notable aptitude for rehydration. Dense hydrothermal alpha monohydrate could not be rehydrated readily (Laubengayer and Weisz).

F. Equilibria in Solution

Many contradictory reports are published on the relative stability of the various hydrates in solution. One of the most satisfactory means of resolving the difficulties is to measure solubilities of the several phases accurately. From extrapolation of solubilities in sodium hydroxide, Russell (1955) found hydrothermally produced alpha monohydrate to be the stable phase at room temperature and above, although the more soluble trihydrates might be precipitated first and persist at low temperature for extremely long times. At solution temperatures above 100°C, the trihydrates transformed to alpha monohydrate. Alpha trihydrate was shown to be stable with respect to beta trihydrate at temperatures up to about 145°C. Equilibrium constants for the reactions

$$Al(OH)_3 + OH^- \longrightarrow AlO_2^- + 2H_2O, \text{ and}$$
$$AlOOH + OH^- \longrightarrow AlO_2^- + H_2O,$$

accurately correlated the effects of sodium hydroxide concentration on the solubilities. Temperature coefficients of the equilibria led to heats of solution of 7.34, 4.76 and 5.24 kcal/mole for the alpha trihydrate, alpha monohydrate and beta trihydrate, respectively.

Calcination of alpha trihydrate in air stepwise at temperatures below 1000°C, where the X ray would indicate a variety of structures, did not produce a major change in the pseudo equilibrium solubility. Calcination of the hydrothermal alpha monohydrate in this same temperature region increased equilibrium solubility to values nearly characteristic of alpha trihydrate. Calcination of either of these phases under conditions that induced strong exothermal transformations lowered solubility, or at least the rate of solubility, substantially.

Ginsberg and Köster found that the transition of alpha trihydrate to alpha monohydrate at temperatures of 150 to 200°C was accelerated by small amounts of alkali. Further increase in the alkali concentration was without effect on the rate of the transformation. At 200°C and an alkali content of 0.13 g/l Na_2O, the decomposition was completed within two hours, while at 150°C and 10 g/l Na_2O, 12 hours were required before the monohydrate was obtained. In the experiments at 150°C, the decomposition products contained about 15.5% water of hydration (theoretical value for monohydrate 15.0%), and at the higher temperatures the water contents were even higher. Another interesting point from their work is that the apparent density of the monohydrate decreased uniformly with increase of alkali concentration. The values were 0.65 g/ml at 0.6Na_2O/l, 0.50 g/ml at 7 g Na_2O/l, 0.40 g/ml at 70 g Na_2O/l and 0.25 g/ml at 140 g Na_2O/l. This difference in apparent density remained even after calcination of the monohydrate into alpha alumina.

These authors suggested that small amounts of Na_2O are built into the hydrate lattice, and that the points of the trihydrate, which are thus disturbed, are most readily converted into monohydrate. They also attributed the change in density of the monohydrate to soda in its structure.

Travers and Clause found that phenol added to sodium aluminate favored monohydrate formation. Kraut, Kohlschütter and co-workers stated that alkalinity accelerated the alpha monohydrate conversion to beta trihydrate.

ACTIVATED ALUMINA

A. Commercial Forms

Alcoa Activated Alumina F (Figure 17) is prepared by the controlled calcination of a rocklike form of alpha alumina trihydrate. The loss of water, with the accompanying recrystallization, creates many large pores which can be seen readily with the optical microscope (Figure 18). Many small pores are resolved only by the electron microscope (Figure 19). Alcoa Activated Alumina H is prepared from a gelatinous alpha alumina monohydrate which has many small pores and a high surface area as precipitated, although it is usually calcined to enlarge the pores and increase its sorptive capacity. Alcoa Activated Aluminas are used commercially for drying air, for the drying of liquids and gases, for chromatography, for the maintenance of transformer and lubricating oils, and as catalysts and catalyst carriers. It is available in the form of balls, tablets and fluidizable microspheres. A photomicrograph of a fluidizable form is shown in Figure 20.

Alcoa Activated Alumina adsorbs water, organic liquids and gases without change of form or properties. It is inert chemically to most gases and vapors, is nontoxic and will not soften, swell or disintegrate when immersed in water. High resistance to shock and abrasion is one of its important physical characteristics. Alcoa Activated Alumina may be reactivated to its original adsorptive efficiency an almost unlimited number of times by employing a heating medium at any temperature between 350 and 600°F (175 and 315°C).

Hüttig, and Hüttig and Markus found that water, hydrogen bromide, sulfur trioxide and hydrogen chloride decreased the stability of a high-area alumina. Péchiney discovered that alumina was rendered nonhygroscopic when it was calcined with a trace of fluoride.

In 1954, Péchiney patented a method for the production of an exceptionally reactive amorphous alumina by slowly heating alumina hydrate not exceeding 300°C, preferably in vacuo or in an atmosphere as dry as possible, immediately eliminating all water liberated in the

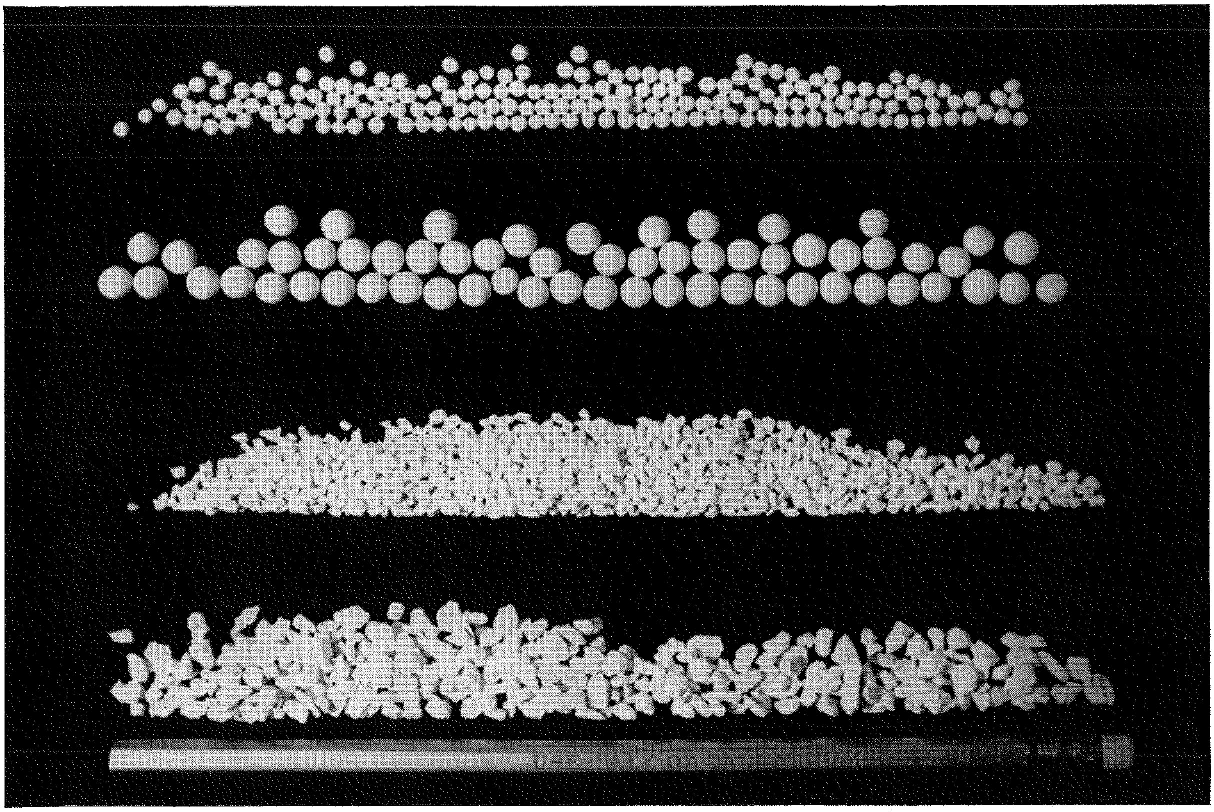

Fig. 17—Types of Alcoa Activated Alumina F

process. A later Péchiney patent (1956) describes an activated alumina (essentially its eta modification) that is prepared by extremely rapid dehydration of Bayer process alumina trihydrate at temperatures in the range of 400 to 1000°C.

B. Drying

Cross may have been the first to report the strong desiccating action of partially calcined alumina hydrate. Johnson showed in 1912 that it would take up water without change in form, sorbing 18% before passing enough moisture to be apparent in a phosphorus pentoxide bulb. Barnitt discovered that the rocklike alpha trihydrate, formed in the precipitation tanks during the Bayer process, maintained its rugged character after calcination and withstood repeated reactivation without loss of sorption efficiency. The market for this product outran the natural supply, and Stowe (1944) developed a synthetic product of superior erosion resistance.

Barnitt and Bower compared agents for drying gases. When 6000 ml of air containing water vapor at 11 mm pressure was passed at a rate of 50 ml/hr over 1 ml of Alcoa Activated Alumina F-1 at 30°C, the residual water content was 0.0018 mg/l of air (1.10^{-3} mm water pressure, dew point −75°C, 0.0004 grain/cu ft of water). In large-scale production equipment, at flow rates approximating 10 to 20 cu ft/hr/lb of alumina, gases are readily dried to dew points below this value. Reactivation is most satisfactory when the desorbed water is swept away before the highest temperatures are reached (Derr). Alcoa Activated Alumina F-1 will adsorb 14% by weight of water at substantially 100% efficiency in a standardized dynamic test.

Kiselev and Smirnova found that adsorption of water by alumina increased with every adsorption-desorption cycle until the sorbent contained 9 to 13% of water, after which adsorption and desorption became reproducible. Imelik pointed out that partially calcined alumina could be rehydrated on exposure to water vapor. Papée found that if the first adsorption isotherm for water on alumina was continued until true saturation was reached subsequent adsorption-desorption isotherms were reproducible. The amount of irreversibly fixed water was high if dehydration was carried out under vacuum.

In 1958, Papée stated that as a result of irreversible adsorption, the initial specific surface was first reduced considerably. As rehydration progressed, the surface area returned to the order of the initial value, and finally slowly decreased as long as the quantitative transformation into beta trihydrate was not completed. Cornelius determined the reversible adsorption of water at 32 to 508°C and 0.05 to 300 mm vapor pressure.

Stowe (1952) found the heat evolved when freshly reactivated aluminas were immersed in liquid water to be 18.0 cal/g adsorbent for Alcoa F-1 and 24.4 cal/g for Alcoa H-51. The heat of wetting by a monolayer of water derived from liquid water was 170 cal/g of water adsorbed, for these forms of Alcoa Activated Alumina. Robert found that the heat of wetting of 15 organic compounds on alumina gel correlated with their degree of adsorbability. Water adsorbed on alumina was judged by Freymann and Freymann to be in the liquid state inasmuch as it showed microwave absorption at 3.15 cm like liquid water. Hydrated alumina does not absorb in this region. Isoteric heats of hydration-dehydration for transition alumina, as determined by Cornelius, vary from 10 kcal/mole water adsorbed at 3% by weight water adsorption level to over 105 kcal/mole at about 0.1% adsorption level. According to Sanlaville, the differential heat of adsorption is 6-7 kcal/mole for 0-30 mg $H_2O/g\ Al_2O_3$ (first layer), 0.9 kcal/mole for 130 mg $H_2O/g\ Al_2O_3$ (second layer) and 0.25 kcal/mole for more than 150 mg water adsorbed per gram of alumina.

Alcoa Activated Alumina is used to reduce the moisture content of cereal grain, yeast, drugs and other biological products to increase their storage life without adverse effects on viability. It is also

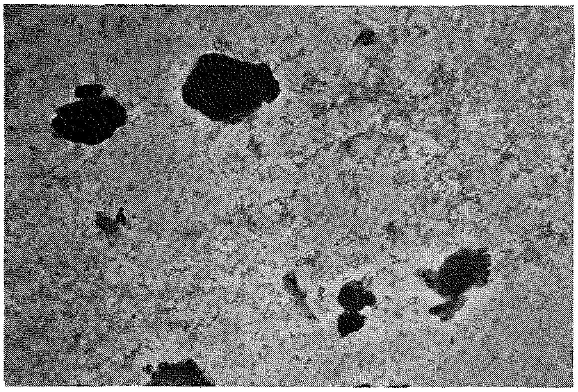

Turkevich, Hubbell and Hillier Faraday Society

Fig. 19—Electron-Micrograph of Alcoa Activated Alumina F, 16,500X

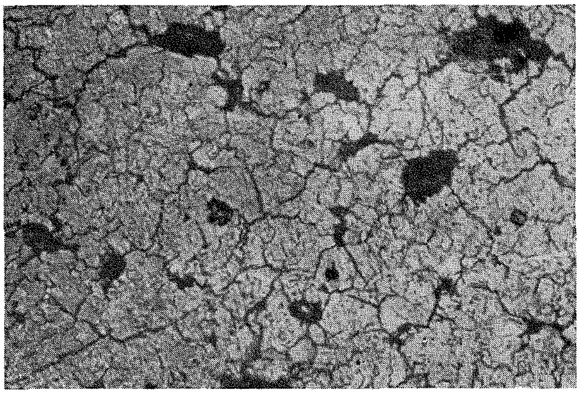

A. S. Russell

Fig. 18—Micrograph of Alcoa Activated Alumina F, 250X

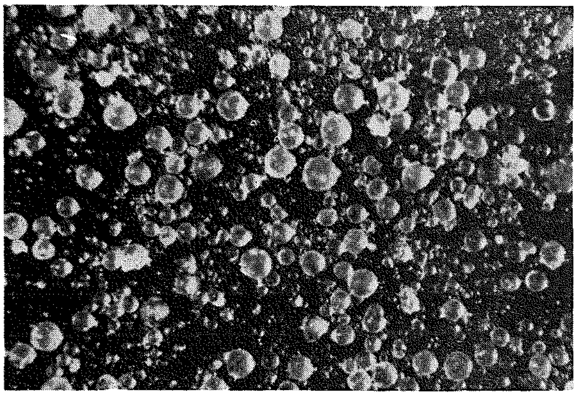

Fig. 20—Alcoa Activated Alumina H-41

used to dry temperature-sensitive chemicals such as ammonium thiosulfate. In these operations, freshly reactivated desiccant is intimately mixed with the solid to be dried. The mixture is allowed to approach equilibrium, then is separated (e.g., by sieving) and the desiccant is reactivated (Moran and Jones). In this system of drying, the heat of adsorption, which may amount to as much as 750 cal/g water adsorbed, flows freely from the desiccant into the material being dried. The transfer of heat in this manner facilitates transfer of moisture without application of heat externally. For drying solids and also for drying enclosed spaces, the equilibrium capacities of the aluminas are of chief interest.

A partial list of liquids that can be commercially dehydrated by Alcoa Activated Alumina includes

LIQUIDS

Benzene
Butane
Butylene
Butyl Acetate
Carbon Tetrachloride
Chlorobenzene
Cyclohexane
Ethyl Acetate
Freon
Gasoline
Hydraulic Oils
Jet Fuel
Kerosene
Lubricating Oils
Naphtha
Nitrobenzene
Oxygen
Pentane
Pipeline Products
Propane
Propylene
Sulfur Dioxide
Toluene
Transformer Oil
Tributylamine
Vegetable Oil
Xylene

References containing engineering data on the drying of some of these products are listed in Table 14.

The heat of wetting by the small amounts of water involved is generally readily dissipated in the liquid being dried. In this case, and if the liquid itself is not adsorbed, the equilibrium capacity for adsorption of water at various levels of saturation approaches that shown in Figure 21, provided that the ordinate be taken as per cent saturation instead of per cent relative humidity. In drying polar liquids, such as methyl chloride and some olefins, capacity is considerably diminished. Possibly these polar liquids compete with water for the adsorbing surfaces. In some cases, the attraction of the liquid for the alumina, as evidenced by the heat of wetting, approximates that of water, and the liquid cannot be successfully dried. Methanol is one example. Another exception must be made in the case of acetone but for a different reason—it is unstable in the presence of activated alumina.

Alcoa Activated Alumina dries air and other gases with great efficiency. The capacity of the alumina depends upon pressure; temperatures of bed and of inlet gas; means of removing heat of adsorption; degree of dryness required; heat capacity of the gas; contaminants in the gas; rate of flow of gas relative to quantity of adsorbent; bed configuration; quality, grade and particle size. Because of the high cost of pressure vessels, the prime factor in the practical design of adsorbers is pressure.

A partial list of gases that can be commercially dehydrated by Alcoa Activated Alumina includes

GASES

Acetylene
Air
Ammonia
Argon
Carbon Dioxide
Chlorine
Cracked Gas
Ethane
Ethylene
Freon
Furnace Gas
Helium
Hydrogen
Hydrogen Chloride
Methane
Natural Gas
Nitrogen
Nitrous Oxide
Oxygen
Propane
Propylene
Sulfur Dioxide

Properties of the principal desiccant grade Alcoa Activated Aluminas are listed in Table 15.

Activated Alumina F-1 is recommended for drying gases at pressures near one atmosphere, for drying refrigerants and for applications where extremely low dew points are desirable. Adsorbents of equilibrium capacity higher than F-1 often give no higher capacities in dynamic drying of gases at one atmosphere because these capacities are limited by the temperatures produced by the adsorbents. Some helpful information and data that are suitable for engineering design may be found in Derr (1938), Rathmell and

Bateman and in *Industrial Heating 18*, 297 (1951).

Some fluorine compounds react chemically with alumina and cannot be dried by this agent. In fact, Alcoa Activated Alumina is used for essentially complete removal of fluorine from the product of the hydrogen fluoride alkylation process. It is also used to diminish the amounts of fluorine in municipal water supplies to safe levels.

Savinelli investigated the effects of a number of variables on the fluoride-ion exchange capacity of activated alumina regenerated with dilute solutions of filter alum. The method appears useful for removal of fluoride from waters of high alkalinity from carbonate hardness but not for those with sodium or potassium bicarbonate.

Alcoa Activated Alumina H-151 is recommended for drying gases under high pressure and for liquids, refrigerants and other applications where maximum absorptive capacity is desirable.

When drying gases under pressure, the heat of adsorption is dissipated readily because of the high heat capacity of the gas. The temperature remains low and adsorption proceeds until capacities fairly near equilibrium capacities are attained. Data on the performance of H-151 in an installation for drying natural gas are given by Getty. The high absorptive capacity, nontoxicity and ease of handling make this ball-type desiccant especially suited for static drying applications such as packaging dried foods and drugs to maintain low moisture contents. The abrasion resistance and crushing strength of H-151 are excellent. Pressure drop through beds of spherical H-151 is lower than the pressure drop through granular desiccant beds.

Activated Alumina F-3 is normally recommended for drying gases, vapors and liquids not requiring maximum moisture adsorptive capacity. But dew point equivalents approximating −80°F are readily obtainable.

Activated Alumina F-5, which is F-1 with calcium chloride impregnation, has about twice the moisture capacity of F-1. This grade is used principally where rapid "one-shot" desiccation requiring maximum moisture removal is desired. Repeated reactivation at temperatures in excess of 350°F is not recommended because of progressive decomposition or ultimate breakdown of the calcium chloride.

Activated Alumina F-6 is made by impregnating F-1 with cobaltous chloride. The moisture adsorptive capacity is essentially that of F-1 with the additional property of changing from indigo blue to pale pink at about 20% relative humidity and to white at the water saturated state. Reactivation restores the deep blue color and the original adsorptive capacity with little or no loss in efficiency. This alumina F-6 is used

TABLE 14

Drying Liquids with Activated Alumina

Liquid	No. of Towers	Dia, in.	Height, ft	Alumina per Tower, lb	Flow Rate per Tower, gal/hr	Water Content, %	Gal per Tower per Cycle	Reference
Benzene	2	40	9	2,500	15,000	0.04	100,000	Derr and Willmore
Toluene	2	40	9	2,500	15,000	0.03	200,000	Derr and Willmore
Gasoline	2	40	9	2,500	400,000	....	1,000,000	Derr and Willmore
Propane	1	14	8	500	....	....	120,000	Lupfer
Pipeline Products	6	48	9	3,000	128,333	Varied	1,540,000	Phipps
Pipeline Products	4	84	7	14,000	80,000	....	1,000,000	Fisher
Furnace Oil	1	30	6	550	....	....	100,000	Nat. Petroleum News Jan. 3, 1945, p. R-63

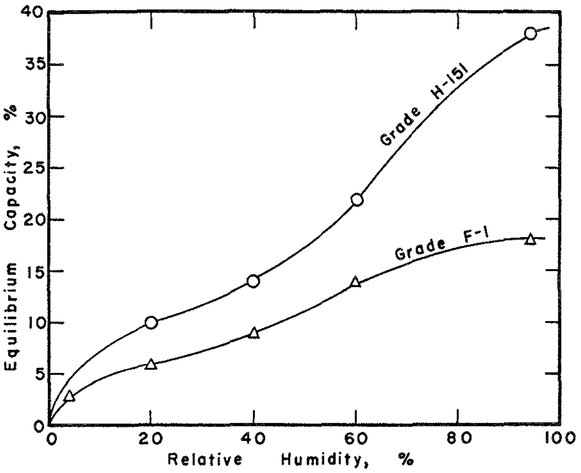

Fig. 21—Activated Alumina Equilibrium Capacities

in breather equipment on tank cars, transformers and storage tanks, and on pneumatic and electrical control equipment, in laboratory desiccators, between multiple-glazed windows and in similar applications requiring a visible indication of the degree of adsorption. If maximum capacity is desired along with visual indication of the degree of adsorption, then F-6 may be intermixed with H-151.

C. *Chromatography*

High surface area alumina has been used extensively in chromatography and a special grade of closely controlled mesh and chemical purity is marketed for this purpose under the trade name Alcoa Activated Alumina F-20. Alcoa Activated Aluminas H-41, H-43 and H-51 offer interesting possibilities as chromatographic media.

Schwab theorized that the adsorption of ions on alumina takes place by the displacement of ions of equal sign contained in the alumina surface, i.e., sodium by cations and nitrate or chloride by anions. Schwab's optical spectra of cations adsorbed by sodium exchange on alumina confirm the view that the adsorption zones contain basic double aluminates. Sacconi has shown that sodium-free sorptive alumina (from amalgamated aluminum) adsorbs cations, the addition of pure alumina to 0.1 N hydrochloric acid raising the pH above 5.6. He has also demonstrated the displacement of aluminum ions during chromatographic adsorption of acid solutions and the lowering of anion concentration. Shuvaeva and Gapon interpreted a number of chromatographic separations on the basis that the alumina predominately functions by exchange and that secondary adsorption occurs in the case of multivalent ions. Grasshof reported no difference in the behavior of alkali-free and alkali-containing alumina toward inorganic ions.

Plank emphasized that alumina gel is primarily an anion sorber, although it also shows some cation sorption. The former is apparently due to a chemical exchange with OH^- groups in the gel structure, and the cation adsorption is associated with the anion uptake as required for electroneutrality. This behavior contrasts with that of silica-alumina gel which is primarily a cation sorber.

Reichstein and Shoppee controlled the chemical activity of the alumina for steroid separations by homogeneous addition of moisture. Before attempting to separate sensitive substances, they removed the alkali from the alumina by boiling it repeatedly with distilled water until the extract was neutral, filtered and washed with methanol and reactivated at 160 to 200°C. For separation of colorless steroids, they adsorbed the mixture on alumina from a suitable solvent and then fractionally eluted, employing the following sequence of solvents of increasing elution power: pentane, petroleum ether, benzene, ether, chloroform or acetone, methanol, water and acetic acid. Boutillon and Prettre changed the Brockmann-Schodder degree for a calcined alpha trihydrate from 1.2 for a freshly activated product of 122 m^2/g, to 2.8 for a sample with 4% water and to 5.0 for a sample containing 16% water.

Solutions of zinc, cadmium, manganese, magnesium, calcium, strontium and barium salts and of ammonium and barium tungstates have been freed from trace impurities of iron, copper, silver and lead by passage through a column packed with high surface area alumina (Lister).

The order of decreasing cation adsorption on alumina was listed by Sacconi as (Th, Al, U^4), (Zr, Cr, Ce^4), (Fe^3, Ti^4, Ce^3), Hg^2, $UO_2{}^2$, Pb, Cu, Ag, Zn, (Fe^2, Co), (Ni, Cd), Tl, Mn; Kubli found

TABLE 15

Typical Properties of Desiccant Grade Activated Aluminas

Chemical Analysis, %	**F-1**	**F-3**	**F-5**	**F-6**	**H-151**
Al_2O_3	92	92	77	88	85
Na_2O	0.80	0.80	0.70	0.76	2.0
Fe_2O_3	0.12	0.12	0.10	0.11	0.15
SiO_2	0.09	0.09	0.08	0.08	6.3
Loss on Ignition 1100°C	6.8	7.2	12.4	8.5	6.2
$CaCl_2$	....	....	9.3	....	....
$CoCl_2$	....	....	....	2.0	....
Physical Properties					
Form	Granular	Granular	Granular	Granular	Balls
Surface Area, m^2/g	210	200	....	....	350
Bulk Density, Packed, lb/ft^3	55	55	60	57	55
Bulk Density, Loose, lb/ft^3	50	50	55	52	52
Specific Gravity	3.3	3.3	....	....	3.1-3.3
Dynamic Sorption①	13-15	11-13	18-23	13-15	21-23
Crushing Strength②	55	55	....	....	60
Pore Volume, ml/g	0.25	0.25	....	0.25	0.3
Pore Diameter, Å	40	40	....	40	50
Static Adsorption at 60% Relative Humidity, %	13.0 (Min.)	11.0 (Min.)	....	....	20.0 (Min.)

The standard sizes for F grade alumina are ½″ to ¼″, ¼″ to 8 mesh and 8 to 14 mesh. Other nonstandard sizes from 2″ granules to 325 mesh powder are available. Activated Alumina H-151 is available in nominal ⅛″ and ¼″ diameter balls.

①Adsorption of moisture at 100% efficiency from air under isothermal conditions at 30°C and 90% relative humidity under dynamic flow of 7.5 $ft^3/hr/lb$ *Activated Alumina: Its Properties and Uses.*

②Method of *Activated Alumina: Its Properties and Uses*

for anions: OH^-, PO_4^{-3}, $C_2O_4^{-2}$, F^-, (SO_3^{-2}, $Fe[CN]_6^{-4}$, CrO_4^{-2}), $S_2O_3^{-2}$, ($Fe[CN]_4^{-3}$, $Cr_2O_4^{-2}$), (NO_2^-, CNS^-), I^-, Br^-, Cl^-, NO_3^-, MnO_4^-, Ac^-, SO_4^{-2}, S^{-2}. Shibata's sequence for decreasing cation absorption is Bi^2, Fe^3, Hg^2, Pb^2, Cu^2, Zn, Co^2, Cd, Ni^2, Fe^2 and Mn^2. He said that calculation of the potential energy for adsorption employing the radius of the hydrated ion gave values in agreement with the order of chromatographic adsorption. Brockmann has listed the functional groups in order of decreasing adsorption affinity for alumina as COOH, $CONH_2$, OH, NH_2, $COOCH_3$, $N(CH_3)_2$, NO_2, OCH_3, H.

Aleixandre Ferrandis has listed values for the per cent sorption onto alumina from solution of many organic acids dissolved in carbon disulfide, carbon tetrachloride, chloroform, ethyl ether, nitrobenzene, and methyl, ethyl, isopropyl and isobutyl alcohols.

Tewari measured the decrease in absorbability with aging for gels precipitated from aluminum chloride solution with 110, 100 and 90% of the equivalent alkali hydroxide solution. The influence of age on sorption of cations and basic dyes was greatest for the material precipitated with the deficiency of alkali. For the adsorption of anion and acid dyes, this influence was greatest for the material precipitated with excess alkali.

TABLE 16

Typical Properties of Catalytic and Chromatographic Grade Aluminas

Chemical Analysis, %	F-10	F-20	H-41	H-42	H-43	H-44	H-51
Al_2O_3	96	92	87	68	93	72	85
Na_2O	0.09	0.80	0.06	0.05	0.04	0.03	2.0
Fe_2O_3	0.09	0.12	0.12	0.10	0.10	0.08	0.10
SiO_2	0.09	0.09	5.8	4.5	0.32	0.25	5.8
Loss on Ignition, 1100°C	3.0	6.8	6.0	27.0	6.0	27.0	6.0
Cl	0.58	....	0.03	0.02	0.03	0.02	0.03
SO_3	....	....	0.32	0.25	0.32	0.25	0.3
CaO	....	....	0.32	0.25	0.19	0.15	0.3
Screen Analysis, %							
+100 mesh	①....	80-200 mesh	....	....	0.5-3.5	....	....
100-200 mesh	....	....	....	....	30-40	....	....
200-325 mesh	....	....	....	....	25-30	....	....
−325 mesh	....	....	....	....	25-35	....	....
Physical Properties							
Form	Granular	Granular	Microspheroidal		Microspheroidal		
Surface Area, m²/g	100	210	350	....	250	....	350
Bulk Density, Packed, lb/ft³	55	68	59	70	60	70	59
Bulk Density, Loose, lb/ft³	50	58	52	60	55	60	52
Pore Vol., ml/g	0.3	....	0.5	....	0.3	....	0.5
Pore Diameter, Å	80	....	60	....	60	....	60
Specific Gravity	3.2	....	2.9	3.7	....	....	....

①The standard sizes for F-10 are ½″ to ¼″, ¼″ to 8 mesh, 8 to 14 mesh and 14 to 28 mesh.

Fricke, Neugebauer, and co-workers, and Venturello and Burdese, investigated the behavior of copper chloride solution on pure gamma-type alumina. $Cu_2(OH)_3Cl$ precipitated in an "immediate reaction" through the surface hydroxyl groups and in a secondary reaction continuing with time as a result of rehydration of the oxide. In addition to these chemical reactions, physical absorption was established with equivalent quantities of Cu^{2+} and Cl^- ions. Quantitative separation of the results permitted the estimation of all of these mechanisms. pH did not change during adsorption of the copper ion; chemically adsorbed copper ion was replaced by aluminum in the solution. Properties of chromatographic aluminas are in Table 16.

D. Catalysis

The catalytic activity of alumina changes drastically with its mode of preparation. The usual forms of high surface area alumina have high dehydrating activity around 350°C. At higher temperatures a dehydrogenating action becomes pronounced.

The most extensive commercial application of alumina in catalysis is as a support for molybdena, chromia and platinum in reforming operations. Thousands of tons of Alcoa Activated Alumina F-10 have been used in hydroforming. Dehydrocyclization activity of molybdena-alumina catalysts was found by Russell and Stokes to vary directly with the amount of impregnated area of the catalyst. Pure alumina, or alumina containing acid sites resulting from incorporation of silica or fluorine, is a favored support for platinum in the reforming reaction for producing high octane gasoline. Highly calcined, low surface area forms of alumina are employed with active agents such as vanadium oxide and silver oxide in oxidation reactions. Alumina by itself or with additives, such as aluminum chloride, or hydrogen fluoride is used extensively in isomerization, alkylation and polymerization reactions.

Holm and Blue reported that pure alumina of high surface area had high activity for hydrogen-deuterium exchange and that this was greatly increased by increasing the calcination temperature of the sample from 400 to 800°C. Incorporation of silica in the catalyst decreased this exchange but increased the rate of hydrogen transfer reactions from naphthenes to olefines.

Alumina-silica cracking catalyst owes its activity primarily to a number of acid sites on the catalyst surface. Trambouze found this acidity at cracking temperatures to comprise both Bronsted and Lewis type acids. Mixing neutral silica sol with fresh neutral alumina sol developed a strong acid. In the presence of an excess of silica sol, no free aluminum hydroxide was precipitated by addition of base to aluminum salt solution, but the primary products of hydrolysis of aluminum ions were consumed by the interaction with silica sol. One equivalent of acid was produced for each atom of aluminum consumed in this reaction. The reaction proceeded well with freshly formed silica gel, less readily with aged gels and very slowly with thoroughly aged silica gel (Tamele). The calcined solid effective in catalysis is essentially a mixture of transition alumina and silica, in which the silicon and aluminum ions share oxygen ions. By exposing a silica-alumina mixture to the vapors of a base such as quinoline, more or less of the alumina became acidic (Milliken). Ewles and Heap reported that alumina was made luminescent by the addition of water, methyl alcohol or ethyl alcohol; the region of excitation, at 2700 Å, being ascribed to surface hydroxyl radicals. The solid lost luminescence on long heating in dry air but gained it again by heating in vacuum or hydrogen. Stowe (1948) reported the cracking activity of alumina containing about 5% silica.

Selwood and Lyon, and Mooi and Selwood were unable to find any effect of alumina crystal structure on the magnetic susceptibility and catalytic action of manganese impregnated on the various transition aluminas or even for high surface area alpha alumina. Dowden related the relative dehydrogenation and dehydration activity of alumina to the number of cation vacancies on the surface. Cornelius proposed that highly strained sites, resulting from dehydration of surface MOH groups, can function as catalytic centers. From an extensive investigation of the physical properties and activity for the hydrogenation of ethylene and hydrogen deuterium exchange of alumina as a function of its dehydration temperature, Mills ascribed the catalytic activity of alumina to centers of high strain resulting from the alumina dehydration. Brey and Krieger found, in the dehydration of ethyl alcohol by alumina to produce ethylene, that both total activity and specific activity decreased as the preparation temperature increased above 600°C. Properties of catalytic grade aluminas are in Table 16.

Although primarily used as a desiccant, Alcoa Activated Alumina F-1 finds application as a catalyst in such reactions as a destructive dehydration of alcohols, in which typical soda content of 0.8 is not harmful.

F-10, a low-soda, granular catalytic alumina, has found considerable application as a fixed bed chemical and petroleum catalyst. It is characterized by its surface area of 100 m^2/g, soda content of less than 0.1% and good physical strength.

Activated Alumina H-41 is an alumina gel catalyst base containing 6% silica. It is produced as spray-dried microspheres well suited for fluid bed operation. Its thermal stability is excellent. This factor coupled with its high surface area makes it a promising material for catalytic use. The unactivated form of this alumina is H-42. This form tablets more readily than H-41. The corresponding grades without silica are H-43 and H-44. Aluminum stearate is an excellent lubricant for tableting H-42 and H-44. A mixture of graphite and Sterotex, a hydrogenated oil, is also a good lubricant.

E. Oil Maintenance

Alcoa Activated Alumina is finding increased use for maintenance of oil in power systems and in large internal combustion engines. The oil is circulated continuously through a bypass filter where the alumina adsorbs the moisture and acids that would otherwise result in sludge and in attack on the metal parts. After being saturated with adsorbed materials, the oil-soaked alumina can be reactivated by heat. Experience has shown that a preventive maintenance program for power system oils offers substantial savings on the operation of transformers, oil circuit breakers and hydroelectric powerhouse equipment. Instructions for such a program are set forth in the booklet, *Activated Alumina Maintenance Program—Power System Oils*. Sawyer, Kipp, Keefer and Shaw reported that Alcoa Activated Alumina was satisfactory for lubricant maintenance for large radial gas engines. Sargent and Kipp also reported that Activated Alumina gave better performance than other adsorbents for maintenance of lubricants in gas burning in-line internal combustion engines. It was superior in maintaining oil quality and in resisting softening or degradation during use.

ALUMINA HYDRATES

A. Alpha Trihydrate

Alpha trihydrate (gibbsite or hydrargillite) is the principal constituent of bauxites in North and South America (Frary). L. H. Milligan early showed alpha trihydrate to be the product of the Bayer process. Investigations by Ginsberg and Hüttig, regarding the precipitation of alpha trihydrate from Bayer process sodium aluminate solution, showed that besides alpha trihydrate some other phases of alumina are effective as seed material to start crystallization.

Alpha trihydrate usually occurs in tabular form with a hexagonal habit (Dana). An electron micrograph of alpha trihydrate prepared in the Bayer process was presented by Nahin and Huffman. Megaw's X-ray analysis (1934) showed all the OH^- ions to be roughly equivalent, so that the material is properly not a hydrate but a hydroxide (Fricke and Hüttig). The crystal (Figures 22 and 23) has a stratified character, each stratum consisting of two layers of hydroxyl ions enclosing aluminum ions in interstices. There are no aluminum ions between the second and third layers of hydroxyl ions. The hydroxyl ions of the third layer are directly over, rather than lying in the depressions of, the second layer. Thus, there

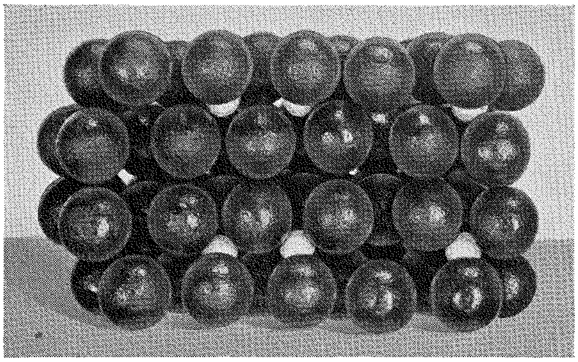

A. S. Russell

Fig. 22—Model of Alpha Alumina Trihydrate b-Plane

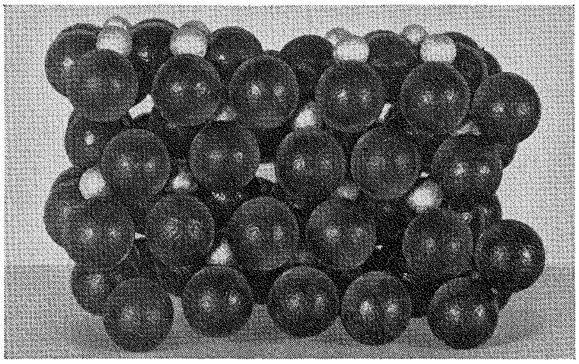

A. S. Russell

Fig. 23—Model of Alpha Alumina Trihydrate c-Plane

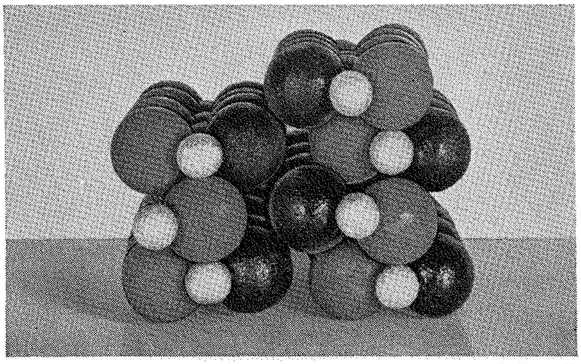

A. S. Russell

Fig. 24—Model of Alpha Alumina Monohydrate Crystal, a-Plane. Glossy Black Balls: Hydroxyl Ions. Large Gray Balls: Oxygen Ions. Small Balls: Aluminum Ions.

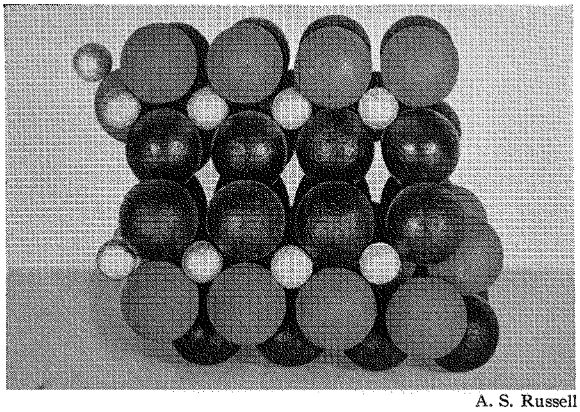

A. S. Russell

Fig. 25—Model of Alpha Alumina Monohydrate c-Plane

are many channels between the strata. In the c-plane the large hydroxyl ions are approximately hexagonal, close packed. The small, hexagonally distributed aluminum ions are surrounded by six nearest hydroxyl ion neighbors, three above and three below. This feature of the structure was deduced also by Duval and Lecomte from infrared absorption. A characteristic of the structure is the hole through the crystal in the center of each hexagon of aluminum ions. Gibbsite was also investigated by Keller and Pickett, and the use of infrared, chemical and X-ray methods for evaluating bauxites was described by Iberg. Asselmeyer considered alpha trihydrate to have in addition to its normal unit cell a "fine structure" which appeared on heating. Kroon and Stolpe assumed a model from proton magnetic resonance measurements where the O-H bonds are directed from an oxygen atom in the lower plane to an oxygen atom in the upper plane in the next "sandwich," but translated over one triangle side. In alternate triangles, these O-H bonds are pointing upward and downward.

This material exhibits neither pyro- nor piezoelectricity (Megaw 1934). Fricke and Keefer gave the isoelectric point at pH = 9.20. Van Bemmelen found that the crystalline hydrate did not adsorb salts from solution to any marked degree. Alpha trihydrate usually contains several tenths per cent alkali ion.

Alpha trihydrate is readily soluble in strong mineral acids and alkalis. Solubility values in the sodium oxide-water system were given by Russell (1955) (see Structure and Phase Transformations, Section F). Fricke and Jucaitis gave values for potassium oxide-water. Elmore estimated the solubility of alpha trihydrate in sodium aluminate, ionic strength 0.6, pH 11.3, temperature 60°C as $5 \cdot 10^{-3}$ mole/liter.

B. Beta Trihydrate

Beta trihydrate (bayerite) is produced by treating aluminum chloride solutions with cold ammonium hydroxide followed by aging and syneresis at room temperature, by saturating a solution of sodium aluminate with carbon dioxide at room temperature (Fricke and Wullhorst) and by autoprecipitation from sodium aluminate solutions under certain conditions. The action of water on aluminum or aluminum alcoholates at temperatures below 40°C (Fricke and Jockers 1947) is a favored means of preparing beta trihydrate. If aluminum metal is used, the production is particularly rapid if the aluminum is amalgamated or finely divided (Schmäh), or if the oxidation is carried out electrolytically. Beta trihydrate has not been identified in nature.

Beta trihydrate, like alpha trihydrate, has a stratified crystal lattice. Each stratum is similar to that of the alpha structure but the third-layer hydroxyl ions in beta trihydrate lie in the depressions between hydroxyl ions of the second layer.

Thus the hydroxyl ions form a closely packed hexagonal lattice.

Stumpf (unpublished) studied X-ray patterns of a number of samples of beta trihydrate prepared by carbon dioxide precipitation from sodium aluminate solutions, and found that stacking faults in the crystal lattice were common. This was shown by distortion of the X-ray reflection from the basal planes of the lattice, i.e., the diffraction peak corresponding to the distance between alternate planes of hydroxyl ions.

The broad nature of the OH infrared vibration pattern was consistent with hydrogen bonding in the crystal (Frederickson).

Beta trihydrate was readily soluble in acid and was more soluble in caustic solution than alpha trihydrate (Fricke 1928).

An electron micrograph of beta trihydrate from carbon dioxide precipitation of aluminate at room temperature was presented by Nahin and Huffman. Electron micrographs of beta trihydrate, prepared by reacting amalgamated aluminum with conductivity water, were shown by Eberspächer, and by Watson. The structural constants of beta trihydrate prepared by the hydrolysis of amalgamated aluminum at room temperature are summarized in Table 13.

Tertian and Papée investigated by X-ray quantitative analysis various procedures of beta trihydrate preparation. They concluded that the conventional methods, especially those starting with aluminum salt or aluminate solutions, led to solids containing only 40 to 75% crystallized beta trihydrate. They stated that the remainder might be: (a) Pseudoböhmite or gel type monohydrate which happens to give a very faint X-ray pattern if under low concentration; nevertheless, its presence is characterized by a lower water content and an increased surface area of the bulk solid, the average properties of pseudoböhmite being a composition of $Al_2O_3 \cdot 1.5H_2O$ and a surface area of 300 m ^{2}/g. (b) Pseudoamorphous trihydrate, the bulk of which has the properties of pure beta trihydrate, namely, a surface area lower than 20 m^2/g, and a composition close to $Al_2O_3 \cdot 3H_2O$; the X-ray pattern does not show any broadening of the beta trihydrate lines, but under special conditions reveals two weak bands at 4.80 and 2.40 Å. Extremely rich or pure beta trihydrate preparations could be achieved only by the Schmäh amalgam method or by rho alumina rehydration.

Beta trihydrate is now on the market. It may well be the origin of some aluminas employed as catalyst supports.

C. Nordstrandite

A new alumina trihydrate, Nordstrandite, based on X-ray studies was reported by Van Nordstrand, Hettinger and Keith. This phase has also been called bayerite II or randomite. Whereas dehydration of alpha trihydrate at 200°C yields chi alumina, beta trihydrate and Nordstrandite yield eta alumina.

From the treatment of solutions of aluminum chloride or nitrate with ammonium hydroxide, all three trihydrates were found after the washed gel was gradually converted to crystalline trihydrate. Papée and co-workers confirmed the existance of the new hydrate, Nordstrandite, and published a more complete X-ray spectrum of the pure material (Table 3).

D. Alpha Monohydrate

Alpha monohydrate (böhmite) is the principal constituent of European bauxites. Natural, well-crystallized specimens were reported by Bonshtedt-Kupletskaya and Vlodavets. Ginsberg

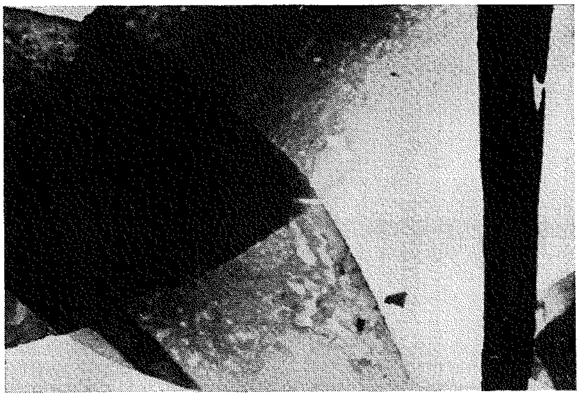

W. H. Gitzen

Fig. 26—Electron-Micrograph of Plate-like Alpha Monohydrate, 25,000X. Alcoa Monohydrated Alumina D-50.

and Köster found heating alumina hydrate in water at 200°C or in caustic at 150°C to be reliable methods for preparing alpha monohydrate. The time for the conversion depended on the initial alpha trihydrate and extended to several hours. Alpha monohydrate was formed by subjecting amalgamated aluminum to boiling water or steam at 100°C (Weiser and Milligan 1936, Fricke and Jockers 1947).

The structure (Figures 24 and 25) consists of oxygen ion layers that do not fit with each other but within which the oxygen ions are in cubic packing. Kroon and Stolpe found the OH-directions to form zig-zag chains between the planes of the oxygen ions. Milligan and McAtee determined the short, unshared O-O distance to be 2.70 Å, consistent with usual hydrogen bond distances. As with all the other so-called hydrates, this material does not contain water molecules (Fricke and Severin), at least in its basic structure. Hill showed extensive solid solution between alpha alumina monohydrate and the corresponding gallia monohydrate.

A fine alpha monohydrate consisting of thin ellipselike plates with sharp points at each end (Figure 26) resulted from heating alpha trihydrate in concentrated sodium hydroxide solution (Tosterud).

Structural regularities in the plates were shown by Bragg reflections from some areas, and the jagged edges indicated a linear arrangement within the plates (Figure 27). These nonporous plates had an area of about 15 m^2/g (Russell and Cochran). Ervin and Osborn published photomicrographs and electron micrographs showing that alpha monohydrate prepared hydrothermally consisted of well-formed thin six-sided plates or laths, some being 150 microns long, the large crystals being similar in habit to the small ones. Structural properties of alpha monohydrate, prepared by hydrolysis of amalgamated aluminum at 100°C, are listed in Table 13.

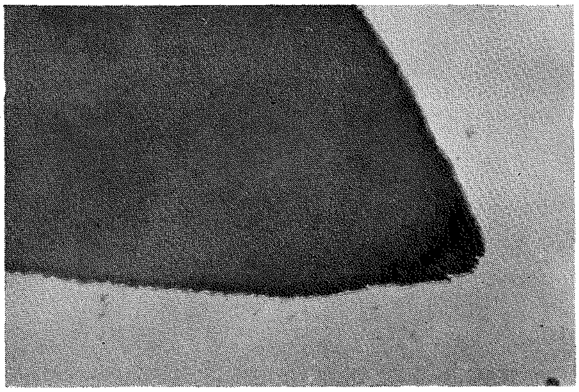

Turkevich and Hillier Analytical Chemistry

Fig. 27—Plate-like Alpha Monohydrate, 47,000X

Transparent films of highly oriented alpha monohydrate have been made by Milligan and Weiser by evaporating a highly thixotropic alumina sol to dryness at room temperature. These films remained transparent and oriented after being transformed into a transition alumina by heating to about 700°C.

The refractive index commonly given for alpha monohydrate was substantially lower than that found recently for large crystals. Ervin (private communication) suggested that the difference was caused by adsorbed water on the usual fine crystals. The permanent adsorption of water vapor increased continuously as alpha monohydrate gel was heated from 100 to 400°C, according to Papée. Fricke and Keefer found the isoelectric point to be in the pH range of 9.40 to 9.45. Alpha monohydrate may show thermoluminescence with peaks like those for the transition aluminas (Rieke). Samples of this material prepared in different ways showed different glow curves.

According to Hüttig and Schaufel, alpha monohydrate swelled greatly in 3.73N hydrochloric acid. It was harder to dissolve in caustic soda solution than the trihydrates (Havestadt and Fricke).

Bryan found that the alpha monohydrate formed by the action of boiling distilled water on aluminum alloys, was made impervious by a certain minimum quantity of silicon in the metal.

The usual samples of alpha monohydrate contain water in excess of the theoretical 15%. Goton pointed out that this excess water acts as if it were a trihydrate phase, located around the surface of crystallites, as judged by the temperature, kinetics and heat requirements of its decomposition.

Concerning this problem of excess water, Tertian and Papée do not accept the trihydrate hypothesis, considering that: (a) the presence of trihydrate in alpha monohydrate may be detected by a refined X-ray examination to an amount as little as 1%, corresponding to less than 2% of excess water; (b) the loss of several per cent—12% for instance—of excess water at about 300°C is followed by neither significant increase in surface area (from 3 to less than 3.5 m^2/g), nor structural change. They rather consider this excess water as intercrystalline.

An unusual fibrous alpha monohydrate has been produced and described by Bugosh. This material must be made in an acid environment; and it is unique in that it is a very fine crystalline powder which forms a gel when mixed with water. It has been described as being a fibrous alumina in the form of fibrils and having an average length in the range from 100 to 700 millimicrons, the remaining average dimensions being in the range from 3 to 10 millimicrons, the axial ratio being from 50:1 to 150:1. It was also claimed that the product has a surface area of 250 to 350 m^2/g.

E. Beta Monohydrate

Deposits of impure beta monohydrate (diaspore) are found in east central Missouri and central Pennsylvania. The pure crystals are rare. Beta monohydrate was grown hydrothermally on seed by Laubengayer and Weisz. Roy and Osborn grew diaspore crystals 1 to 2 mm long at pressures above 20,000 psi.

The beta monohydrate structure is shown in Figures 28 and 29. The oxygen ions are nearly equivalent, each being joined to one other oxygen by way of a hydrogen ion and being arranged in hexagonal close packing (Ewing). Busing and Levy, by neutron diffraction, established the position of the hydrogen on a line at an angle of 12° with the line of centers of the two different types of oxygen atoms and closest to the oxygen farthest from the aluminum ion. This structure lacks the shafts characteristic of the alpha monohydrate. The compact arrangement is consistent with the greater density of this monohydrate and with the low frequency of the OH$^-$ stretching vibration shown by infrared absorption. Coblentz, and van Arkel and Fritzius were unable by infrared absorption to identify bands characteristic of water in beta monohydrate.

The infrared spectra of diaspore were examined by a number of observers. Cabannes-Ott included diaspore in his study of natural hydroxides of the type XO·OH (Table 10). Nakamoto, and Rundle and Parsol discussed the relation between the wave length of the OH absorption

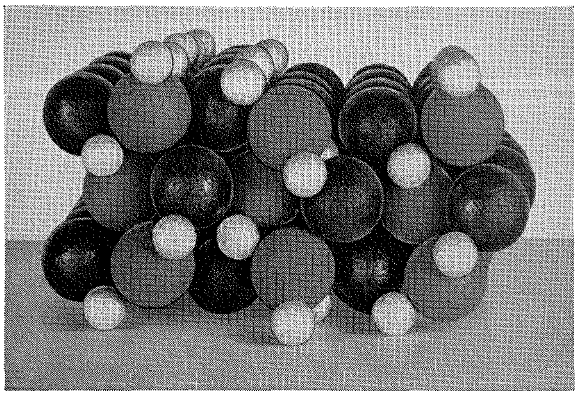

A. S. Russell

Fig. 28—Model of Beta Alumina Monohydrate c-Projection

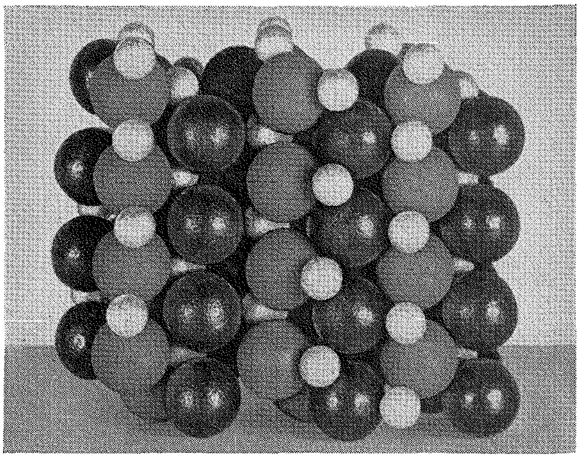

A. S. Russell

Fig. 29—Model of Beta Alumina Monohydrate a-Plane

TABLE 17

Typical Properties of Hydrated Aluminas

Chemical Analysis (dry basis), %	C-31	C-33	C-730	C-740	C-741
Al_2O_3	64.9	64.9	64.4	63.7	63.6
Na_2O	0.35	0.35	0.45	0.45	0.45
Fe_2O_3	0.010	0.003	0.02	0.02	0.02
SiO_2	0.02	0.02	0.05	0.05	0.05
Insoluble	0.04	0.04	....	....	....
Combined Water	34.7	34.7	34.9	34.3	34.2
Water Adsorbed at 50% Humidity	0.03	0.03	0.21	0.25	0.43
Coconut Oil	....	....	....	1.0	....
Stearic Acid	....	....	....	....	1.0
Cumulative Screen Analysis, %					
+100 mesh	0-0.6	0-0.6	....	....	....
+200 mesh	0-8	0-8	....	....	....
+325 mesh	20-40	20-40	....	....	....
−325 mesh	60-80	60-80	....	....	....
Physical Properties					
Bulk Density, Packed, lb/ft^3	75-85	75-85	21-28	32-42	32-42
Bulk Density, Loose, lb/ft^3	60-70	60-70	16-21	27-37	27-37
Specific Gravity	2.42	2.42	2.40	2.38	2.38
Surface Area, m^2/g	0.1	0.2	10	10	10
Average Number Particle Diameter, microns	....	....	0.05	0.06	0.06

and the OH—O distance, i.e., the length of the hydrogen bond. Diaspore is included in these discussions and is also mentioned in Lecompte's review paper on the infrared spectra of water in solids.

The crystals are generally flattened in the [010] direction; they are readily divided and have parallel fibers in the direction [001]. From photomicrographs and electron micrographs, Ervin and Osborn showed beta monohydrate to develop hydrothermally as square prisms, sometimes twinned, with growth predominantly in the c-axis direction resulting in needles or even fibers. During his investigations Hill showed a complete series of solid solutions between beta monohydrate and the corresponding gallia monohydrate.

Beta monohydrate is scarcely attacked by caustic soda solutions under conditions where alpha monohydrate can be dissolved.

USES OF HYDRATED ALUMINAS

A. *Hydrated Alumina C-30 Series*

These aluminas are fine, white crystals of alpha trihydrate. The Combination Process (a development of Alcoa Research Laboratories) enables production of snow-white, organic-free hydrated alumina with higher reactivity and lower insoluble content than ever before. Two grades are available (Table 17), Hydrated Alumina C-33 having lower iron content than C-31. Hydrated Aluminas C-30 Series find applications in the manufacture of chemicals, catalysts, glass, vitreous enamel and ceramic whitewares. The first two of these are most important in terms of tonnage consumed. Compounds made from hydrated alumina are aluminum sulfate, aluminum chloride (hydrated), aluminum nitrate, sodium aluminate and sodium aluminum sulfate. "Iron-free alum" is low-iron aluminum sulfate as distinguished from commercial "filter alum." The purer form of aluminum sulfate is used in the paper industry and also in the manufacture of other aluminum compounds. Aluminum chloride (anhydrous) is a catalyst in organic reactions, and the hydrous form is used in the reprocessing of used wool. Aluminum nitrate is a mordant in the dyeing of textiles. Sodium aluminate is marketed as a coagulant and softener for water supplies, and sodium aluminum sulfate goes into baking powder.

Many aluminum compounds are made using aluminum sulfate as an intermediate. The more important of these are the acetate, formate, stearate and resinate, and also such pharmaceutical compounds as the citrate, gluconate and lactate, and gelatinous aluminum hydroxide. Aluminum acetate and formate are used in textile dyeing. The stearate and resinate have applications in paint and varnish and in waterproofing. Aluminum stearate is also used in lubricating greases. Another product made from aluminum sulfate is "light" aluminum hydrate, which is a fine, fluffy basic aluminum sulfate used in lake pigments and as a bodying agent for lithographic ink.

For preparation of alumina catalysts, one type of process involves precipitation of gelatinous aluminum hydroxide by neutralization of aluminum sulfate or other soluble aluminum salt. Other metal oxides or salts are often either co-precipitated with the alumina or subsequently mixed with it, after which it is dried and calcined to produce the catalyst. In other catalytic preparations, hydrated alumina is used directly. It is formed into pills or briquettes, often with small amounts of other metal salts. The briquettes are then calcined to produce the active catalyst.

In glass manufacture, hydrated alumina is added directly to the glass melt in a proportion between 2 and 4% of the total batch. It has been shown (Seger, Schweig) that alumina reduces viscosity of the molten glass, assists fusion, reduces corrosion of the furnace refractories, facilitates annealing, retards devitrification, increases resistance to chemical attack, improves mechanical strength and improves the appearance of the finished glass.

For vitreous enamel and as a part of the glazing mixture for whiteware bodies, the function of hydrated alumina is to improve the luster and smoothness of the surface.

B. Hydrated Alumina C-700 Series

The applications of Hydrated Alumina C-700 Series (see Table 17 for typical properties of the several grades) are dependent in most cases on some of the following physical properties: uniformly fine (less than one micron) particles, white color, low refractive index, low specific gravity, nonhygroscopic quality and resistance to physical or chemical change at temperatures up to 150°C.

Almost all rubber products contain some small-particle filler to improve physical properties, reduce raw material cost, or facilitate factory operations. Hydrated alumina is a reinforcing filler, which increases abrasion resistance, tear resistance, tensile strength and modulus of elasticity. Foam rubber is not usually reinforced by even the best of the fillers. However, C-730 improves the load-carrying capacity of foam rubber in addition to reducing its volume cost.

Hydrated alumina in plastics reduces volume cost with a minimum decrease in physical properties. In polyvinyl chloride, C-730 actually increases tensile strength and tear resistance up to ten parts of the hydrate in one hundred parts of resin.

Clay is the basic pigment used for book and magazine paper coatings. Calcium carbonate is sometimes added to the clay to increase the whiteness of the coating. Hydrated Alumina C-730 replaces all or part of the calcium carbonate with a resulting improvement in whiteness, opacity, gloss and smoothness.

For adhesive tape, hydrated alumina gives body to the adhesive mixture without detracting from its adhesiveness. It is about equal to zinc oxide and superior to other fillers in this respect.

In varnish and oil paints, this alumina increases viscosity, and thus acts as a bodying agent. Its low refractive index permits its use in some varnishes without reduction in the clarity. In water paints, hydrated alumina acts as an opacifying agent. In the presence of oil, the hydrate loses its opacity because of its relatively low refractive index.

In tooth paste, C-730 acts as a bodying agent and, being thixotropic, produces a firm paste that does not run off the brush. For tooth powder, the soft texture and absence of grit are desirable properties. The bodying properties and smooth, soft texture of this alumina are desirable in both cosmetic creams and cosmetic powders.

Hydrated Alumina C-730 is a general-purpose grade. Hydrated Alumina C-740 is the same as C-730 except that the particles are coated with coconut oil. It is recommended as a reinforcing pigment for rubber compounds. Hydrated Alumina C-741 is the same as C-730 except that the particles are surface coated with stearic acid. It is recommended as a reinforcing pigment for rubber compounds and as a filler for plastics.

AMORPHOUS AND GEL ALUMINAS

Amorphous alumina is frequently encountered in the decomposition of aluminum compounds, in the precipitation of alumina from solution and in the oxidation of aluminum. In the dehydration sequences, Stumpf assigned a characteristic broad X-ray line at 4.5 Å to the amorphous phase.

A model consisting of two Al_2O_3 molecules, was found by Wilsdorf to agree satisfactorily with the electron diffraction rings of the amorphous alumina produced by 75-hour air oxidation of aluminum. This contains an octahedron of six closely packed oxygen ions with four aluminum ions in a tetrahedral arrangement and ionic distances of 2.80 and 3.95 Å for O-O; 1.72 and 3.28 Å for O-Al; and 2.80 Å for Al-Al.

Dinwiddie and co-workers produced alpha monohydrate by hydrolyzing an aluminum alcoholate above the boiling point of water, providing excess water and alcohol were removed from the hydrolysis distillation zone within 45 minutes.

Watson (1957) investigated the structure of Wislizenus fibrous alumina produced by the action of a small amount of water on slightly amalgamated aluminum. The material was composed of amorphous fibrils 70-80 Å in diameter, orientated parallel to the length of the fiber. Amorphous particles arranged linearly, less than 50 Å in diameter, were the ultimate building blocks of these fibrils.

Papée (1958) described a strictly amorphous alumina gel prepared by precipitation of aluminum nitrate at pH 8 with ammonia, followed by rapid washing and drying under vacuum at 25°C to constant weight. The composition of the product was $Al_2O_3 \cdot 3.45H_2O$ contaminated with less than 0.1 per cent NO_3^-. Its surface area was 170 m^2/g. It showed a broad X-ray band at 1.4 Å.

Harris and Sing discussed the surface area of alumina formed by interaction of sodium hydroxide and aluminum salt solutions, and by hydrolysis of aluminum isopropoxide. The latter gave a peak area of 1130 m^2/g and retained 300 m^2/g on aging.

The three types of aluminum hydroxide gel C_α, C_β and C_γ, which were originally prepared by Willstätter, have (Kraut, Fricke and Schmäh, Souza Santos, Watson) the following aging sequences and properties: C_α, the initial form, transforms in a few hours to C_β which goes over to C_γ in a matter of several weeks at a pH of 7.5 but in one week at pH 10.2. C_α corresponds in water content to a trihydrate, is amorphous, and is easily soluble in hydrochloric acid or sodium hydroxide. C_β consists of fibrils of $Al_2O_3 \cdot 2.2H_2O$ which show alpha monohydrate lines. C_γ has the water content of a trihydrate and shows the lines of both alpha and beta trihydrate, the two phases having different crystal habits. C_γ is not changed by hot ammonia and is only difficultly soluble in hydrochloric acid or sodium hydroxide.

To find a more convenient method for producing the C_γ gel required for purification of enzymes, Watson prepared gels and sols from ammonium

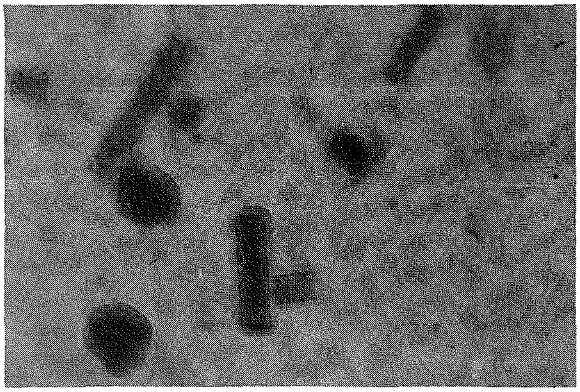

Turkevich and Hillier Analytical Chemistry

Fig. 30—Alumina Sol, 100,000X

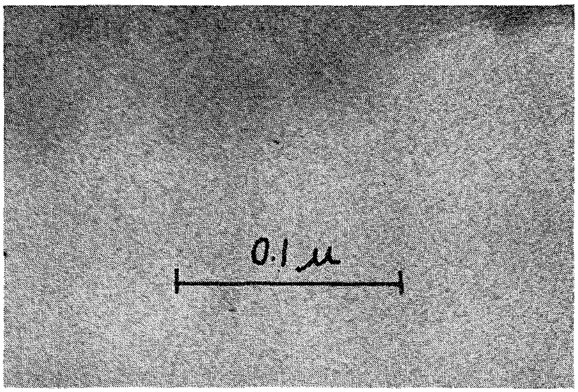

Turkevich and Hillier Analytical Chemistry

Fig. 31—Alumina Gel Dried at 80°C, 300,000X

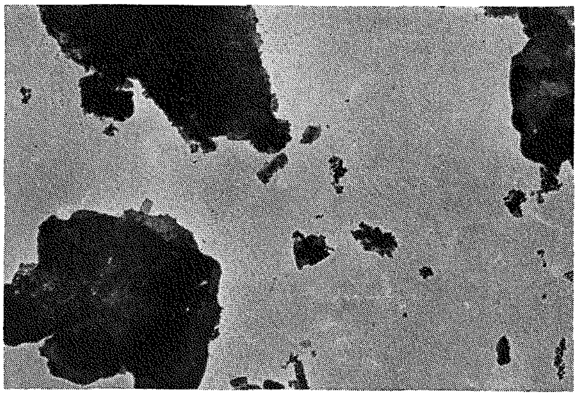

Turkevich and Hillier Analytical Chemistry

Fig. 32—Alumina Gel Steamed at 600°C, 16,500X

alum and from amalgamated aluminum. The several methods based on alum produced mixtures of alpha and beta trihydrates after aging, the sol and gel portions having identical X-ray patterns and electron microscope morphologies. Hexagonal prisms of alpha trihydrate and triangular or hour-glass somatoids of beta trihydrate constituted the principal structures. The somatoids had serrated edges and appeared to have an intrinsic structure of 40 Å thick platelets perpendicular to the long axis of the somatoids. An electron micrograph was shown of an alpha trihydrate hexagon mosaic, 40-80 Å high, 2000 Å long and 1200 Å wide, apparently formed directly by concentration of tiny particles of the background gel.

Souza Santos (1958) showed by X-ray diffraction and electron microscopic examination that Schmidt's modification of Willstätter's gel resembles Willstätter's C_β gel.

Sawamura observed a few fibers of 200 to 500 Å diameter on two-hour aging of a gel. In 24 hours, most of the crystals were arranged in fibers of this diameter, the crystals themselves being less than 50 Å in size.

Turkevich's and Hillier's electron micrographs of fresh hydrous alumina from aluminum nitrate plus ammonia showed finely divided spherical particles about 30 Å in diameter combined into fibers (Figure 30). On aging, these flexible fibers lined up to form rectangular plates. The fibrous nature of the alumina was retained on drying at 80°C (Figure 31) and even on heating to 350°C where the solid gel consisted of 30 Å particles arranged in nonrigid fibers. On further heating, particularly in steam, the granular fibers became rigidly arranged in plates and the fibers gradually disappeared to give smooth lathlike surfaces (Figure 32).

The aging by ammonia of an alumina sol prepared from aluminum metal with acetic acid is shown in Figures 33-35. Coagulation of fine fibrils into plates and then into hard structures is shown.

Calvet and Thibon pointed out the differences between the X-ray patterns of alpha monohydrate gels (pseudoböhmite a and b) and of well-crystallized alpha monohydrate. The well-crystallized gel prepared at over 150°C had a specific

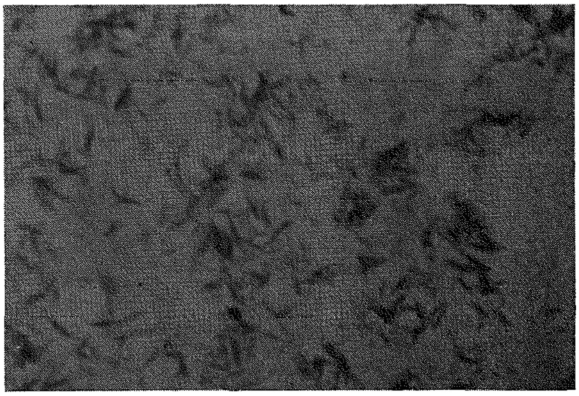

Fig. 33—Alumina Sol, 50,000X

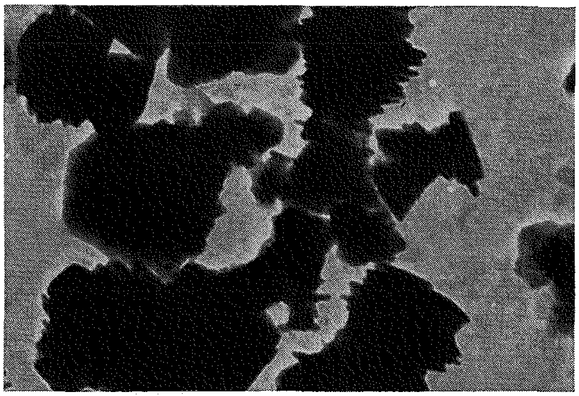

Fig. 35—Alumina Sol Further Aged, 50,000X

surface less than 10 m^2/g and a dehydration temperature of 350-400°C. The gel type prepared at less than 100°C had specific surface of 100 m^2/g or more and a progressive dehydration between 200 and 400°C. They also investigated the transformation of amorphous alumina to crystalline compounds. Gels prepared at pH less than 6 were amorphous. At pH 9 the gels were alpha monohydrate. The temperature at which the gel was dried, the adsorbed anion content and the degree of crystallinity affected the heat of wetting of the gel for normal sodium hydroxide. The temperature effect was attributed to the irreversible dehydration of the gel and confirmed by infrared spectra studies in these gels, water being absent. As the temperature was raised to 100°C, desiccation of the gel involved condensation of the hydroxyl ions. Aging of alumina gels at 100°C, in the presence of water or alkali, improved their crystallinity. Heating to 400°C did not change the structure of gels aged at 100°C. The difference between amorphous and alpha monohydrate gels was shown by differential thermal analysis. In the presence of sodium carbonate or bicarbonate, amorphous gels of alumina were transformed at room temperature into a crystalline double carbonate of sodium and aluminum. Crystallized gels of alumina did not give this reaction.

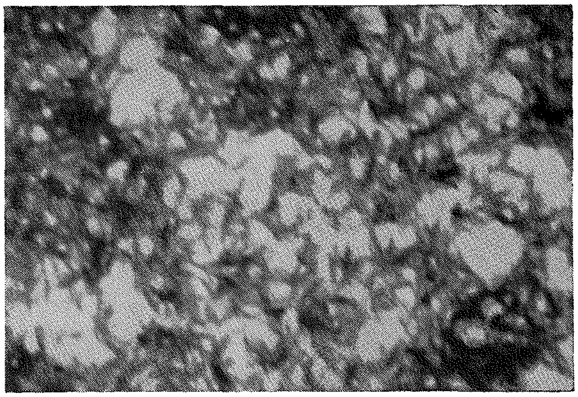

Fig. 34—Alumina Sol Partially Aged, 50,000X

Teichner and Imelik prepared pure amorphous aluminas by the action of water vapor or heat on aluminum methylate. The water content of the amorphous materials varied with the temperature of treatment and could be zero. Those with the water content of trihydrate lost water more readily than the usual alpha or beta trihydrates. Alumina from aluminum methylate decomposed at low temperature had a surface area of 300 m^2/g, and an X-ray pattern with weak halos at 4.5, 2.3 and 1.4 Å.

Teichner and Imelik also prepared gels from ammonia and aluminum nitrate of varying pH at the end of the precipitation. As pH increased from 5.1 to 9.1, the contained nitrate diminished from 0.4 to 0.00%, the water of constitution fell from 4.3 to 3.3 moles/mole of alumina, and the specific surface increased from 0 to 190 m^2/g. The gels changed with increasing pH from translucent to opaque grains, and the degree of crystallinity increased, alpha monohydrate being the phase, except for the preparation of pH 9.1 which also contained some beta trihydrate. For the gel prepared at pH 5.1, crystallinity increased with the number of washings. The gel precipitated at pH 5.1 increased in area to 25 m^2/g after calcination at 500°C where it still retained 0.3 mole of water/mole of alumina. Gels precipitated at higher pH lost their water of crystallization more readily and increased to higher surface areas. A gel precipitated at pH 5.1 was treated with potassium hydroxide in methanol. The nitrate was almost completely eliminated, and this solid had a surface area of 600 m^2/g. The gel produced in the cold had a composition $Al_2O_3 \cdot 3H_2O$ after evacuation at room temperature. This composition remained unchanged on standing in air, but the surface diminished progressively. X-ray diffraction analysis showed many lines in common with alpha monohydrate. Infrared bands ascribed to alpha or beta trihydrates or to alpha monohydrate were found in all the samples as well as in all their products of partial or complete decomposition.

The amorphous aluminas from the foregoing processes lost oxygen ($Al_2O_{2.96}$) by heating at 500°C in a 10^{-6} mm Hg vacuum. They turned black and became n-type semiconductors. Loss of oxygen from the surface led to a corresponding increase in specific surface. The black oxide became white in air at 500°C while its crystallinity increased (Teichner 1959).

The size of the primary crystals of the monohydrate varies widely with the nature of the anion, sulfate giving much finer diffraction bands (and hence finer particles) than chloride or nitrate. The highly dispersed adsorptive alumina floc in water purification practice is obtained from aluminum sulfate. The size of the primary crystals increased with increase in pH, with decrease in concentration, and with precipitant in this order: sodium sulfide, sodium carbonate, ammonia and sodium hydroxide (Weiser and Milligan 1952; Milligan 1951).

Weiser (1941) found that fresh alumina floc from aluminum sulfate solution at pH less than 5.5 was an amorphous basic salt of the formula $Al_2O_3 \cdot SO_3 \cdot 1.5H_2O$. No basic salts were formed in this way with aluminum chloride or nitrate at pH between 4 and 8. Kuczynski and Zagorski pointed out that alumina precipitated from aluminum sulfate solution by ammonia at pH 3.4, had low sorption and low mechanical strength, both properties being improved by basic precipitation. Arimori precipitated a basic alum from ammonium alum or aluminum sulfate heated with ammonia at 120 to 180°C, but this was transformed to alpha monohydrate in fresh water.

Gyani reported that hard, fairly transparent alumina can be prepared by precipitation from boiling solutions and immediate washing. Aging of the precipitated alumina at room temperature, particularly in the presence of a large quantity of soluble salts, leads to soft, chalky gels. The transformation of the precipitated hydroxide can be prevented by addition of acetic acid.

Lacroix stated that aluminum hydroxide starts to precipitate at a pH of 3.95 with 0.01 N hydrochloric acid solution, and that the pH of complete solution is 11.0. Marion and Thomas gave 7.7 as the pH of maximum precipitation of alumina from 0.02 M aluminum chloride solution by potassium hydroxide. Fluoride or oxalate raised the pH of maximum precipitation; sulfate, lactate and chloride lowered the value; and citrate and tartrate caused a sharp drop. Pavella determined photometrically that about half the stoichiometric quantity of base (ammonia or sodium hydroxide) was required to precipitate the alumina from aluminum sulfate solution.

Graham and Thomas found that the rate of neutralization of various 0.2 N acids by hydrous alumina at 25°C was most rapid for HF and decreased in the order H_3PO_4, $H_2C_2O_4$, H_2SO_4, HNO_3, HCl, CH_3COOH, H_2NSO_3H, $HClO_4$, which agrees in general with the tendency of the negative ion to form stable aluminum complexes. Graham and Horning found the addition of hydrous alumina at 25°C to 0.1 M or 0.05 M solutions of the potassium salts at pH 7.00 to increase the pH to the following values: fluoride 9.6, oxalate 8.6, sulfate 8.0, nitrate 7.3, chloride 7.3, perchlorate 7.1 and phosphate 7.0, the increase being ascribed to displacement of OH groups from the surface by the anions. Schmäh reported very pure alumina gel to have an alkaline surface reaction, adsorbing potassium chloride, perchlorate and sulfate from neutral solutions to a pH of 8.5 to 9.5.

Szabo listed the following values for the solubility products:

	20°C	30°C
$(Al^{+3}) \times (OH^-)^3 =$	$1.25 \cdot 10^{-33}$	$1.92 \cdot 10^{-32}$
$(AlO_2^-) \times (H^+) =$	$1.80 \cdot 10^{-13}$	$1.34 \cdot 10^{-13}$

The paper summarizes many earlier determinations. Fricke and Schmäh gave the solubility of very pure aluminum hydroxide in water as less than 10^{-6} mole/liter.

Dekker and Van Geel found the dielectric constant of the amorphous and crystalline layers formed by anodic oxidation of alumina to be equal. Gulbransen and Wysong found the formation of amorphous alumina from purest aluminum and oxygen to have an energy of activation of 22.8 kcal/mole and an entropy of activation of -26 cal/mole deg. This is equivalent to a rate of about 8 micrograms/cm^2 hr at 500°C or a thickness increase of 400 Å/hr.

MOLTEN AND GASEOUS ALUMINA

Brewer and Searcy concluded from vapor pressure measurements that Al_2O gas was evolved from alumina heated with aluminum and that AlO was the principal aluminum species when alumina volatilized. Cochran also found that Al_2O was evolved from the aluminum-alumina reaction but that no AlO was present in the reaction vapors. By high-temperature X-ray techniques, Hoch and Johnston found that Al and Al_2O_3 were the stable phases below 1000°C, Al_2O between 1050 and 1600°C and AlO above 1500°C. Both Al_2O and AlO are cubic, the lattice constants being 4.98 Å (at 1100°C) and 5.67 Å (at 1700°C), respectively. Intense ion currents of Al_2O^+ formed from gaseous Al_2O in the aluminum-alumina system were identified mass spectrometrically by Porter. At 1477°C ions formed from other gaseous oxides were very much less intense than Al_2O^+. The appearance potential of Al_2O^+ was 7.7 ± 0.2 ev. For the reaction, $Al_2O(g) = 2Al(g) + O(g)$, $\Delta H_{298} = 256 \pm 7$ kcal/mole.

More recently Navias made studies of the chemical stability of certain electronic tube structures, as being pertinent to the volatility of aluminum oxide. From his data an upper limit for the evaporation rate of aluminum oxide out of contact of possible reactants has been estimated to be about 4,000 times less at 1900°C than the extrapolated value from Brewer and Searcy's data. A sapphire rod was used in subsequent tests by Sears and Navias.

Wartenberg (1951) found molten alumina to absorb water and concluded that the water must be bound as a hydroxide. He claimed that alumina was more volatile in the presence of water vapor than in dry air, so that gaseous aluminum hydroxide is also stable.

BIBLIOGRAPHY

Note: Figures appearing in **boldface** indicate locations within the text where these references may be found.

Achenbach, H., Chem. Erde *6*, 307-56 (1931). **P. 44.**

Activated Alumina: Its Properties and Uses, Aluminum Company of America, Pittsburgh (1949). **Tables 4, 15.**

Activated Alumina Maintenance Program: Power System Oils, Aluminum Company of America, Pittsburgh (1955). **P. 61.**

Adelsköld, V., Arkiv Kemi, Mineral. Geol. *12A*, No. 29, 9 pp. (1938). **Table 2.**

Akiyama, K., J. Soc. Chem. Ind. Japan *42*, Suppl. 394-5 (1939). **P. 19.**

Aleixandre Ferrandis, V., Anales fis. y. quim. (Madrid) *41*, 709-45 (1945). **P. 58.**

Alfred University, Final Report "Study of Heat Transfer of Ceramic Materials" (1957). Contract Nonr-1503(02), NR-32-022. **P. 16.**

Arimori, T., J. Soc. Chem. Ind. Japan *45*, 370-5 (1942). **P. 71.**

Arizumi, T. and Tani, S., J. Phys. Soc. Japan *5*, 442-7 (1950). **Table 5.**

Arkel, A. E. van and Fritzius, C. P., Rec. trav. chim. *50*, 1035-45 (1931). **P. 65.**

Asselmeyer, F., Z. angew. Physik *1*, 26-35 (1948). **P. 62.**

Attinger, C., Bull. Soc. Suisse Chronometrie, June, 1951. **P. 17.**

Austin, C. R., Schofield, H. Z. and Haldy, N. L., J. Am. Ceram. Soc. *29*, 341-54 (1946). **P. 23.**

Avdalian, D., Compt. rend. acad. sci. U.R.S.S. *1*, 173-5 (1936). **P. 38.**

Bailey, W. A., Jr. and Bittner, C. W., U. S. Patent 2,398,610 (March 16, 1946). **P. 11.**

Barlett, H. B., J. Am. Ceram. Soc. *15*, 361-4 (1932). **Pp. 8, 19.**

Barnitt, J. B., U. S. Patent 1,868,869 (July 26, 1932). **P. 53.**

Barnitt, J. B., Derr, R. B. and Scripture, E. W., Jr., Ind. Eng. Chem. Anal. Ed. *2*, 355-7 (1930). **P. 53.**

Bárta, R., Bartuška, M., Hlaváč, J. and Procházka, S., (Chem. Technol. Univ., Prague) Silikáty *1*, 77-83 (1957). **P. 16.**

Bates, J. L. and Gibbs, P., "Some Optical Properties of Corundum," University of Utah Progress Report V, ASTIA AD 140406 (1957). **P. 15.**

Baumann, H. N., Jr., Bull. Am. Ceram. Soc. *35*, 387-90 (1956). **P. 28.**

Bauple, R., Gilles, A., Romand, J. and Vodar, B., J. Opt. Soc. Am. *40*, 788-9 (1950). **P. 16.**

Beckman, J., "A History of Inventions, Discoveries and Origins," Translated from the German by William Johnston, 4th Ed. Revised and Enlarged by William Francis and J. W. Griffith. Henry G. Bohn, London (1846). **P. 7.**

Beevers, C. A. and Brohult, S., Z. Krist. *95*, 472-4 (1936). **Table 2.**

Belova, E. N. and Ikornikova, N. Yu., Doklady Akad. Nauk S.S.S.R. *81*, 829-32 (1951). **P. 13.**

Bemmelen, J. M. van, Rec. trav. chim. *7*, 75-87 (1888). **P. 62.**

Bergmann, O., Thesis T. H. Graz nr. 25,000/428 (1958). **P. 38.**

Berman, R., Proc. Roy. Soc. (London) *A208*, 90-108 (1951). **Table 4.**

Bentley, F. J. L. and Feachem, C. G. P., J. Soc. Chem. Ind. (London) *64*, 148-9 (1945). **P. 51.**

Bhagavantam, S. and Venkatarayudu, T., Proc. Indian Acad. Sci. *9A*, 224-58 (1939). **P. 16.**

Bhimasenachar, J., Current Sci. (India) *18*, 372-3 (1949). **Table 7.**

Biegler, Hanns, Thesis T. H. Graz nr. 25,000/429$_1$ (1957). **P. 37.**

Bienvenue, L. L. and Dixon, C. E., Bull. Am. Phys. Soc. *4*, 464 (1959). **P. 17.**

Biltz, W. and Lemke, A., Z. anorg. allgem. Chem. *186*, 373-86 (1930). **Fig. 16.**

Blackburn, A. R., Shevlin, T. S. and Lowers, H. R., J. Am. Ceram. Soc. *32*, 81-9 (1949). **P. 32; Table 9.**

Blanchin, L., Thesis, University of Lyon, June 24, 1952. **Pp. 40, 43; Fig. 16; Table 13.**

Blanchin, L., Imelik, B. and Prettre, M., Compt. rend. *233*, 1106-8 (1951); 1029-31 (1951). **P. 40.**

Boehm, J. and Jäntsch, J., Collection Czechoslov. Chem. Communs. *15*, 708-16 (1951). **P. 50.**

Boerskov, G. K., Dzis'ko, V. A. and Borisova, M. S., Zhur. Fiz. Khim. *27*, 1176-80 (1953). **P. 49.**

Boerskov, G. K., Dzis'ko, V. A., Borisova, M. S. and Krasnopol'skaya, V. N., Zhur. Fiz. Khim. *26*, 492-9 (1952). **P. 49.**

Bogoroditskii, N. P. and Polyakova, N. L., Doklady Akad. Nauk S.S.S.R. *95*, 257-9 (1954). **P. 23.**

Böhm, J., Z. anorg. allgem. Chem. *149*, 203-16 (1925). **P. 8; Table 1.**

Böhm, J. and Nichassen, H., Z. anorg. allgem. Chem. *132*, 1-9 (1924). **P. 8.**

Bonshtedt-Kupletskaya, E. M. and Vlodavets, N. I., Compt. rend. acad. sci. U.R.S.S. *49*, 587-9 (1945). **P. 63; Table 8.**

Bor, L., J. Am. Ceram. Soc. *33*, 375-6 (1950). **P. 19.**

Boutillon, G. and Prettre, M., Compt. rend. *240*, 1216-8 (1955). **P. 57.**

Bowen, N. L. and Greig, J. W., J. Am. Ceram. Soc. *7*, 242 (1924). **Fig. 4.**

Bower, J. H., J. Res. Bur. Stds. *33*, 199-200 (1944). **P. 53.**

Bragg, W. L., Gottfried, G. and West, J., Z. Krist. *77*, 255-74 (1931). **Pp. 19, 64; Table 2.**

Braun, P. B., Nature *170*, 1123 (1952). **P. 37; Table 2.**

Brewer, L. and Searcy, A. W., J. Am. Chem. Soc. *73*, 5308-14 (1951). **P. 72; Table 4.**

Brey, W. S., Jr. and Krieger, K. A., J. Am. Chem. Soc. *71*, 3637-41 (1949). **P. 60.**

Bridgman, P. W., Proc. Am. Acad. Arts Sci. *77*, 187-234 (1949). **Table 7.**

Brindley, G. W. and Nakshira, M., Nature *183*, 1620 (1959). **P. 35.**

Brockmann, H., Dis. Faraday Soc. No. *7*, 58-64 (1949). **P. 58.**

Bron, V. A., Ogneupory *16*, 312-23 (1951). **P. 11.**

Brownmiller, L. T., Am. J. Sci. *29*, 260-77 (1935). **P. 18.**

Bryan, J. M., J. Soc. Chem. Ind. (London) *69*, 169-72 (1950). **P. 64.**

Budnikov, P. P., Tresvyatskii, S. G. and Kushakovskii, V. I., Doklady Akad. Nauk S.S.S.R. *93*, 281-3 (1953). **Fig. 4.**

Bugosh, J., U. S. Patent 2,915,475 (December 1, 1959). **P. 65.**

Burgers, W. G., Claassen, A. and Zernike, J., Z. Physik. *74*, 593-603 (1932). **P. 34.**

Burnham, J. and Robinson, P., Natl. Research Council, Div. Eng. and Ind. Research Ann., Rept. Conf. on Elect. Insulation 1948, 68-71 (1949). **P. 38.**

Busing, W. R. and Levy, H. A., Acta Cryst. *11*, 798-803 (1958). **P. 65.**

Cabannes-Ott, C., Compt. rend. *244*, 2491-5 (1957). **P. 65; Table 10.**

Caglioti, V. and D'Agostino, O., Gazz. chim. ital. *66*, 543-8 (1936). **P. 34.**

Cahoon, H. P. and Christensen, C. J., Tech. Rept. XLII, Inst. for the Study of Rate Processes, Univ. of Utah (1955). **Pp. 11, 17.**

Cahoon, H. P. and Christensen, C. J., J. Am. Ceram. Soc. *39*, 337-44 (1956). **P. 18.**

Calvet, E., J. Polymer Sci. *8*, 163-71 (1952). **P. 43.**

Calvet, E. and Thibon, H., Bull. soc. chim. France 696-702 (1953). **P. 69.**

Calvet, E. and Thibon, H., Bull. soc. chim. France 1343-6 (1954). **P. 51.**

Calvet, E., Boivinet, P., Noel, M., Thibon, H., Maillard, A. and Tertian, R., Bull. soc. chim. France 99-108 (1953). **P. 69.**

Cannon, H. S., Metal Prog. *67*, 83-7 (April, 1955). **P. 29.**

Carnahan, R. D., Johnston, T. L. and Li, C. H., J. Am. Ceram. Soc. *41*, 343-7 (1958). **P. 18.**

Carruthers, T. G., Metallurgia *44*, 103-7 (1951). **P. 32.**

Carruthers, T. G. and Gill, R. M., Trans. Brit. Ceram. Soc. *54*, 59-68, 69-82 (1955). **Pp. 32, 43.**

Chang, R., "Creep of Al_2O_3 Single Crystals," Atomics International Report NAA-SR-4297 (1959). **P. 17.**

Chang, R., J. Nuclear Materials *1*, 174-81 (1959). **P. 17.**

Charles, R. J., "The Strength of Silicate Glasses and Some Crystalline Oxides," 9-1 to 9-32; Conference on Fracture (held by National Academy of Sciences, Washington, D. C., April 1959). **P. 17.**

Charrier, J. and Papée, D., Compt. rend. *237*, 897-9 (1953). **P. 38.**

Charvat, F. R. and Kingery, W. D., J. Am. Ceram. Soc. *40*, 306-15 (1957). **P. 16.**

Chesters, J. H., See Ceramics, a Symposium, Green, A. T. and Stewart, G. H., British Ceramic Society, Stoke-on-Trent, 637-650 (1953). **P. 25.**

Chrêtien, A. and Papée, D., Compt. rend. *234*, 214-6 (1952). **P. 47.**

Coble, R. L., J. Am. Ceram. Soc. *41*, 55-62 (1958). **P. 13.**

Coble, R. L. and Kingery, W. D., J. Am. Ceram. Soc. *39*, 377-85 (1956). **P. 17.**

Coblentz, W. W., Jahrb. Radioakt. *3*, 397 (1906). **P. 65.**

Cochran, C. N., J. Am. Chem. Soc. *77*, 2190-1 (1955). **P. 72.**

Cohen, J., Bull. Am. Ceram. Soc. *38*, 441-6 (1959). **P. 16.**

Cooke, P. W. and Haresnape, J. N., Trans. Faraday Soc. *43*, 395-8 (1947). **Fig. 8.**

Cornelius, E. B., Milliken, T. H., Mills, G. A. and Oblad, A. G., J. Chem. Phys. *59*, 10-14, 809-13 (1955). **Pp. 54, 60.**

Courtial, R., Trambouze, Y. and Prettre, M., Compt. rend. *242*, 1976-9 (1956). **P. 42.**

Courtial, R. and Trambouze, Y., Compt. rend. *244*, 1764-6 (1957). **P. 42.**

Cowley, J. M., Acta Cryst. *6*, 53-4, 846-53 (1953). **Pp. 8, 37.**

Cross, C. F., J. Chem. Soc. *35*, 796 (1879). **P. 53.**

Cutler, I. B., Bradshaw, C., Christensen, C. J. and Hyatt, E. P., J. Am. Ceram. Soc. *40*, 134-9 (1957). **P. 11.**

Damerell, V. R., Hovorka, F. and White, W. E., J. Phys. Chem. *36*, 1255-67 (1932). **P. 44.**

Dana, J. D., System of Mineralogy I, 7th Ed. Revised and Edited by Palache, C., Berman, H. and Frondel, C., New York, Wiley (1944). **Pp. 13, 61; Tables 2, 8.**

Davy, H., Phil. Trans. *95*, 155, 1621 (1805). **P. 7.**

Day, M. K. B. and Hill, V. J., Nature *170*, 539 (1952); J. Phys. Chem. *57*, 946-50 (1953). **P. 51.**

Day, M. K. B. and Hill, V. J., J. Phys. Chem. *57*, 946-50 (1953). **Table 1.**

De Boer, J. H. and Houben, G. M. M., Proc. Intern. Symposium Reactivity of Solids (Gothenburg) Part 1, 237-44 (1952). **P. 37.**

De Boer, J. H., Angew. Chem. *70*, 383-9 (1958). **Pp. 40, 43; Figs. 13, 14.**

De Kayser, W. L., Rev. gen. sci. appl. (Brussels) *1*, No. 3, 84-108 (1952); Bull. soc. chim. Belges *60*, 516-41 (1952). **P. 45.**

De Lapparent, J., Compt. rend. *184*, 1661-2 (1927). **P. 8.**

De Morveau, L. B. Gyton, Encyclopedie methodique, Paris (1786); Dictionaire de Physique, Article "Alun." **P. 7.**

De Pablo-Galan, L. and Foster, W. R., J. Am. Ceram. Soc. *42*, 491-8 (1959). **P. 22.**

Deadmore, D. L., Ceram. Age *56*, No. 7, 15-17, 23-24 (1951). **P. 30.**

Deflandre, M., Bull. soc. franc. mineral. *55*, 140-65 (1932). **P. 50.**

Dekker, A. J. and Geel, W. Ch. van, Philips Research Repts. 2, 313-20 (1947). **P. 72.**

Derr, R. B., U. S. Patent 2,015,593 (September 24, 1935). **P. 53.**

Derr, R. B., Ind. Eng. Chem. *30*, 384-8 (1938). **P. 55.**

Derr, R. B. and Willmore, C. B., Ind. Eng. Chem. *31*, 866-8 (1939). **Table 14.**

Desmarquest, J. M., Métaux (Corrosion-Ind.) *28*, 24-7 (1953). **P. 18.**

Dewey, C., Am. J. Sci. (1) *2*, 249 (1820). **P. 7.**

Dinwiddie, J. A., Milligan, W. O. and Mosesman, M. A., Light Metals Bull. *18*, 554 (1956); U. S. Patent 2,749,216 (June 5, 1956). **P. 68.**

Dontsova, E. I., Doklady Akad. Nauk S.S.S.R. *103*, 155-7; *105*, 305-8 (1955). **P. 39.**

Dowden, D. A., J. Chem. Soc. 242-65 (1950). **P. 60.**

Dragsdorf, R. D. and Webb, W. W., Bull. Am. Phys. Soc. *2*, 342 (1957). **P. 18.**

Drake, L. C. and Ritter, H. L., Ind. Eng. Chem. Anal. Ed. *17*, 787-91 (1945). **P. 43.**

Duval, C. and Lecomte, J., Bull. soc. chim. *8*, 713-24 (1941). **P. 62.**

Eberspächer, O., Z. Wiss. Mikroskopie *60*, 393 (1952). **P. 63.**

Economos, G., Ind. Eng. Chem. *45*, 458-9 (1953). **Table 9.**

Edwards, J. D., Frary, F. C. and Jeffries, Z., The Aluminum Industry: Aluminum and Its Production, New York, McGraw-Hill, 1930, 164-9. **P. 8; Table 1.**

Eliasson, B. A. E., Canadian Patent No. 504,385 (1954). **P. 11.**

Elmore, K. L., Mason, C. M. and Hatfield, J. D., J. Am. Chem. Soc. *67*, 1449-52 (1945). **P. 62.**

Ernst, T. and Wartenberg, H. von, Z. angew. Mineral. *1*, 115-24 (1938). **P. 32.**

Ervin, G., Acta Cryst. *5*, 103-8 (1952). **Pp. 37, 50.**

Ervin, G. and Osborn, E. F., Office of Naval Research Contract N6onr-26909, NR071-062, Code 428, August 26, 1949; J. Geol. *59*, 381-94 (1951). **Pp. 49, 50, 51, 64, 66; Fig. 8; Table 8.**

Ewing, F. J., J. Chem. Physics *3*, 203-7 (1935). **P. 65.**

Ewles, J. and Heap, C. N., Trans. Far. Soc. *48*, 331-8 (1952). **P. 60.**

Eyraud, C. and Goton, R., J. Chim. Phys. *51*, 430-33 (1954). **Pp. 40, 49.**

Eyraud, C., Goton, R. and Prettre, M., Compt. rend. *238*, 1028-31 (1954); *240*, 1082-4 (1955). **Pp. 40, 49.**

Eyraud, C., Goton, R., Trambouze, Y., Tran-Huu-The and Prettre, M., Compt. rend. *240*, 862-4 (1955). **Pp. 40, 49.**

Fichter, R., Helv. Phys. Acta *19*, 21-40 (1946); Helv. Chim. Acta *30*, 2010-13 (1947). **Table 10.**

Fisher, H. E., Oil Gas J. *48*, No. 22, 229 (1949). **Table 14.**

Foster, A. G., Dis. Faraday Soc. No. 3, 41-51 (1948). **P. 43.**

Foster, L. M. and Stumpf, H. C., J. Am. Chem. Soc. *73*, 1590-5 (1951). **Pp. 34, 38.**

Foster, L. M., Long, G. and Hunter, M. S., J. Am. Ceram. Soc. *39*, 1-11 (1956). **P. 35.**

Foster, P. A., J. Electrochem. Soc. *106*, 971-5 (1959). **P. 37; Table 8.**

Frary, F. C., Ind. Eng. Chem. *38*, 129-31 (1946). **P. 61; Table 1.**

Frederickson, L. D., Anal. Chem. *26*, 1883-5 (1954). **P. 63; Table 10.**

Freymann, M. and Freymann, R., Compt. rend. *232*, 401-3 (1951). **P. 54.**

Fricke, R., Z. anorg. allgem. Chem. *175*, 249-56 (1928). **Pp. 8, 63.**

Fricke, R., Z. anorg. allgem. Chem. *179*, 287-92 (1929). **P. 8.**

Fricke, R. and Eberspächer, O., Z. anorg. Chem. *265*, 21-40 (1951). **Pp. 37, 45; Table 13.**

Fricke, R. and Hüttig, G. F., Handbuch der allgemeinen Chemie IX, Hydroxyde und Oxyhydrate, Leipzig: Akad. Verlagsges (1937) 57-113. **P. 61.**

Fricke, R., Handbuch der Katalyse IV, 144. **Table 4.**

Fricke, R. and Jockers, K., Z. Naturforsch. *2b*, 244 (1947). **Pp. 51, 62, 64; Fig. 16.**

Fricke, R. and Jockers, K., Z. anorg. Chem. *265*, 41-8 (1951). **Pp. 43, 45; Table 13.**

Fricke, R. and Jockers, K., Z. anorg. Chem. *262*, 3 (1950). **P. 35.**

Fricke, R. and Jucaitis, P., Z. anorg. allgem. Chem. *191*, 129-49 (1930). **P. 62.**

Fricke, R. and Keefer, H., Z. Naturforsch. *4a*, 76-7 (1949). **Pp. 39, 62, 64.**

Fricke, R. and Neugebauer, W., Naturwissenschaften *37*, 427 (1950). **P. 59.**

Fricke, R., Neugebauer, W. and Schäfer, H., Z. anorg. Chem. *273*, 215-26 (1953). **P. 59.**

Fricke, R., Niermann, F. and Feichtner, C., Ber. *70B*, 2318-30 (1937). **P. 39.**

Fricke, R. and Schmäh, H., Z. anorg. Chem. *255*, 253-68 (1948). **Pp. 68, 72.**

Fricke, R. and Severin, H., Z. anorg. allgem. Chem. *205*, 287-308 (1932). **Pp. 40, 47, 64; Tables 2, 5.**

Fricke, R. and Weitbrecht, G., Z. anorg. Chem. *253*, 30-6 (1945). **P. 11.**

Fricke, R. and Wullhorst, B., Z. anorg. allgem. Chem. *205*, 127-44 (1932). **P. 62; Table 5.**

Fulda, W. and Ginsberg, H., Tonerde und Aluminium, Part I, Die Tonerde, Berlin, Walter de Gruyter (1951). **P. 7.**

Funaki, K., Bull. Tokyo Inst. Tech. B-1 (1950). **P. 18.**

Funaki, K. and Shimizu, Y., J. Chem. Soc. Japan, Ind. Chem. Sect. *55*, 194-6 (1952); *56*, 53-6 (1953). **P. 47.**

Furukawa, G. T., Douglas, T. B., McCoskey, R. E. and Ginnings, D. C., J. Research Natl. Bur. Standards *57*, 67-82 (1956). **P. 16; Table 4.**

Gallup, J., J. Am. Ceram. Soc. *18*, 144-8 (1935). **P. 18.**

Garrido, J., Bol. acad. cienc. exactas, fis. nat. (Madrid) *2*, No. 7, 1-3 (1936). **P. 50.**

Geller, R. F. and Yavorsky, P. J., J. Research Natl. Bur. Standards *35*, 87-110 (1945). **P. 23; Table 4.**

Geller, R. F., Yavorsky, P. J., Steierman, B. L. and Creamer, A. S., J. Research Natl. Bur. Standards *36*, 277-312 (1946). **P. 23.**

Gerdien, H., Z. Elektrochem. *39*, 13-20 (1933). **Table 5.**

Getty, R. J., Lamb, C. E. and Montgomery, W. C., Petroleum Eng. *25*, B-7-B-10 (1953). **P. 56.**

Gibbs, P., Kinetics of High-Temperature Processes, John Wiley and Sons, New York, 21-37 (1959). **Pp. 15, 16.**

Gilles, A., J. phys. radium *13*, 247 (1952). **P. 16.**

Ginsberg, H. and Hüttig, W., Z. anorg. allgem. Chem. *285*, 160-72 (1956). **P. 61.**

Ginsberg, H., Hüttig, W. and Strunk-Lichtenberg, G., Z. anorg. allgem. Chem. *293*, 33-46, 204-13 (1957). **Pp. 8, 34, 37, 39, 44; Tables 1, 2.**

Ginsberg, H. and Köster, M., Z. anorg. Chem. *271*, 41-8 (1952). **Pp. 52, 63, 64.**

Gitzen, W. H., Hart, L. D. and MacZura, G., Am. Ceram. Soc. Bull. *35*, 217-23 (1956); J. Am. Ceram. Soc. *40*, 158-67 (1957). **P. 26.**

Glemser, O., Z. Elektrochem. *45*, 865-70 (1939). **Table 5.**

Gomel'skii, K. Z., Zhur, Fiz. Khim. *32*, 1859-62 (1958). **P. 14.**

Gorbunova, O. E. and Vaganova, L. I., Khim. Referat. Zhur. *2*, No. 5, 31-2 (1939). **P. 34.**

Goton, R., Thesis, No. 146, University of Lyon, July 9, 1955. **Pp. 45, 49, 64.**

Graham, R. P. and Horning, A. E., J. Am. Chem. Soc. *69*, 1214-5 (1947). **P. 71.**

Graham, R. P. and Thomas, A. W., J. Am. Chem. Soc. *69*, 816-21 (1947). **P. 71.**

Grasshof, H., Angew. Chem. *63*, 96-7 (1951). **P. 57.**

Gregg, S. J. and Sing, K. S. W., J. Phys. and Colloid Chem. *55*, 592-7, 597-604 (1951); *56*, 388-91 (1952). **P. 43; Fig. 16.**

Gregory, J. N. and Moorbath, S., Trans. Faraday Soc. *47*, 844-59 (1951). **P. 45.**

Greville, C., See Encyclopaedia Brittanica "Corundum," 7, 11th Ed. (1910) 207. **P. 7.**

Gulbransen, E. A. and Wysong, W. S., J. Phys. and Colloid Chem. *51*, 1087-1103 (1947). **P. 72.**

Gyani, B. P., J. Phys. Chem. *56*, 762-3 (1952). **P. 71.**

Haber, F., Naturwissenschaften *13*, 1007-12 (1925). **Pp. 8, 49; Table 1.**

Hannah, R. W., Correspondence, January 13, 1960. **Table 10.**

Hansen, W. C. and Brownmiller, L. T., Am. J. Sci. *15*, 225-42 (1928). **Table 8.**

Harbison-Walker Refractories Co., "Modern Refractory Practice," Third Edition, Pittsburgh, Pa. (1950). **P. 23; Fig. 4.**

Harris, M. R. and Sing, K. S., J. Appl. Chem. *5*, 223 (1955); *7*, 397 (1957); *8*, 386-9 (1958). **P. 68.**

Hass, G., Optik *1*, 134-43 (1946). **P. 38.**

Hauth, W. E., Jr., J. Am. Ceram. Soc. *32*, 394-8 (1949); J. Phys. and Colloid Chem. *54*, 142-56 (1950). **P. 32.**

Haüy, R. J., Traite de mineralogie, Paris *4*, 358 (1801). **P. 7.**

Havestadt, L. and Fricke, R., Z. anorg. allgem. Chem. *188*, 357-95 (1930). **P. 64.**

Heilman, R. H., Mech. Eng. *58*, 291-2 (1936). **P. 16.**

Heldt, K. and Haase, G., Z. angew. Phys. *6*, 157-60 (1954). **Table 5.**

Hensler, J. R. and Henry, E. C., J. Am. Ceram. Soc. *36*, 76-83 (1953). **Table 5.**

Herold, P. G. and Dodd, C. M., J. Am. Ceram. Soc. *22*, 388-91 (1939). **P. 18.**

Hill, V. G., Roy, R. and Osborn, E. F., J. Am. Ceram. Soc. *35*, No. 6, 135-42 (1952). **Pp. 64, 66.**

Hippel, A. von, Table of Dielectric Materials. Vol. IV, Technical Report 57 (January 1953) and Vol. VI, Technical Report 126 (June 1959) M.I.T. Laboratory for Insulation Research. **Table 5.**

Hoch, M. and Johnston, H. L., J. Am. Chem. Soc. *76*, 2560-1 (1945). **Pp. 13, 72; Table 9.**

Hoffman, F., Observationum physico-chymicarum selectorium, Halae (1722). **P. 7.**

Holm, V. C. F. and Blue, R. W., Ind. Eng. Chem. *43*, 501-5 (1951). **P. 60.**

Houben, G. M. M., Refractories J. Abstracts (England) *28*, 252 (1952). **P. 37.**

Huffman, H. C., U. S. Patents 2,437,531-3 (March 9, 1948). **P. 11.**

Hunter, M. S. and Fowle, P., J. Electrochem. Soc. *103*, 482-5 (1956). **P. 34.**

Hüttig, G. F., Angew. Chem. *53*, 35-9 (1940). **P. 52.**

Hüttig, G. F. and Kölbl, F., Z. anorg. allgem. Chem. *214*, 289-306 (1933). **P. 50.**

Hüttig, G. F. and Markus, G., Kolloid-Z. *88*, 274-88 (1939). **P. 52.**

Hüttig, G. F. and Schaufel, A., Kolloid-Z. *55*, 199-207 (1931). **P. 64.**

Hüttig, W. and Ginsberg, H., Z. anorg. Chem. *278*, 93-107 (1955). **Pp. 44, 49, 50.**

Iberg, R., Helv. Chim. Acta *40*, 102-6 (1957). **P. 62.**

Imelik, B., Compt. rend. *233*, 1284-6 (1951). **Pp. 54, 70.**

Imelik, B., Petitjean, M. and Prettre, M., Compt. rend. *238*, 900-2 (1954). **P. 45; Table 10.**

Imelik, B., Mathieu, M. C., Prettre, M. and Teichner, S., J. chim. phys. *51*, 651-662 (1954). **P. 45.**

Iwase, E., Nishiyama, S. and Isono, T., Bull. Chem. Soc. Japan, *29*, 147-63 (1956). **P. 45.**

Jackson, E. A. and Roberts, J. B., Trans. Brit. Ceram. Soc. *54*, 389-98 (1955). **P. 18.**

Jaeger, G. and Krasemann, R., Werkstoffe u. Korrosion *3*, 401-15 (1952). **P. 30; Table 9.**

Jellinek, M. H. and Fankuchen, I., Ind Eng. Chem. *37*, 158-63 (1945); *41*, 2259-65 (1949). **P. 43.**

Jockers, K., Z. anorg. Chem. *265*, 49-55 (1951). **P. 45.**

Johnson, F. M. G., J. Am. Chem. Soc. *34*, 911-2 (1912). **P. 53.**

Jones, J. T., Maitra, P. K. and Cutler, I. B., J. Am. Ceram. Soc. *41*, 353-7 (1958). **P. 11.**

Karpacheva, S. M. and Rozen, A. M., Doklady Akad. Nauk S.S.S.R. *81*, 425-6 (1951); *75*, 55-8 (1950). **P. 39.**

Kebler, R. W., Linde Air Products Co. **Table 8.**

Keller, W. D. and Pickett, E. E., Am. J. Sci. *248*, 264-73 (1950). **P. 62.**

Kelley, K. K., Correspondence, May 12, 1959. **Table 4.**

Kelman, L. R., Wilkinson, W. D. and Yaggu, F. L., Argonne National Laboratory Report ANL-4417, July, 1950. **Table 9.**

Kengott, A., The Minerals of Switzerland, Leipzig (1866). **P. 50.**

Kilham, J. K., Third Symposium on Combustion Flame and Explosion Phenomena 733-40, The Williams and Wilkins Co., Baltimore, Md. (1949). **P. 16.**

Kimberlin, C. N. and Gladrow, E. M., U. S. Patent 2,796,326 (June 1957); Light Metals Bull. *19*, 684 (1957). **P. 34.**

Kingery, W. D., Francl, J., Coble, R. L., and Vasilos, T., J. Am. Ceram. Soc. *37*, 107-10 (1954). **Table 4.**

Kiselev, A. V. and Smirnova, I. V., Zhur. Fiz. Khim. *23*, 1018-24 (1949). **P. 53.**

Kiyoura, R. and Sayta, T., Yogyo Kyokai Shi *66*, 23-7 (1958). **P. 18.**

Klassen-Neklyudova, M. V., J. Tech. Phys. (U.S.S.R.) *12*, 519-34, 535-51 (1942). **Table 7.**

Klassen-Neklyudova, M. V., Ikornikova, N. Yu. and Tomilovskii, G. E., Trudy Inst. Krist. Akad. Nauk. S.S.S.R. No. *8*, 237 (1953). **P. 15.**

Klein, D. J., U. S. Atomic Energy Comm. NAA-SR-25-42, 24 pp. (1958). **P. 14.**

Klevens, H. B. and Platt, J. R., J. Am. Chem. Soc. *69*, 3055-62 (1947). **P. 16.**

Knapp, H., Z. angew. Phys. *9*, 233-9 (1957). **P. 18.**

Kohlschütter, V., Beutler, W., Sprenger, L. and Berlin, M., Helv. Chim. Acta *14*, 3-49 (1931). **P. 52.**

Kohlschütter, V. and Beutler, W., Helv. Chim. Acta *14*, 305-54 (1931). **P. 52.**

Kohn, J. A., Katz, G. and Broder, J. D., Am. Mineralogist *42*, 398-407 (1957). **P. 34; Table 2.**

Kolesova, V. A., Optika I Spektroskopiia VI, 20 (1959). **Table 10.**

Komarov, V. A. and Chernikova, E. A., Zhur. Fiz. Khim. *29*, 1876-82 (1955). **P. 38.**

König, G., Naturwissenschaften *35*, 92-3 (1948). **P. 38.**

Kordes, E., Z. Krist. *91*, 193-228 (1935). **Tables 2, 8.**

Korenstein, B., Z. anorg. allgem. Chem. *279*, 194-204 (1955). **P. 13.**

Kraut, H., Flake, E., Schmidt, W. and Volmer, H., Ber. *75B*, 1357-73 (1942). **Pp. 52, 68.**

Krishnan, R. S., Nature *160*, 26 (1947). **P. 16.**

Kröger, F. A., Some Aspects of the Luminescence of Solids, Elsevier Publishing Co., New York, 1948. **Pp. 15, 19.**

Kronberg, M. L., Acta Met. *5*, 507-24 (1957). **P. 15.**

Kronberg, M. L., Science *122*, 599 (1955). **P. 18.**

Kroon, D. J. and Stolpe, C. V. D., Nature *183*, 944 (1959). **Pp. 49, 62.**

Kubli, H., Helv. Chim. Acta *30*, 453-63 (1947). **P. 57.**

Kuczynski, W. and Zagorski, Z., Roczniki Chem. *24*, 211-7 (1950). **P. 71.**

Kuczynski, G. C., Abernethy, L. and Allan, J., University of Notre Dame, Notre Dame, Ind., and Argonne National Laboratory, Lement, Ill.; Plansee Proceedings, 1-12 (1958). **P. 11.**

Kukolev, G. V. and Leve, E. N., Zhur. Priklad. Khim. *28*, 909-15 (1955). **P. 11.**

Lacroix, S., Anal. Chim. Acta *1*, 260-90 (1947). **P. 71.**

Lägerqvist, K., Wallmark, S. and Westgren, A., Z. anorg. Chem. *234*, 1-16 (1937). **Table 2.**

Lang, S. M., "Properties of High-Temperature Ceramics and Cermets. Elasticity and Density at Room Temperature," Communication from J. B. Wachtman, Jr., January, 1960. **P. 17.**

Laubengayer, A. W. and Weisz, R. S., J. Am. Chem. Soc. *65*, 247-50 (1943). **Pp. 47, 50, 51, 65; Fig. 8.**

Layng, E. T., U. S. Patent 2,487,564 (November 8, 1949). **P. 11.**

LeChatelier, H., Compt. rend. *104*, 1443-6; 1517-20 (1887). **P. 38.**

Lecompte, J., J. Chem. Phys. *50*, C53-61 (1953). **P. 66.**

Lecuir, R., Bull. soc. chim. France, D227-30 (1949). **P. 32.**

Leedy, R. M., Westinghouse Engineer *14*, No. 4, 147-51 (1954). **P. 16.**

Levin, E. M., McMurdie, H. F. and Hall, F. P., Phase Diagrams for Ceramists, Columbus, Ohio, The American Ceramic Society (1956). **P. 15.**

Levin, E. M. and McMurdie, H. F., Phase Diagrams for Ceramists, Part II, Columbus, Ohio, The American Ceramic Society (1959). **P. 15.**

Levy, P. W., Bull. Am. Phys. Soc. *4*, 159 (1959). **P. 15.**

Lister, B. A. J., J. App. Chem. *2*, 280-3 (1952). **P. 57.**

Lomer, P. D., Proc. Phys. Soc. (London) *B63*, 818-9 (1950). **Table 5.**

Lupfer, R., Petroleum Processing *7*, 993 (1952). **Table 14.**

MacKenzie, J. K., Proc. Phys. Soc. (London) *63B*, 2-11 (1950). **P. 17.**

Mah, A. D., J. Phys. Chem. *61*, 1572-3 (1957). **Table 4.**

Mahl, H., Kolloid-Z. *100*, 219-28 (1942). **P. 38.**

Makhov, G., Kikuchi, C., Lambe, J. and Terhune, R. W., Phys. Rev. *109*, 1399-1400 (1958). **P. 16.**

Mandarino, J. A., "Some Optical and Stress-Optical Properties of Synthetic Ruby," University of Michigan, ASTIA AD 146029 (1957). **P. 15.**

Marggraf, A. S., Mem. Acad. Berlin *41* (1754). **P. 7.**

Marion, S. P. and Thomas, A. W., J. Colloid Sci. *1*, 221-34 (1946). **P. 71.**

Mauer, F. A. and Bolz, L., Wright Air Development Center Technical Report, 55-473, Supplement 1. **Table 4.**

May, J. E., Kinetics of High-Temperature Processes, John Wiley and Sons, New York, 1959, 30-37. **P. 18.**

McCandless, E. L. and Yenni, D. M., U. S. Patents 2, 485,978-9 (October 25, 1949). **P. 16.**

Megaw, H. D., Proc. Roy. Soc. (London) *A142*, 198-214 (1933). **Table 4.**

Megaw, H. D., Z. Krist. *A87*, 185-204 (1934). **Pp. 61, 62; Table 2.**

Michaud, M., Compt. rend. *228*, 1115-6 (1949). **P. 16.**

Michel, M., Compt. rend. *244*, 73-4, 595-6 (1957). **Table 4.**

Milligan, L. H., J. Phys. Chem. *26*, 247 (1922). **P. 61.**

Milligan, W. O., J. Phys. and Colloid Chem. *55*, 497-506 (1951). **P. 71.**

Milligan, W. O. and Weiser, H. B., J. Phys. and Colloid Chem. *55*, 490-6 (1951). **P. 64.**

Milligan, W. O. and McAtee, J. L., J. Phys. Chem., *60*, 273-77 (1956). **P. 64.**

Milliken, T. H., Jr., Mills, G. A. and Oblad, A. G., Dis. Faraday Soc. No. *8*, 279-90 (1950). **P. 60.**

Mills, G. A., Weller, S., Hindin, S. G. and Milliken, T. H., Jr., Z. Electrochem. *60*, 823-7 (1956). **P. 60.**

Minerals Yearbook, U. S. Dept. Int., Bur. Mines (1958). **P. 7.**

Miyazawa, H. and Okada, J., J. Phys. Soc. Japan *6*, 55-9 (1951). **Table 5.**

Modi, H. J. and Fuerstenau, D. W., J. Phys. Chem. *61*, 640-3 (1957). **P. 16.**

Moiseev, P. S., Kolloid-Zhur. *9*, 53-6 (1947). **Table 1.**

Montoro, V., Ricerca sci. *13*, 565-71 (1942). **Table 8.**

Mooi, J. and Selwood, P. W., J. Am. Chem. Soc. *74*, 1750-4 (1952). **P. 60.**

Moorbath, S., Atomic Energy Research Establishment Report C/M 127 (August, 1952). **P. 45.**

Moore, B., J. Soc. Chem. Ind. (London) *59*, 119-20 (1940). **Table 7.**

Moran, T. and Jones, C. R., British Patent 569, 710. **P. 55.**

Nahin, P. G. and Huffman, H. C., Ind. Eng. Chem. *41*, 2021-7 (1949). **Pp. 44, 61, 63.**

Nakamoto, K., Margoshes, M. and Rundle, R. E., J. Am. Chem. Soc. *77*, 6480-6 (1955). **P. 65.**

Neugebauer, W. and Schäfer, H., Z. anorg. Chem. *274*, 281-8 (1953). **P. 59.**

Newsome, J. W., U. S. Patent 2,642,337. **P. 45.**

Nieuwenburg, C. J. van, and Pieters, H. A. J., Rec. trav. chim. *48*, 31 (1929). **P. 50.**

O'Connor, D. J., Johansen, P. G. and Buchanan, A. S., Trans. Far. Soc. *52*, 229-36 (1956). **P. 16.**

Orsini, L. and Petitjean, M., Compt. rend. *237*, 326-8 (1953). **P. 45.**

Pampuch, R., Prace Inst. Hutnic. *10*, 333-47 (1958). **P. 11.**

Papée, D., Thesis A2737, 3610, Univ. of Paris, March 10, 1953. **P. 51.**

Papée, D., Compt. rend. *234*, 952-4, 2536-8 (1952). **Pp. 47, 54, 64.**

Papée, D., Charrier, J., Tertian, R., Houssemaine, R., Congress of Aluminum, Paris 1954, Investigation of the Constitution of Activated Alumina. **P. 51.**

Papée, D. and Tertian, R., Compt. rend. *236*, 1668-70 (1953); Bull. soc. chim. (France), 983-9 (1955). **Pp. 8, 42, 51.**

Papée, D., Compt. rend. *246*, 2377-80 (1958). **P. 54.**

Papée, D., Tertian, R. and Biais, R., Bull. soc. chim. (France) 1301-10 (1958). **Pp. 37, 49, 63, 68; Tables 1, 3.**

Parché, M. C., "Facts About Fused Alumina," Niagara Falls, N. Y., The Carborundum Company (Revised 1954). **Pp. 27, 28, 30.**

Parravano, N. and Montoro, V., Atti. Accad. Lincei *7*, 885-91 (1928). **P. 38.**

Partridge, J. H. and Rooksby, H. P., Trans. Soc. Glass Tech. *23*, *338* (*1953*). **Fig. 4.**

Pascal, P., Compt. rend. *178*, 481-3 (1924). **Table 6.**

Pauling, L. and Hendricks, S. B., J. Am. Chem. Soc. *47*, 781-90 (1925). **P. 13.**

Pavella, F., Kolloid-Z. *107*, 139-41 (1944). **P. 71.**

Pavlushkin, N. M., Steklo i Keram. *13*, 19-23 (1956). **P. 11.**

Pearson, S., Proc. Phys. Soc. (London) *69B*, 1293-6 (1956). **P. 17.**

Péchiney, A. R., French Patent 349,709 (April 8, 1904). **P. 52.**

Péchiney, French Patent 1,077,116 (November 4, 1954); French Patent 1,108,011 (January 9, 1956). **Pp. 52, 53.**

Petitjean, M., Thesis No. 79. University of Lyon, March 4, 1955. **Pp. 45, 47, 49.**

Phipps, H. K., Oil Gas J. *45*, No. 29, 67-9, 101-2 (1946). **Table 14.**

Pike, R. G. and Hubbard, D., Highway Research Board, *37*, 256 (1958). **P. 16.**

Pingard, L. G. (to Péchiney) U. S. Patent 2,881,051 (April 7, 1959). **P. 51.**

Plank, C. J., J. Phys. Chem. *57*, 284-90 (1953). **P. 57.**

Plummer, M., J. Appl. Chem. (London) *8*, 35-44 (1958). **P. 35.**

Podszus, E., Z. Elektrochem. *39*, 75-81 (1933). **Table 5.**

Pointud, R. and Caillat, R., Light Metals Bull. *17*, 8776 (1955). Rev. Met. *54*, 277-82 (1957). **P. 13.**

Pollak, P., Private Communication, 1960. **Table 12.**

Porter, R. F., Schissel, P. and Inghram, M. G., J. Chem. Phys. *23*, 339-42 (1955). **P. 72.**

Pott, J. H., Lithogeognosia; Potsdam (1746), Berlin (1754). **P. 7.**

Prettre, M., Bull. assoc. franc. techniciens pétrole No. 91, 23-41 (1952). **P. 40.**

Prettre, M., Imelik, B., Blanchin, L. and Petitjean, M., Angew. Chem. *65*, No. 22, 549-55 (1953). **P. 40.**

Railton, E. C., Ceramics and Glass, Selected Government Res. Rpts., Ministry of Supply (London) *10* (1952). **Table 5.**

Raman, C. V., Proc. Indian Acad. Sci. *34A*, 61-71 (1951). **P. 16.**

Rankin, G. A. and Merwin, H. E., J. Am. Chem. Soc. *38*, 568-88 (1916). **P. 8; Table 8.**

Rao, R. V. G. S., Proc. Indian Acad. Sci. *29A*, 352-60 (1949). **Table 7.**

Rao, S. R. and Leela, M., Current Sci. (India) *22*, 72-3 (1953). **Table 6.**

Rathmell, B. L. and Bateman, P. J., J. Inst. Heating Ventilating Engrs. (London) *19*, 471-523 (1952). **P. 55.**

Reed, E. L., J. Am. Ceram. Soc. *37*, 146-53 (1954). **Table 9.**

Reichstein, P. and Shoppee, C. W., Dis. Faraday Soc. No. 7, 305-11 (1949). **P. 57.**

Reinhard, F., Glas-Email-Keramo-Tech. *5* [5] 180-4 (1954). **P. 11.**

Remmey, G. B., Am. Ceram. Soc. Bull. *27*, 477-85 (1948). **Fig. 5.**

Ridgway, R. R., Ballard, A. H. and Bailey, B. L., Trans. Electrochem. Soc. *63*, *369-93* (*1933*). **P. 19.**

Ridgway, R. R., Klein, A. A. and O'Leary, W. J., Trans. Electrochem. Soc. *70*, 71-86 (1936). **P. 8.**

Rieke, J. K. and Daniels, F., J. Phys. Chem. *61*, 629-33 (1957). **Pp. 15, 39, 64.**

Robert, L., Compt. rend. *233*, 1103-4 (1951). **P. 54.**

Roberts, J. P. and Watt, W., Ceramics and Glass, Selected Government Res. Rpts., Ministry of Supply (London) *10* (1952); Trans. Brit. Ceram. Soc. *48*, 343-51 (1949); *50* (3) 122-43 (1951). **Pp. 17, 32; Table 7.**

Rodigina, E. W. and Gomel'skii, K. Z., Zhur. Fiz. Khim. *29*, 1105-12 (1955). **P. 14.**

Rögener, H., Z. Elektrochem. *46*, 25-7 (1940). **Table 5.**

Rooksby, H. P., Chapter 10, X-ray Identification and Crystal Structure of Clay Minerals, Edited by Brindley, G. S., The Mineralogical Society British Museum (Natural History) London, S. W. 7 (1951). **Table 1.**

Rooksby, H. P., J. Appl. Chem. (London) *8*, 44-9 (1958). **P. 35; Tables 2, 3.**

Rooymans, C. J. M., J. Inorg. and Nuclear Chem. *11*, 78-9 (1959). **P. 37.**

Rooymans, C. J. M., (Communication to H. P. Rooksby, 1959). **P. 35; Table 2.**

Roth, A., Z. anorg. allgem. Chem. *244*, 48-56 (1940). **P. 38.**

Roth, W. A., Wirths, G. and Berendt, H., Z. Elektrochem. *48*, 264-7 (1942). **Tables 2, 4.**

Roy, R., Hill, V. G. and Osborn, E. F., Ind. Eng. Chem. *45*, 819-20 (1953). **P. 34.**

Roy, R. and Osborn, E. F., Am. Mineralogist *39*. 853-85 (1954). **P. 65.**

Rueger, L. J., Todd, F. C. and Nelson, H. R., Battelle Memorial Institute Report S-725-4 to Aluminum Company of America, August 6, 1948. **Table 5.**

Ruh, E., Am. Ceram. Soc. Bull. *32*, No. 4, 150 (1953). **Table 4.**

Rundle, R. E. and Parsol, M., J. Chem. Phys. *20*, 1487-8 (1952). **P. 65.**

Russell, A. S. and Cochran, C. N., Ind. Eng. Chem. *42*, 1336-40 (1950). **Pp. 18, 43, 45, 47, 49, 64; Fig. 15.**

Russell, A. S. and Lewis, J. E., Ind. Eng. Chem. *46*, 1305-10 (1954). **P. 29.**

Russell, A. S. and Stokes, J. J., Jr., Ind. Eng. Chem. *38*, 1071-4 (1946); *40*, 520-4 (1948). **P. 60.**

Russell, A. S., Edwards, J. D., Taylor, C. S., J. Metals, 1123-8, October, 1955. **Pp. 51, 62; Table 4.**

Ryshkewitch, E., Ber. deut. keram. Ges. *20*, 477-84 (1939). **P. 30.**

Ryshkewitch, E., Ber. deut. keram. Ges. *22*, 54-65, 363-71 (1941). **P. 17; Table 7.**

Ryshkewitch, E., Ber. deut. keram. Ges. *23*, 243-60 (1942). **Table 7.**

Ryshkewitch, E., Ber. deut. keram. Ges. *25*, 95-112 (1944). **P. 17.**

Ryshkewitch, E., Oxydkeramik der Einstoffsysteme vom Standpunkt der Physikalischen Chemie (1948) 280 pp. Berlin: Springer-Verlag. **Table 7.**

Ryshkewitch, E., J. Am. Ceram. Soc. *36*, 42-3, 65-8 (1953). **P. 11.**

Saalfeld, H., Z. anorg. allgem. Chem. *286*, 174-9 (1956); *291*, 117-21 (1957). **P. 19.**

Saalfeld, H., Clay Minerals Bull. *3*, 249-56 (1958). **P. 35.**

Sacconi, L., Dis. Faraday Soc. No. 7, 173-9 (1949). **P. 57.**

Sanlaville, J., Génie chim. *78*, 102-22 (1957). **Pp. 43, 54.**

Sargent, L. B., Jr. and Kipp, E. M., Iron Steel Eng. *31*, 73-6 (1954). **P. 61.**

Saucier, H., Bull. soc. franc. mineral. et Crist. *76*, 480-2 (1953). **P. 16.**

Savinelli, E. A., J. Appl. Chem. *6*, 9 (1956). **P. 56.**

Sawamura, H., J. Sci. Research Inst. (Japan) *46*, 15-6 (1952). **P. 69.**

Sawyer, D. W., Keefer, H. D., Kipp, E. M. and Shaw, R. W., Lubrication Engineering, *12*, No. 3, 183-192 (1956). **P. 61.**

Schmäh, H., Z. Naturforsch. *1*, 323-4 (1946). **Pp. 62, 72.**

Schneider, A. and Gattow, G., Z. anorg. Chem. *277*, 41-8 (1954). **P. 35; Table 4.**

Schwab, G., Dis. Faraday Soc. No. 7, 170-3 (1949). **P. 57.**

Schwartz, B., J. Am. Ceram. Soc. *35*, 325-33 (1952). **Tables 4, 7.**

Schweig, B., Glass *22*, 263-5 (1945). **P. 67.**

Schwiersch, H., Chem. Erde *8*, 252-315 (1933). **Pp. 18, 50.**

Scott, R., Metallurgia *44*, 50-2 (1951). **P. 32.**

Sears, G. W. and Navias, L., J. Chem. Phys., *30*, 1111 (1959). **P. 72.**

Seemann, A. K., "Gems, Synthetic," Encyclopedia of Chemical Technology *7*, Interscience Encyclopedia, Inc. (1951). **Pp. 16, 33; Tables 2, 5, 7, 8.**

Seger, W. A., Am. Glass Rev. *50*, No. 9, 15-6 (1930). **P. 67.**

Selected Values of Chemical Thermodynamic Properties, Nat. Bur. Stds. **Table 4.**

Selwood, P. W., Correspondence, August 2, 1950. **Table 6.**

Selwood, P. W. and Lyon, L., J. Am. Chem. Soc. *74*, 1051 (1952). **P. 60.**

Selwood, P. W., Magnetochemistry, Interscience, 163-8 (1956). **P. 16.**

Shalnikova, N. A. and Yakovlev, I. A., Kristallogramiya *1*, 531-3 (1936). **Table 4.**

Sharma, S. S., Proc. Indian Acad. Sci. *33A*, 245-9 (1951). **Table 4.**

Shibata, M., Science (Japan) *19*, 570-1 (1949). **P. 58.**

Shishakov, N. A., Zhur. Fiz. Khim. *26*, 106-11 (1952). **P. 8.**

Shubnikov, A. V., Klassen-Neklyudova, M. V. and Grum-Gizhimăilo, S. V., "Physical Properties of Synthetic Corundum — A Symposium," Trudy Inst. Krist. Akad. Nauk S.S.S.R. No. 8, 356 pp. (1953). **P. 32.**

Shul'man, A. R. and Rozentsveig, I. Yu, Doklady Akad. Nauk S.S.S.R. *74*, 497-500 (1950). **Table 5.**

Shuvaeva, G. M. and Gapon, E. N., Zhur. Anal. Khim. *8*, 50-2 (1953). **P. 57.**

Singer, F. and Thurnauer, H., Metallurgia *36*, 237-42, 313-5 (1947). **Tables 5, 7, 9.**

Smith, A. E. and Beeck, O. A., U. S. Patent 2,422,172 (June 10, 1947). **P. 19.**

Smothers, W. J. and Reynolds, H. J., J. Am. Ceram. Soc. *37*, No. 12, 588-96 (1954). **Pp. 11, 23.**

Souza Santos, P., Vallejo-Freire, A. and Souza Santos, H. L., Kolloid-Z. (Germany) *133*, 101-7 (1953). **P. 68.**

Souza Santos, P., Vallejo-Freire, A., Parsons, J. and Watson, J. H. L., Experienta *14*, 318-20 (1958). **P. 69.**

Stavrolakis, J. A. and Norton, F. H., J. Am. Ceram. Soc. *33*, 263-8 (1950). **Table 7.**

Steinheil, A., Ann. Physik. *19*, 465-83 (1934). **P. 8.**

Stirland, D. J., Thomas, A. G. and Moore, N. C., Trans. Brit. Ceram. Soc. *57*, 69-84 (1958). **P. 44.**

Stott, V. H., Trans. Ceram. Soc. (Engl.) *37*, 346, 353 (1938). **P. 30.**

Stott, V. H., Metallurgia *44*, No. 263, 157-62, Cont. 164; *44*, No. 264, 212, Cont. 218 (1951). **P. 32.**

Stowe, V. M., J. Phys. Chem. *56*, 484-6, 487-9 (1952). **P. 54.**

Stowe, V. M., U. S. Patent 2,352,867 (July 4, 1944). **P. 53.**

Stowe, V. M., Marshall, E. E., Nickel, L. L. and Greenwood, R. S., Petroleum Processing *3*, 217-24 (1948). **P. 60.**

Stumpf, H. C., Russell, A. S., Newsome, J. W. and Tucker, C. M., Ind. Eng. Chem. *42*, 1398-1403 (1950). **Pp. 8, 50, 68; Fig. 7; Tables 1, 2, 3.**

Swanson, H. E. and Fuyat, R. K., Natl. Bur. Standards Circular 539, Vol. 2 (1953), Vol. 3 (1954). **Tables 2, 3.**

Szabo, Z. G., Csányi, L. J. and Kávai, M., Z. anal. chem. *146*, 401-14 (1955). **P. 72.**

Tamele, M. W., Dis. Faraday Soc. No. 8, 270-9 (1950). **P. 60.**

Taylor, C. S. and Edwards, J. D., Heating, Piping, Air Conditioning (Journal Section) *11*, 59-63 (1939). **P. 16.**

Taylor, C. S., Tucker, C. M. and Edwards, J. D., Trans. Electrochem. Soc. *88*, 325-33 (1945). **P. 38.**

Taylor, R. J., J. Soc. Chem. Ind. (London) *68*, 23-6 (1949). **P. 43.**

Teichner, S., Compt. rend. *237*, 810-2, 900-2 (1953). **P. 70.**

Teichner, S., Correspondence, December 24, 1959. **Pp. 37, 71.**

Tertian, R. and Papée, D., Compt. rend. *236*, 1565-67 (1953), *241*, 1575-7 (1955). **Pp. 37, 51.**

Tertian, R., Papée, D. and Charrier, J., Compt. rend. *238*, 98-9 (1954). **P. 51.**

Tertian, R. and Papée, D., J. chim. phys. *55*, 341-53 (1958). **Pp. 42, 63, 65; Table 1.**

Teter, J. W., Gring, J. L. and Keith, C. D., U. S. Patent 2,838,375 (June 10, 1958). **Table 1.**

Tewari, S. N., Dey, A. K. and Ghosh, S., Z. anorg. Chem. *271*, 150-2 (1953). **P. 58.**

Thibon, H. and Charrier, J., Bull. soc. hist. nat. Toulouse *85*, 394-8 (1950). **P. 44.**

Thibon, H., Charrier, J. and Tertian, R., Bull. soc. chim. France 384-92 (1951). **P. 51; Fig. 16; Tables 2, 8.**

Thilo, E., Vander, E. and Seemann, H., Z. anorg. allgem. Chem. *279*, 2-17 (1955). **P. 32.**

Thompson, J. G. and Mallett, M. W., J. Research Natl. Bur. Standards *23*, 319-27 (1939). **P. 32.**

Tomashov, N. D., Vestnik Inzhenerov i Tekh. No. 2, 59-65 (1946). **Table 4.**

Torkar, K. and Worel, H., Monatshefte für Chem. *88*, 739-48 (1957). **Table 4.**

Toropov, N. A., Compt. rend. acad. sci. U.R.S.S. *1*, No. 2-3, 147-9 (1935). **Tables 2, 8.**

Toropov, N. A. and Galakhov, F. Y., Doklady Akad. Nauk S.S.S.R. *78*, 299-302 (1951). **Fig. 4; Table 2.**

Torrey, J., New York Med. Phys. Journ. *1*, 68 (1822); Edin. Phil. Journ. *7*, 388 (1822). **P. 7.**

Tosterud, M., Canadian Patent 285,147 (November 27, 1928); U. S. Patent 1,953,201 (April 3, 1934). **P. 64.**

Trambouze, Y. and Perrin, M., Compt. rend. *236*, 1261 (1953). **P. 45.**

Trambouze, Y., Mourgue, L. de and Perrin, M., J. chim. phys. 723-8 (1954). **P. 60.**

Tran-Huu-The and Prettre, M., Compt. rend. *234*, 1366-8 (1952). **P. 38.**

Travers, A. and Clause, F., Bull. soc. chim. France, 209-10 (1947). **P. 52.**

Tromimov, A. K. and Tolkachov, S. S., Doklady Akad. Nauk S.S.S.R. *104*, 154-5 (1955). **P. 45.**

Tscherbow, S. I., and Tschernjak, E. L., Chem. J. Ser. B., J. Appl. Chem. (Russian) *10*, 1220 (1957). **P. 14.**

Turkevich, J. and Hillier, J., Anal. Chem. *21*, 475-85 (1949). **P. 69; Figs. 27, 30, 31, 32.**

Turkevich, J., Hubbell, H. H. and Hillier, J., Dis. Faraday Soc. No. 8, 348-52 (1950). **Fig. 19.**

Ueda, I. and Okada, T., Proc. Phys. Soc. Japan *4*, 8-9 (1949). **Table 5.**

Ulrich, F., Norsk Geol. Tidsskrift *8*, 115-22 (1925). **P. 8.**

Unmack, A., Second International Congress of Crystallography. Abstracts of Papers, Stockholm. June 27 to July 5, 1951 (Inorganic Structures No. 8, Section G). **Table 2.**

Van Nordstrand, R. A., Hettinger, W. P. and Keith, C. D., Nature *177*, 713-4 (1956). **Pp. 8, 63; Table 3.**

Van Oosterhout, G. W. and Rooymans, C. M. J., Nature *181*, 44 (1958). **Pp. 35, 37.**

Vauquelin, L. N., Ann. Chim. Phys. (1) *42*, 113 (1802). **P. 7.**

Venturello, G. and Burdese, A., Ann. chim. (Rome) *41*, 155-62 (1951). **P. 59.**

Verwey, E. J. W., Z. Krist. *91*, 317-20 (1935); J. Chem. Phys. *3*, 592-3 (1935). **P. 37.**

Voltz, S. E. and Weller, S. W., U. S. Patents 2,810,698-9 (October, 1957). **P. 11.**

Wachtman, J. B., Jr. and Maxwell, L. H., Am. Ceram. Soc. Bull. *32*, No. 4, 145 (1953); J. Am. Ceram. Soc. *37*, 291-299 (1954); WADC Technical Report 53-265 Supplement 1, November 1954. **P. 17; Tables 5, 7.**

Wachtman, J. B., Jr. and Maxwell, L. H., Wright Air Development Center Technical Report 57-526 (1957). **P. 17.**

Wachtman, J. B., Jr. and Maxwell, L. H., J. Am. Ceram. Soc. *42*, 432-3 (1959). **P. 18.**

Wachtman, J. B., Jr. and Lam, D. G., Jr., J. Am. Ceram. Soc. *42*, 254-60 (1959). **P. 17.**

Wachtman, J. B., Jr., Tefft, W. E., Lam, D. G., Jr. and Stinchfield, R. P., Wright Air Development Center Technical Report 59-278. **P. 17.**

War Production Board, The Special Aluminum Committee, "The World Aluminum Industry," April 1945, p. 105 cited by Report of the Surplus Property Board to the Congress, Aluminum Plants and Facilities, Washington 25, D. C., September 21, 1945, 125-126. **P. 7.**

Wartenberg, H. von., Z. anorg. Chem. *264*, 226-9 (1951); *269*, 76-85 (1952); *270*, 328 (1952). **Pp. 11, 72; Table 4.**

Wartenberg, H. von, and Prophet, E., Z. Elektrochem. *38*, 849-50 (1932). **Table 5.**

Wartenberg, H. von, Wehner, G. and Saran, E., Nachr. Ges. Wiss. Gottingen, Math.-physik, Klasse Fachgruppe II [N.F.] *2*, 73-5 (1936). **Table 2.**

Watson, J. H. L., Parsons, J., Vallejo-Freire, A. and Souza Santos, P., Kolloid-Z. *140*, 102-112 (1955). **Pp. 63, 68.**

Watson, J. H. L., Vallejo-Freire, A., Souza Santos, P. and Parsons, J., Kolloid-Z. *154*, 4-15 (1957). **P. 68.**

Watt, W. and Roberts, J. P., Metallurgia *43*, 307-8 (June, 1951). **P. 32.**

Webb, W. W. and Forgeng, W. D., Bull. Amer. Phys. Soc. *2*, 342 (1957). **P. 18.**

Weeks, J. L. and Seifert, R. L., J. Am. Ceram. Soc. *35*, 15 (1952). **Table 4.**

Weiser, H. B., Inorganic Colloid Chemistry, Vol. II, The Hydrous Oxides and Hydroxides, New York, John Wiley and Sons, 1935, 90-120. **P. 8.**

Weiser, H. B. and Milligan, W. O., J. Phys. Chem. *38*, 1175-82 (1934). **P. 8; Table 1.**

Weiser, H. B. and Milligan, W. O., J. Phys. Chem. *40*, 1-7 (1936). **P. 64.**

Weiser, H. B. and Milligan, W. O., "The Constitution of Inorganic Gels" in Advances in Colloid Science I, Interscience Publishers, New York (1952). **P. 71.**

Weiser, H. B., Milligan, W. O. and Purcell, W. R., Ind. Eng. Chem. *32*, 1487-90 (1940); *33*, 669-72 (1941). **P. 71.**

Werner, K., Feuerfest *8*, 70 (1932). **Table 5.**

Whalley, E. and Winter, E. R. S., J. Chem. Soc. 1175-7 (1950). **P. 39.**

Willstätter, R., Kraut, H. and Erbacher, O., Ber. *58B*, 2448-58 (1925). **P. 68.**

Wilsdorf, H. G. F., Nature *168*, 600-1 (1951). **P. 68.**

Winter, E. R. S., J. Chem. Soc. 1170-5 (1950). **P. 39.**

Winter, E. R. S. and Houghton, G., Mass Spectrometry (Institute of Petroleum, London) 127-40 (1950). **P. 39.**

Winzer, R., Angew. Chem. *45*, 429-31 (1932). **P. 30; Table 9.**

Yamaguchi, G. and Tanabe, H., J. Japan Ceram. Assoc. *62*, 34-8 (1954). **P. 29.**

Yamanouchi, S. and Kato, S., J. Japan Ceram. Assoc. *54*, 29-32 (1946). **P. 22.**

Yamauchi, T. and Kato, S., J. Japan Ceram. Assoc. *52*, 194-6, 255-8 (1944). **P. 18.**

Yamauchi, T. and Kondo, R., J. Japan Ceram. Assoc. *57*, 160-3; *62*, 34-8 (1954). **P. 32.**

SUBJECT INDEX